

**T.C.
REPUBLIC of TURKEY
HACETTEPE UNIVERSITY
GRADUATE SCHOOL of HEALTH SCIENCES**

**DEVELOPMENT of RADIOPHARMACEUTICAL
FORMULATIONS for IMAGING of NON HODGKIN'S
LYMPHOMA**

Pharm. Elif Tugce SARCAN BOZKIR

**Doctorate Program of Radiopharmacy
DOCTOR of PHILOSOPHY THESIS**

**ANKARA
2022**

**T.C.
REPUBLIC of TURKEY
HACETTEPE UNIVERSITY
GRADUATE SCHOOL of HEALTH SCIENCES**

**DEVELOPMENT of RADIOPHARMACEUTICAL
FORMULATIONS for IMAGING of NON HODGKIN'S
LYMPHOMA**

Pharm. Elif Tugce SARCAN BOZKIR

**Doctorate Program of Radiopharmacy
DOCTOR of PHILOSOPHY THESIS**

SUPERVISOR of THE THESIS

Prof. Dr. A. Yekta OZER

CO-SUPERVISOR of THE THESIS

Prof. Neil HARTMAN

ANKARA

2022

HACETTEPE UNIVERSITY
GRADUATE SCHOOL of HEALTH SCIENCES

**Development of Radiopharmaceutical Formulations
for Imaging of Non Hodgkin's Lymphoma**

Elif Tugee Sarcan Bozkır

Supervisor: Prof. Dr., A. Yekta OZER

Co-supervisor: Prof. Dr., Neil HARTMAN

This thesis study has been approved and accepted as a PhD dissertation in "Radiopharmacy Doctorate Program" by the assesment committee, whose members are listed below, on 22.09.2022.

- Chairman of the Committee :** *Prof. Dr., Suna, ERDOĞAN*
Hacettepe Uni. Faculty of Pharm,
Department of Radiopharmacy
- Member :** *Doç., Dr., Derya, İLEM ÖZDEMİR*
Ege Uni. Faculty of Pharm,
Department of Radiopharmacy
- Member :** *Prof. Dr., Özlem, KÜÇÜK*
Ankara Uni. Faculty of Med.
Department of Nuclear Medicine
- Member :** *Prof. Dr., Fani, BOZKURT*
Hacettepe Uni. Faculty of Med.
Department of Nuclear Medicine
- Member :** *Dr. Öğr. Üyesi, Mine, SİLİNDİR GÜNAY*
Hacettepe Uni. Faculty of Pharm,
Department of Radiopharmacy ı

This dissertation has been approved by the above committee in conformity to the related issues of Hacettepe University Graduate Education and Examination Regulation.

29 Eylül 2022

Prof. Müge YEMİŞCI ÖZKAN, MD, PhD

Director

YAYIMLAMA VE FİKRİ MÜLKİYET HAKLARI BEYANI

Enstitü tarafından onaylanan lisansüstü tezimin/raporumun tamamını veya herhangi bir kısmını, basılı (kağıt) ve elektronik formatta arşivleme ve aşağıda verilen koşullarla kullanıma açma iznini Hacettepe Üniversitesine verdiğimi bildiririm. Bu izinle Üniversiteye verilen kullanım hakları dışındaki tüm fikri mülkiyet haklarım bende kalacak, tezimin tamamının ya da bir bölümünün gelecekteki çalışmalarda (makale, kitap, lisans ve patent vb.) kullanım hakları bana ait olacaktır.

Tezin kendi orijinal çalışmam olduğunu, başkalarının haklarını ihlal etmediğimi ve tezimin tek yetkili sahibi olduğumu beyan ve taahhüt ederim. Tezimde yer alan telif hakkı bulunan ve sahiplerinden yazılı izin alınarak kullanılması zorunlu metinlerin yazılı izin alınarak kullandığımı ve istenildiğinde suretlerini Üniversiteye teslim etmeyi taahhüt ederim.

Yükseköğretim Kurulu tarafından yayınlanan “**Lisansüstü Tezlerin Elektronik Ortamda Toplanması, Düzenlenmesi ve Erişime Açılmasına İlişkin Yönerge**” kapsamında tezimin aşağıda belirtilen koşullar haricince YÖK Ulusal Tez Merkezi / H.Ü. Kütüphaneleri Açık Erişim Sisteminde erişime açılır.

- Enstitü / Fakülte yönetim kurulu kararı ile tezimin erişime açılması mezuniyet tarihimden itibaren 2 yıl ertelenmiştir. ⁽¹⁾
- Enstitü / Fakülte yönetim kurulunun gerekçeli kararı ile tezimin erişime açılması mezuniyet tarihimden itibaren 6 ay ertelenmiştir. ⁽²⁾
- Tezimle ilgili gizlilik kararı verilmiştir. ⁽³⁾

22 /09/2022

Elif Tuğçe
SARCAN BOZKIR

¹“Lisansüstü Tezlerin Elektronik Ortamda Toplanması, Düzenlenmesi ve Erişime Açılmasına İlişkin Yönerge”

(1) Madde 6. 1. Lisansüstü teze ilgili patent başvurusu yapılması veya patent alma sürecinin devam etmesi durumunda, tez **danışmanın** önerisi ve **enstitü anabilim dalının** uygun görüşü üzerine **enstitü** veya **fakülte yönetim kurulu** iki yıl süre ile tezin erişime açılmasının ertelenmesine karar verebilir.

(2) Madde 6. 2. Yeni teknik, materyal ve metotların kullanıldığı, henüz makaleye dönüşmemiş veya patent gibi yöntemlerle korunmamış ve internetten paylaşılması durumunda 3. şahıslara veya kurumlara haksız kazanç imkanı oluşturabilecek bilgi ve bulguları içeren tezler hakkında tez **danışmanın** önerisi ve **enstitü anabilim dalının** uygun görüşü üzerine **enstitü** veya **fakülte yönetim kurulunun** gerekçeli kararı ile altı ay aşmamak üzere tezin erişime açılması engellenebilir.

(3) Madde 7. 1. Ulusal çıkarları veya güvenliği ilgilendiren, emniyet, istihbarat, savunma ve güvenlik, sağlık vb. konulara ilişkin lisansüstü tezlerle ilgili gizlilik kararı, **tezin yapıldığı kurum** tarafından verilir *. Kurum ve kuruluşlarla yapılan işbirliği protokolü çerçevesinde hazırlanan lisansüstü tezlere ilişkin gizlilik kararı ise, **ilgili kurum ve kuruluşun önerisi** ile **enstitü** veya **fakültenin** uygun görüşü üzerine **üniversite yönetim kurulu** tarafından verilir. Gizlilik kararı verilen tezler Yükseköğretim Kuruluna bildirilir.

Madde 7.2. Gizlilik kararı verilen tezler gizlilik süresince enstitü veya fakülte tarafından gizlilik kuralları çerçevesinde muhafaza edilir, gizlilik kararının kaldırılması halinde Tez Otomasyon Sistemine yüklenir

* Tez **danışmanın** önerisi ve **enstitü anabilim dalının** uygun görüşü üzerine **enstitü** veya **fakülte yönetim kurulu** tarafından karar verilir.

ETHICAL DECLARATION

In this thesis study, I declare that all the information and documents have been obtained in the base of the academic rules and all audio-visual and written information and results have been presented according to the rules of scientific ethics. I did not do any distortion in data set. In case of using other works, related studies have been fully cited in accordance with the scientific standards. I also declare that my thesis study is original except cited references. It was produced by myself in consultation with supervisors (Prof. Dr., A. Y. ÖZER and Prof. Dr., N. HARTMAN) and written according to the rules of thesis writing of Guidance Hacettepe University Institute of Health Sciences .

Pharm. Elif Tuğçe SARCAN BOZKIR

APPRECIATION

Endless thanks to,

My supervisor **Prof. Dr. A. Yekta ÖZER** who always helped and guided me with her knowledge and experience. I learned many things from her at every stage of my thesis work, and also helped me to realize my thesis work with UK partnership as my goal, and whom I took as an idol throughout my professional life.

Prof. Neil HARTMAN, who was the advisor of my thesis work in abroad, whom I learned from his knowledge and experience, and I always felt his support throughout my work and social life in the UK,

Prof. Dr. Christopher MARSHALL, who did not hesitate to exhibit his support and help in every problem we encountered during my studies in UK,

Dr. Stephen PAISEY, who taught me everything he knew during my all studies, guided and helped me at every stage of my studies in UK,

Dr. Martin RUTHGARD, who helped me in cell culture, in-vitro and in-vivo studies and did not hesitate to give his kind help during my research,

Staff of the Nuclear Medicine Department of Singleton Hospital/Swansea and Nuclear Medicine Clinical and Preclinical Departments of University Hospital of Wales/Cardiff, whose did not hesitate to give their kind help during my studies,

Prof. Dr. Suna ERDOĞAN, who supported me with her information and opinions,

Prof. Dr. N. Özlem KÜÇÜK, who supported me with her information and opinions,

Dr. Mine SİLİNDİR-GÜNAY, who supported me with her knowledge and opinions,

F. Hoffman-La Roche Company, that provided the monoclonal antibody "Obinutuzumab" used in my thesis,

Cardiff University PETIC, that provided the monoclonal antibody "Tocilizumab" used in my thesis as a control formulation,

TUBITAK, that supported my thesis with the scholarship of "**TUBİTAK 2214-A International Research Fellowship Programme for PhD Students**", during 12 months I have been studied in UK,

My dear **family** and my **husband/collague Pharm. Rıdvan Bozkır** for their endless, heartfelt and valuable support and love throughout the whole hard times of my professional life.

TEŞEKKÜR

Tez çalışmamın her aşamasında bilgi ve deneyiminden yararlandığım, bana yardımcı olan, yol gösteren, tez çalışmamı hayalimde olduğu gibi yurtdışı ile ortak yapmamı sağlayan, meslek hayatım boyunca kendime örnek aldığım danışman hocam Sn. Prof. Dr. A. Yekta ÖZER'e,

Tez çalışmamın yurtdışı danışmanlığını yapan, bilgi ve deneyiminden yararlandığım, güleryüzlü ve anlayışlı tavrıyla Birleşik Krallık'taki çalışma ve sosyal hayatım boyunca desteğini hissettiğim Sn. Prof. Neil HARTMAN'a,

Çalışmalarım esnasında bildiği herşeyi bana öğreten, yol gösteren, çalışmamın her aşamasında yardımcı olan Sn. Dr. Stephen PAISEY'e,

Çalışmalarım esnasında desteğini ve karşılaştığımız her problemde yardımını esirgemeyen Sn. Prof. Dr. Christopher MARSHALL'a,

Hücre kültürü, in-vitro ve in-vivo çalışmalarında yardımını gördüğüm ve çalışmalarımız esnasında yardımlarını esirgemeyen Sn. Dr. Martin RUTHGARD'a,

Çalışmalarım esnasında yardımlarını esirgemeyen Singleton Hospital Nuclear Medicine Departmanı/Swansea ve University Hospital of Wales Nuclear Medicine Clinic and Preclinic Departmanı/Cardiff çalışanlarına,

Değerli bilgi ve görüşlerini esirgemeyen, desteğini ve yardımlarını her zaman hissettiğim Radyofarmasi ABD Başkanı Sn. Prof. Dr. Suna ERDOĞAN'a,

Değerli bilgi ve görüşlerini esirgemeyen, desteğini ve yardımlarını her zaman hissettiğim Radyofarmasi ABD Başkanı Sn. Prof. Dr. Özlem KÜÇÜK'e,

Değerli bilgi ve görüşlerini esirgemeyen, desteğini ve yardımlarını her zaman hissettiğim Sn. Dr. Öğr. Üyesi Sn. Mine SİLİNDİR GÜNAY'a,

Çalışmamızda kullandığımız monoklonal antikor olan "Obinutuzumab"ı sağlayan F. Hoffman- La Roche firmasına,

Çalışmamızda kullandığımız diğer monoklonal antikor olan "Tocilizumab"ı sağlayan University Hospital of Wales PETIC merkezine,

Çalışmalarımı yurtdışı ile ortak sürdürebilmem için 12 aylık bursumu karşılayarak Birleşik Krallık'a gitmemde katkısı olan "TUBITAK 2214-A Yurtdışı Doktora Esnasında Araştırma Bursu" ile çalışmalarımı destekleyen TUBITAK'a,

Hayatta attığım her adımda yanımda olan, özellikle yurtdışındaki çalışmalarım için beni gönülden destekleyen, sevgi ve ilgilerini her daim yanımda hissettiğim canım aileme ve sevgili eşim/meslektaşım Ecz. Rıdvan BOZKIR'a,

Sonsuz teşekkürler.

ABSTRACT

Sarcan Bozkır E. T., Development of Radiopharmaceutical Formulations for Imaging of Non Hodgkin's Lymphoma. Hacettepe University Graduate School of Health Sciences Radiopharmacy Doctoral Programme, Ph.D. Thesis in Radiopharmacy, Ankara, 2022. Non Hodgkin's Lymphoma (NHL) is the most common subtype of lymphoma, which consists of tumour cells originating from B lymphocyte cells. Burkitt's lymphoma is one of the most common subtypes of NHL, and it is one of the most common type, especially in children. Treatment, diagnosis and imaging can be obtained by targeting the CD20 epitope, which is available on the surface of B lymphocytes and shows increased expression. In this study, CD20 specific, new generation humanized-monoclonal antibody "Obinutuzumab" was radiolabelled with ^{89}Zr and formulations were developed. In-vitro and in-vivo studies were carried out with the optimum formulation determined as a result of quality control tests among these developed formulations. Ramos cells (CD20(+)) were used to establish Burkitt's lymphoma in in-vitro and in-vivo studies, while HL60 (CD20(-)) cells were used as the control group. In order to determine the in-vitro activity of ^{89}Zr -Obinutuzumab, immuno-reactivity and binding constant studies were performed. Immuno-reactivity studies were performed on Ramos and HL60 cells using ^{89}Zr -Obinutuzumab and ^{89}Zr -Tocilizumab (control) formulations. Following the data obtained here, binding constant studies of the ^{89}Zr -Obinutuzumab formulation were conducted on Ramos cells. In the light of the data obtained from in-vitro studies, in-vivo studies were started. In-vivo studies were performed on 3 groups of female SCID mice by taking PET/CT images and completing biodistribution studies. The resulting data showed that the labeling efficiency and stability of ^{89}Zr -Obinutuzumab were high. In the light of in-vitro studies, immuno-reactivity (%) and binding constant values were found promising for ^{89}Zr -Obinutuzumab formulation. Although the results obtained from in-vivo studies were not as high as expected, it suggested that the ^{89}Zr -Obinutuzumab formulation is a promising agent for lymphoma and requires further research.

Keywords: monoclonal antibody, zirconium-89, obinutuzumab, radiopharmaceutical, immuno-PET, tocilizumab.

This thesis was supported by Nuclear Medicine Department at Swansea Bay University Health Board and PhD student was supported by a "TUBITAK 2214-A International Fellowship Programme for PhD Students" scholarship throughout 12 months .

ÖZET

Sarcan Bozkır E. T., Non Hodgkin's Lenfoma Görüntülenmesinde Kullanılacak Radyofarmasötik Formülasyonlarının Geliştirilmesi. Hacettepe Üniversitesi, Sağlık Bilimleri Enstitüsü, Radyofarmasi Doktora Programı, Radyofarmasi Doktora Tezi, Ankara, 2022. Non Hodgkin's Lenfoma, B lenfosit hücrelerinden köken alan tümör hücrelerinden oluşan lenfoma türünün en sık karşılaşılan alt türüdür. B lenfositlerinin yüzeyinde bulunan ve artmış ekspresyon gösteren CD20 epitopuna hedefleme yapılarak tedavi, teşhis yapılabilen, görüntü alınabilmektedir. Bu çalışmada CD20'ye spesifik, yeni jenerasyon mAb olan "Obinutuzumab", ⁸⁹Zr ile radyoışaretlenmiştir. Geliştirilen bu formülasyonlar arasından yapılan kalite kontrol testleri sonucu belirlenen optimum formülasyon ile in-vitro ve in-vivo çalışmalar yapılmıştır. Burkitt's lenfomanın, in-vitro ve in-vivo çalışmalarda oluşturulması için Ramos hücreleri (CD20 (+)) ve kontrol grubu için de HL60 (CD20 (-)) hücreleri kullanılmıştır. ⁸⁹Zr-Obinutuzumab'ın in-vitro aktivitesinin belirlenebilmesi için immuno-reaktivite ve bağlanma sabiti çalışmaları yapılmıştır. Immuno-reaktivite çalışmaları için Ramos ve HL60 hücreleri üzerinde ⁸⁹Zr-Obinutuzumab ve ⁸⁹Zr-Tocilizumab formülasyonları kullanılarak karşılaştırılmalı çalışmalar yapılmıştır. Burada elde edilen veriler ardından ⁸⁹Zr-Obinutuzumab formülasyonunun Ramos hücreleri üzerinde bağlanma sabiti çalışmaları yürütülmüştür. In-vitro çalışmalardan elde edilen veriler ışığında in-vivo çalışmalara geçilmiştir. In-vivo çalışmalar 3 grup dışı SCID fareleri üzerinde PET/CT görüntüleri alınarak ve biyodağılım çalışmaları tamamlanarak yapılmıştır. Sonuç olarak elde edilen veriler, ⁸⁹Zr-Obinutuzumab'ın işaretleme veriminin ve stabilitesinin yüksek olduğunu göstermiştir. In-vitro çalışmalar ışığında immuno-reaktivite (%) ve bağlanma sabiti değerleri ⁸⁹Zr-Obinutuzumab formülasyonu için umut verici bulunmuştur. Her ne kadar in-vivo çalışmalardan elde edilen sonuçlar beklendiği kadar yüksek olmasa da ⁸⁹Zr-Obinutuzumab formülasyonunun lenfoma için gelecek vaadedici bir ajan olduğu ve üzerinde daha fazla araştırma yapılmasının gerektiği anlaşılmıştır.

Anahtar Kelimeler: Monoklonal antikor, zirkonyum-89, obinutuzumab, radyofarmasötik, immuno-PET, tocilizumab.

Bu tez, Swansea Bay Üniversitesi Sağlık Kurulu, Nükleer Tıp Departmanı ile; doktora tez öğrencileri için 12 ay süreyle "TUBITAK 2214-A Uluslararası Doktora Sırası Araştırma Bursu" programı tarafından desteklenmiştir

CONTENTS

CONFIRMATION	iii
YAYIMLAMA VE FİKRİ MÜLKİYET HAKLARI BEYANI	iii
ETHICAL DECLARATION	v
APPRECIATION	vi
TEŞEKKÜR	vii
ABSTRACT	viii
ÖZET	viii
CONTENTS	x
SYMBOLS and ABBREVIATIONS	xiii
FIGURES	xvi
TABLES	xviii
1. INTRODUCTION	1
2. GENERAL INFORMATION	5
2.1. Radiopharmacy and Radiopharmaceuticals	5
2.2. Imaging Methods in Nuclear Medicine	6
2.3. Positron Emission Tomography	6
2.3.1. Working Principles	7
2.3.2. Radionuclides in PET Imaging	8
2.4. Immuno-PET	9
2.4.1. Radionuclides in Immuno-PET	10
2.4.2. Zirconium-89	11
2.5. Cancer and Lymphoma	12
2.5.1. Lymphoma Types	13
2.5.2. Diagnosis and Imaging of Lymphoma	14
2.5.3. Immuno-PET Imaging of Lymphoma	15
2.6. Monoclonal Antibodies	15
2.6.1. mAbs Used in Lymphoma	18
2.7. ⁸⁹ Zr Radiolabelled mAbs	19
2.8. ⁸⁹ Zr Radiolabelled mAbs and Non Hodgkin's Lymphoma	21
3. MATERIALS and METHODS	23
3.1. Materials and Equipment	23

3.2.	Characterization Studies on mAbs	24
	3.2.1. ELISA	25
	3.2.2. SDS PAGE	25
3.3.	⁸⁹ Zr Production and Purification	25
3.4.	⁸⁹ Zr Formulation Studies	27
3.5.	⁸⁹ Zr Radiolabelling Process	28
	3.5.1. DFO-p-Bz-NCS -Antibody Conjugation	28
	3.5.2. ⁸⁹ Zr Radiolabelling	31
3.6.	Quality Control Tests	31
	3.6.1. Radiochemical Purity	32
3.7.	Stability	32
3.8.	In-vitro Cell Culture Studies	32
	3.8.1. Immuno-reactivity Studies	33
	3.8.2. Binding Assay Studies	33
3.9.	In-vivo Animal Studies	34
	3.9.1. PET/CT Imaging Studies	35
	3.9.2. Biodistribution Studies	35
3.10.	Statistical Analyzes	36
4.	RESULTS	37
4.1.	Characterization Studies on mAbs	37
	4.1.1. ELISA	37
	4.1.2. SDS-PAGE	37
4.2.	⁸⁹ Zr Production and Purification	37
4.3.	⁸⁹ Zr Formulation Studies	38
4.4.	⁸⁹ Zr Radiolabelling Process	38
	4.4.1. DFO-p-Bz-NCS -Antibody Conjugation	38
	4.4.2. ⁸⁹ Zr Radiolabelling	42
4.5.	Quality Control Results	42
	4.5.1. Radiochemical Purity	42
4.6.	Stability	49
4.7.	In-vitro Cell Culture Study Results	53
	4.7.1. Immuno-reactivity Studies	53

4.7.2. Binding Assay Studies	56
4.8. In-Vivo Animal Study Results	58
4.8.1. PET/CT Imaging Studies	58
4.8.2. Biodistribution Studies	61
5. DISCUSSION	65
5.1. ⁸⁹ Zr Production and Purification	66
5.2. ⁸⁹ Zr Formulation Studies	67
5.3. ⁸⁹ Zr Radiolabelling Process	67
5.4. Quality Control Tests	68
5.4.1. Radiochemical Purity	68
5.5. Stability Studies	71
5.6. In-vitro Cell Culture Studies	72
5.6.1. Immuno-reactivity Studies	72
5.6.2. Binding Assay	74
5.7. In-vivo Animal Studies	75
5.7.1. PET/CT Imaging	75
5.7.2. Biodistribution Studies	76
6. CONCLUSION	78
7. REFERENCES	79
8. SUPPLEMENTS	
Supplement 1. Certificates for animal studies.	
Supplement 2. Ethics Committee Approval/ Project Licence	
Supplement 3: Dissertation originality report, Turnitin	
Supplement 4: Turnitin Digital Receipt	
9. CURRICULUM VITAE	

SYMBOLS and ABBREVIATIONS

Abs	Antibodies
AHA	AcetoHydroxamic Acid
B	Competitor
Bo	Non-Competitor
Br	Bromide
Bsg	Bstrongomab
C	Carbon
CPS	Cound per seconds
Cu	Copper
DFO	Desferrioxamine
DFO-p-Bz-NCS	p-isothiocyanotobenxyl-desferrioxamine
DMSO	Dimethylsulfoxide
DOTA	1,4,7,10-Tetraazocyclododecane
DTPA	DiethyleneTriamine PentaAcetate
EC	Electron Capture
EC50	Effective Concentration
ELISA	Enzyme Linked Immunosorbent Assay
EMA	European Medicines Agency
F	Fluorine
FBS	Fetal Bovine Serum
Fc	Fragment Crystallizable
FDA	Food and Drug Administration
FDG	Fluoro Deoxy Glucose
Ga	Gallium
HCl	HydroChloric Acid
HEPES	N-2-HydroxyEthylPiperazine-N-2-EthaneSulfonic Acid
HL	Hodgkin's Lymphoma
HL 60 cells	Human Leukemia 60 cells
HOPO	2-HydroxyPyridine-N-oxide

HPLC	High Pressure Liquid Chromatography
HRP	Horse Radish Peroxide
I	Iodine
ID	Intensity Dose
Ig	Immunoglobulin
In	Indium
i.v.	Intravenous
kBq	Kilo Becquerel
Kd	Dissociation Constant
keV	Kiloelectron Volt
mAb	Monoclonal Antibody
MBq	Mega Becquerel
Mi	Million
N	Nitrogen
NHL	Non Hodgkin's Lymphoma
O	Oxygen
Obi	Obinutuzumab
PBS	Phosphate Buffered Saline
PET	Positron Emission Tomography
PET/CT	Positron Emission Tomography/ Computed Tomography
RHPLC	Radio High Pressure Liquid Chromatography
ROI	Region of Interest
RPMI 1640	Roswell Park Medium Institute 1640
RT	Room Temperature
RTLC	Radio Thin Layer Chromatography
SCID	Severe Combined Immuno Deficient Mice
SD	Standart Deviation
SDS-PAGE	Sodium Dedocyl Sulphate Polyacrylamide Gel Electrophoresis
SE	Standart Error
SPECT	Single Photon Emission Computed Tomography

Sq	Squalene
Suc-N-DFO	Succinylated-N-DFO
Tl	Thallium
TMB	Tetramethyl Benzidine
Toc	Tocilizumab
UHW	University Hospital of Wales
UK	United Kingdom
WHO	World Health Organization
Y	Yttrium
Zr	Zirconium

FIGURES

Figure	Page
2.1. SPECT camera.	6
2.2. PET camera.	7
2.3. PET imaging working principle.	8
2.4. Decay schema and energy of ^{89}Zr and daughter radionuclide of ^{89}Zr .	11
2.5. Lymphoma types and classification schema.	14
2.6. mAb types.	16
2.7. Different types of conjugated mAbs.	18
2.8. Anti CD20 mAbs (Rituximab, Tositumomab, Obinutuzumab and Ofatumumab) activation mechanism.	19
2.9. Schema of ^{89}Zr radiolabelling of mAb.	19
2.10. DFO schematic representation.	20
3.1. The cassette system which is used ^{89}Zr purification in hot cell.	27
3.2. Preparation Flow-chart for DFO-p-Bz-NCS and mAbs (Obi and Toc) conjugation.	30
3.3. DFO-p-Bz-NCS and mAb conjugation.	30
3.4. ^{89}Zr radiolabelling of mAb schema.	31
3.5. Immuno-reactivity study schema.	33
4.1. Free ^{89}Zr RTLC chromatogram.	43
4.2. ^{89}Zr -Obi RTLC chromatogram.	44
4.3. ^{89}Zr -Toc RTLC chromatogram.	45
4.4. RHPLC chromatograms of formulations.	47
4.5. Stability results in saline (0.9% NaCl) after 96 h incubation at 37°C (n:3).	49
4.6. Stability results of ^{89}Zr -Obi incubated at 37°C in saline (0.9% NaCl) between 0-96 hours.	50
4.7. RHPLC chromatograms of ^{89}Zr -Obi stability tests.	51
4.8. Immuno-reactivity determination of ^{89}Zr -Obi with Ramos cells (n:3).	55
4.9. Immuno-reactivity determination of ^{89}Zr -Toc with Ramos cells (n:3)	55
4.10. Immuno-reactivity determination of ^{89}Zr -Obi with HL 60 cells (n:3).	56
4.11. Binding activity of ^{89}Zr -Obi with Ramos cells	57
4.12. Nano PET/CT images of Ramos cell injected mice six days after ^{89}Zr -Obi injection	59

4.13.	Nano PET/CT images of HL 60 cell injected mice six days after ^{89}Zr -Obi injection	59
4.14.	Nano PET/CT images of control mice six days after ^{89}Zr -Obi injection	60
4.15.	Percentage of ID/g value for each organ of each group of female SCID mice.	60
4.16.	Biodistribution results of ^{89}Zr -Obi in different animal models (HL60 cells, Ramos cells and control groups).	64

TABLES

Table	Page
2.1. PET imaging advantages and disadvantages .	7
2.2. Conventional and new radionuclides used in PET.	9
2.3. Radionuclides used in immuno-PET.	10
2.4. Advantages and disadvantages of ⁸⁹ Zr.	12
2.5. Several mAbs approved by FDA initially.	17
2.6. Different derivatives of DFO used in ⁸⁹ Zr-radiolabelling.	20
2.7. ⁸⁹ Zr-radiolabelled mAbs in preclinical and clinical stages.	21
3.1. Chemicals.	23
3.2. Equipments and softwares.	24
3.3. Molar ratio and composition of prepared formulations.	28
3.4. Obi molarity calculation.	34
3.5. Obi concentration calculation.	34
3.6. Summary of the ⁸⁹ Zr-Obi injections into animals with different cancer models.	36
4.1. Reaction vials and their activity/time (MBq).	38
4.2. ⁸⁹ Zr activity before and after neutralization.	38
4.3. Formulations of mAbs and total volume measurements before and after pH adjustment and solvent exchange.	39
4.4. Obi and Toc amounts for pH adjustment and DFO-p-Bz-NCS conjugation.	40
4.5. ⁸⁹ Zr and mAb amounts for radiolabelling.	42
4.6. ROI (%) values of each formulations.	46
4.7. Stability test results of ⁸⁹ Zr-Obi formulation by RHPLC.	49
4.8. Immuno-reactivity results of ⁸⁹ Zr-Obi and ⁸⁹ Zr-Toc in Ramos and HL 60 cells (mi: million).	54
4.9. Immuno-reactivity values of studied formulations.	54
4.10. Obi concentration and competitor values.	57
4.11. Binding assay results of ⁸⁹ Zr-Obi with Ramos cells.	57
4.12. Biodistribution results of ⁸⁹ Zr-Obi injected mice in different animal groups.	62

1. INTRODUCTION

Lymphoma is a type of cancer in which tumour cells originate from lymphocyte cells and classified depending on the cell type that can be B or T lymphocytes (1). Non-Hodgkin's Lymphoma (NHL) is the most common subtype of B cell lymphoma. The increased CD20 expression on the surface of B lymphocytes is the most commonly used target epitope in drugs developed for diagnosis and therapy. This transmembrane protein (CD20) has 33-35 kiloDalton (kDa) in size and it expresses on the normal and malignant B lymphocytes. CD20 is also used for the diagnosis and therapy as a targeting agent and/or therapy of NHL and other autoimmune diseases (2). The high expression level which is less than or equal to 95% of transmembrane protein present on the cell surface gives them high recognition ability for monoclonal antibodies (mAbs) while allowing the connection of the mechanism of effector dependent on Fragment Crystallizable (Fc) (3).

Antibodies (Abs)/immunoglobulins (Igs) are molecules which are synthesized by lymphoid and plasma cells and consequently they react specifically to antigenic epitopes as a result of antigenic stimulations in an organism. mAbs production have started in 1975 when hybridoma technology was discovered by Kohler and Milstein (4, 5). Murine, chimeric, humanized and human mAbs have been produced with developing technology (respectively) and the immune response has decreased from murine to human mAbs (6).

The use of mAbs and mAb-linked products have gradually been increasing since the first mAb was approved in 1986. Besides their use for therapeutic purposes, they can also be benefited for targeting due to their specificity for the target (7). Although the purpose of these mAbs for cancer is primarily therapeutic, it can also be used for the diagnosis by Positron Emission Tomography (PET), Single Photon Emission Computed Tomography (SPECT) and optic imaging methods (8).

The use of radionuclides in medicine is mainly based on the concept of "Tracer Principle" and "Magic Bullet". "Magic Bullet" concept which was developed by Paul Ehrlich emphasizes how to use target molecules for the transport of the antibodies and toxins to the cancer cells selectively (9, 10).

Radiopharmaceuticals, used in PET, SPECT imaging, consist of two parts which are pharmaceutical and radionuclidic parts. Briefly, SPECT system allows the

detector to rotate 180°-360 ° around the patient and receives images with gamma cameras in various positions by using gamma-emitting radionuclides. PET is the system that transform gamma-rays which are emitted to two opposite directions with 511 kiloelectron volt (keV) energies from positron-emitting radionuclides to the images and determines the distribution and provides the cross-sectional images. 11-Carbon (^{11}C), 13-Nitrogen (^{13}N), 15-Oxygen (^{15}O), and 18-Fluorine (^{18}F) are the most popular and conventional radionuclides for PET while 68-Gallium (^{68}Ga), 64-Copper (^{64}Cu), 89-Zirconium (^{89}Zr) are the new radiometals for PET imaging. Also, these radiometals are the most popular radionuclides for immuno-PET imaging (11, 12).

Immuno-PET is the method that combination of bio-molecules (widely mAbs) and radionuclides having appropriate half-lives to mAbs. It is currently quite popular method for diagnosis, imaging due to high precision and resolution of PET cameras and specificity of mAbs (12).

The use of radiolabelled mAbs in NHL diagnosis and therapy started with the use of 90-Yttrium (^{90}Y) labelled with Ibritumomab Tiuxetan. Later, images and therapy were obtained by 131-Iodine (^{131}I) labelled Tositumomab (13, 14). Until now, the 20 mAbs have been labelled with various radionuclides, and most of them are under the early clinical trials (15). Radionuclide choice is a crucial decision for Immuno-PET imaging. In recent years, ^{89}Zr is one of the most popular radionuclides in mAb radiolabelling and researchers are interested in (10).

^{89}Zr ; is the radionuclide which has a half-life of 78.42 h, and nowadays it is preferred frequently for tumour diagnosis with mAbs. Although having low positron energy, a long half-life and high radiation dose, it provides long-term monitoring of antibody and nanoparticles with slow clearance. ^{89}Zr , which is a product of cyclotron, is produced in high amounts and 99% purity. Furthermore, their 395.9 keV positron energy provides high resolution (16).

Obinutuzumab (Gazyva/Roche); is a humanized Type 2 mAb which is approved by FDA on 26 February 2016 for lymphoma treatment. Obinutuzumab (Obi) has been found more effective than rituximab, and also have more anti-tumour activity and cytotoxicity than rituximab (17).

Yoon et al. (2018) studied different kinds of anti-CD20 mAbs which are ofatumumab, Obi, rituximab, tositumomab and human IgG (as a control) and they

compared the data of biodistribution and PET images after radiolabelling with ^{89}Zr (17). Biodistribution studies and micro-PET images were obtained at 1, 3 and 7th days. As a conclusion, ^{89}Zr -labelled ofatumumab and Obi were found to be more specific to tumour than rituximab and tositumomab. Obi (humanized) and ofatumumab (fully human) are next-generation mAbs which are similar to tositumomab and rituximab, respectively (17-19).

Zettlitz et al. (2017), compared the ^{89}Zr and ^{124}I radiolabelling CD20 specific mAb fragments based on rituximab and Obi for immuno-PET imaging of a murine lymphoma model. As a result, ^{89}Zr labelled Ab fragments showed slightly higher tumour activity and retention (Tumour/Blood) at 24 hours. ^{89}Zr labelled antibody fragments obtained better images for small structure while ^{124}I antibody fragments showed higher image contrast due to lower background. Also, Obi fragments outperform over rituximab fragments when ^{124}I -labeled Obi and rituximab fragments were compared (20).

Tocilizumab (RoActemra/Roche); is a humanized mAb which is firstly approved in Japan in 2005 as an orphan drug. In 2009 Tocilizumab (Toc) was approved for rheumatoid arthritis, systemic juvenile idiopathic arthritis treatment in Europe (21). In this study, Toc was used as a control formulation.

In the base of these information mentioned above, Obi was radiolabelled with ^{89}Zr in different ratio of (mAb:DFO: ^{89}Zr) and quality control tests were performed in this study. After the optimum formulation was determined, formulation and quality control tests were followed by in-vitro and in-vivo studies. Ramos cells were used as a main cell line which is CD20 (+) cells that forms Burkitt's Lymphoma which is a subtype of NHL while HL60 cells were used as control cell line which are CD20 (-). ^{89}Zr radiolabelled Obi was evaluated in Ramos and HL60 cells and their immuno-reactivity and binding constants were compared. ^{89}Zr -Toc was also prepared to compare the immuno-reactivity with ^{89}Zr -Obi in Ramos cells. As the last stage, in-vivo studies were performed on 15 female Severe Combined Immuno Deficient (SCID) mice. 15 mice were divided into three groups as Ramos cells injected, HL60 cells injected and control groups. PET/CT images were obtained in all groups and after that, biodistribution studies were performed.

This study is a collaborated thesis study between Turkey and the United Kingdom (UK). It has great importance (for the studies to be conducted Nuclear Medicine practice in Turkey in the near future) to learn radiochemistry and radiolabelling of mAbs with ^{89}Zr radionuclide from whom having valuable expertise scientifically and clinically. In addition, since there are very limited studies in the literature with the antibody Obi labelled with ^{89}Zr , our study still add a novelty to the literature. Furthermore, stability, immuno-reactivity and binding assay studies (in-vitro) on the ^{89}Zr labelled Obi formulations and their in-vivo observations are the innovative sides brought to the literature.

2. GENERAL INFORMATION

2.1. Radiopharmacy and Radiopharmaceuticals

Radiopharmaceuticals are the radioactive drugs used for diagnosis and treatment that do not cause a pharmacological response in the patient. The radiopharmaceuticals consist of two parts, the radionuclidic and the pharmaceutical part.

Pharmaceutical part; generally is chosen according to the preferential localization in the organs and physiological function of the organs (11). This part is the target agent that enables the radiopharmaceutical to reach the targeted organ and tissue. This molecule should have the appropriate half-life and properties with the radionuclide to be used in the labelling. It is expected that the molecular structure will not decompose after labelling and have a suitable half-life (11).

Radionuclidic part; is the atom whose nucleus undergoes spontaneous decay and emits one or more ionizing radiation (11). In this part, radionuclidic decomposition provides the detection (diagnose, imaging) and/or therapy by irradiating in the organ or region where the pharmaceutical part is localized (11).

Radiopharmaceuticals are used in nuclear medicine for diagnosis (95%) and for (5%) treatment. Radiopharmaceuticals administered to the body for diagnostic purposes; It provides obtaining physiological images of the relevant organ and system and is used in the evaluation of the functions of many organs and tissues in this way (11).

The use of radionuclides in medicine is mainly based on the concept of “tracer principle” and "magic bullet". “Magic Bullet” concept developed by Paul Ehrlich emphasizes how to use target molecules for the transport of the antibodies and toxins to the cancer cells selectively (9). Nowadays, besides the gamma cameras, SPECT and PET; hybrid systems including SPECT/Computed Tomography (SPECT/CT), PET/CT as dual imaging systems are being used for diagnostic purposes in Nuclear Medicine applications (9).

2.2. Imaging Methods in Nuclear Medicine

Imaging methods used in nuclear medicine is intrinsically a technique showing the body's biochemistry as a result of the gamma rays emitted by the applied radiopharmaceuticals by the scanners (Gamma camera, SPECT, PET) by detecting and processing them. Gamma photons emitted in one direction from radiopharmaceuticals administered to the body are detected by SPECT detectors and processed in the computer unit, based on the principle of forming a cross-sectional image (22). The agents radiolabelled by gamma emitting radionuclides need to use in SPECT, which are detected by gamma-camera or SPECT instruments (Figure 2.1).

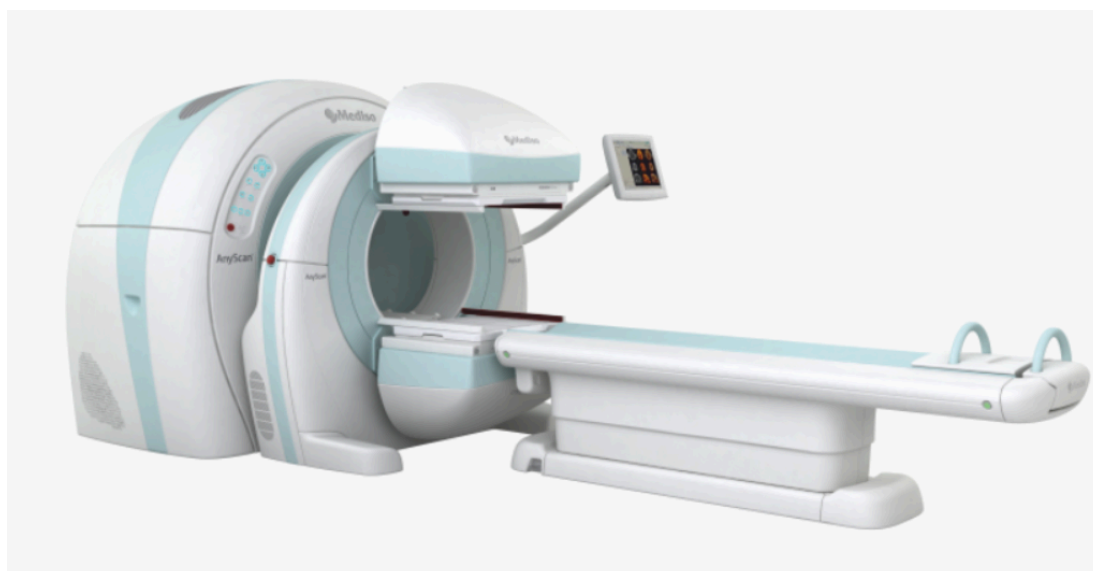


Figure 2.1. SPECT camera.

SPECT have been used clinically from early 1970s. SPECT is a system that allows the detector to rotate 180° - 360° around the patient and receives images with gamma cameras in various positions. SPECT images are taken by using gamma-emitting radionuclides. The low resolution of SPECT cameras and lack of anatomical detail in SPECT images have increased the tendency to use PET cameras (12).

2.3. Positron Emission Tomography

PET is the most common non-invasive imaging technique in nuclear medicine, based on the radiopharmaceuticals that are labelled with positron emitting radionuclides such as ^{18}F , ^{13}N , ^{15}O . These are traditional PET radionuclides and ^{124}I ,

^{68}Ga , ^{89}Zr , ^{64}Cu are recent and under investigation PET radionuclides (9, 23). The PET camera is shown in Figure 2.2.



Figure 2.2. PET camera.

PET imaging have some advantages compared to the other imaging techniques, especially, to SPECT (Table 2.1). PET has better specificity and sensitivity, and also it shows higher resolution and contrast than SPECT (24, 25).

Table 2.1. PET imaging advantages and disadvantages (26).

Advantages	Disadvantages
No collimator required	Most of the radionuclides are produced from cyclotron
Biologically interesting radionuclides are used : ^{11}C , ^{15}O , ^{13}N	Cyclotron cost
Radiopharmaceutical amount can be measured in a region of the body	High cost of radiochemistry and imaging
Spatial resolution	About 5 mm

2.3.1. Working Principles

Positron emitting radionuclides, such as ^{18}F , ^{13}N , ^{15}O , ^{124}I , ^{68}Ga , ^{89}Zr , ^{64}Cu etc., are used in PET imaging and those positrons from the radionuclides travel and are

rapidly annihilated with an electron. After that, two 511 keV gamma rays via the travel indirectly to the opposite positions (180 °) (23) (Figure 2.3).

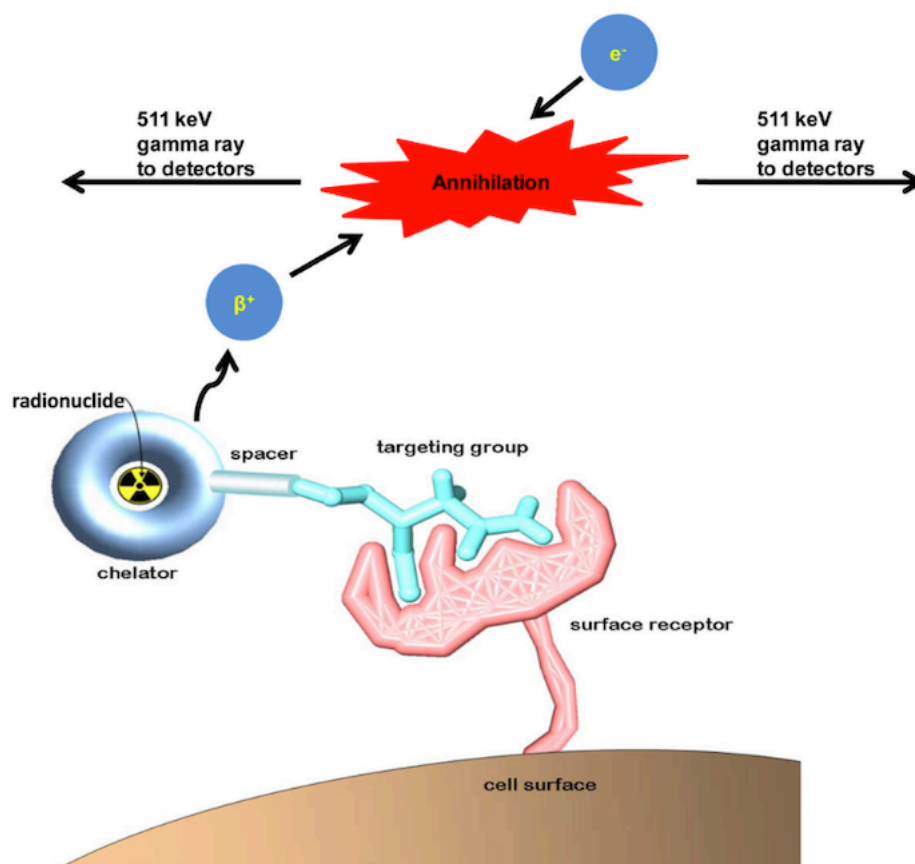


Figure 2.3. PET imaging working principle (23).

2.3.2. Radionuclides in PET Imaging

PET imaging radiopharmaceuticals are generally based on small radionuclides with short half-lives (27). These are ^{18}F , ^{13}N , ^{15}O , ^{11}C called as conventional radionuclides (Table 2.2), most of them in clinical and preclinical stage (28) and some of them are registered by pharmacopoeias. In addition to conventional radionuclides, radiometals (^{89}Zr , ^{64}Cu) and also other radionuclides (^{76}Br , ^{68}Ga) show increasing popularity and existence in preclinical and clinical stage (Table 2.2).

Table 2.2. Conventional and new radionuclides used in PET (29).

Radionuclide	Half-life
¹¹ C	20.4 mins
¹³ N	9.96 mins
¹⁵ O	2.03 mins
¹⁸ F	109.8 mins
⁶⁸ Ga	68 mins
⁶⁴ Cu	12.8 hs
¹²⁴ I	4.2 days
¹¹¹ In	2.8 days
⁸⁹ Zr	78.4 mins
⁷⁶ Br	16.2 hs
⁸² Rb	1.273 mins

2.4. Immuno-PET

Immuno-imaging was developed in early 1990s (30). Immuno-PET is based on the detection of bioactive molecules labelled with positron emitting radionuclides. It is like PET imaging agents but, with the difference that the pharmaceutical part consists of mAbs, mAb fragments or proteins (31). Especially, combination of mAbs and PET radionuclides is attractive formulations/radiopharmaceuticals for immuno-PET imaging because it provides high sensitivity and resolution (12). On the one hand, positron-emitting radionuclides used for immuno-PET show an appropriate emission for optimum resolution and quantitative verification. On the other hand, they can easily bind to mAbs with high efficiency as well. As mAbs can circulate (in the body) over a long time, they can be labelled and monitored via radionuclides with a long half-life (12).

The positron of radionuclides travel a few millimeters depending on the energy and density of radionuclides. Afterwards, annihilation process is occurred with electron and positron encounters and 2 photons with 511 keV are emitted in opposite directions (12).

Immuno-PET provides better understanding of diseases due to several advantages of combination of mAbs and radionuclides (10). Various positron emission radionuclides are still under investigation for immuno-PET while some of the

radionuclides with long half-life are getting popular for immuno-PET, such as ^{64}Cu , ^{89}Zr , ^{124}I , ^{86}Y , ^{76}Br (12) (Table 2.3.).

Table 2.3. Radionuclides used in immuno-PET (12).

Radionuclide	Production	Half-life (min)	Energy (β^+)	
			(keV)	(%)
^{89}Zr	$^{89}\text{Y}(\text{p},\text{n})$	78.4	897	22.7
^{64}Cu	$^{64}\text{Ni}(\text{d},2\text{n})$	12.7	653	17.4
	$^{64}\text{Ni}(\text{p},\text{n})$			
^{86}Y	$^{86}\text{Sr}(\text{p},\text{n})$	14.7	1,221	11.9
^{76}Br	$^{75}\text{As}(3\text{He},2\text{n})$	16.2	871	6.3
	$^{76}\text{Se}(\text{p},\text{n})$		990	5.2
^{124}I	$^{124}\text{Te}(\text{p},\text{n})$	100.3	1,535	11.8
	$^{124}\text{Te}(\text{d},2\text{n})$		2,138	10.9
	$^{125}\text{Te}(\text{p},2\text{n})$			

2.4.1. Radionuclides in Immuno-PET

The considered radionuclides for immuno-PET should match with several aspects: The duration for labelling and transportation, the methods for stable coupling, image quality and quantification with bioactive molecules (31). Positron-emitting radionuclides be used for immuno-PET show an appropriate emission for optimum resolution and quantitative verification, while they should easily be bound to mAbs with high efficiency as well. As mAbs can circulate (in the body) over a long time, they can be labelled and monitorized via radionuclides with a long half-life. Recently, the most commonly used positron-emitting radionuclides for this purpose are ^{89}Zr , ^{64}Cu , ^{124}I radionuclides (12).

The main limitation for immuno-PET is the half-life of the most of the PET radionuclides used in clinics. Their half-lives are shorter than mAbs' biological half-lives. In this purpose, limited radionuclides can be used in immuno-PET. These are: ^{89}Zr , ^{64}Cu , ^{124}I etc. Other radionuclides such as ^{68}Ga , ^{18}F etc. with shorter half-lives can only be used with mAb's fragment or other bioactive molecules which have shorter

biological half-lives (32). Among them, ^{89}Zr shows increasing popularity in labelling to mAbs, recently (15).

^{89}Zr is an attractive radionuclide besides, it is a long half-life positron emitter. It is under investigation for decades, and several preclinical and clinical studies on ^{89}Zr -mAbs such as ^{89}Zr -cetuximab (33); ^{89}Zr -ibritumomab tiuxaten (34); ^{89}Zr -rituximab (35); ^{89}Zr -trastuzumab (36); ^{89}Zr -J591; ^{89}Zr -c-mAb U36 (37) are ongoing.

2.4.2. Zirconium-89

^{89}Zr is a transition radiometal and it decays to ^{89}Y by 23% positron emission and 77% electron capture (EC) (Figure 2.4). It has a long physical half-life of 3.3 days, allowing its use as an immuno-PET radionuclide especially for labelling of mAbs and similar molecules with a long biological half-life (38). It is produced by cyclotron. The first study on the ^{89}Zr radiolabelled mAb was carried out in 1986 with the ^{89}Zr produced by $^{89}\text{Y}(p,n) \rightarrow ^{89}\text{Zr}$ reaction (19).

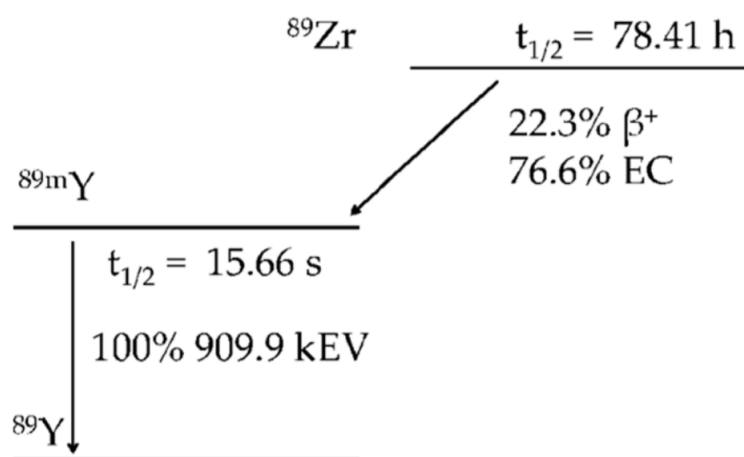


Figure 2.4. Decay schema and energy of ^{89}Zr and daughter radionuclide of ^{89}Zr (39).

^{89}Zr is produced by several reactions using a cyclotron. $^{89}\text{Y}(p,n) \rightarrow ^{89}\text{Zr}$; $^{89}\text{Y}(d,2n) \rightarrow ^{89}\text{Zr}$ reactions can be used in ^{89}Zr production, however the most common reaction is $^{89}\text{Y}(d,2n) \rightarrow ^{89}\text{Zr}$ (32).

^{89}Zr has many advantages for radiolabelling of mAbs and its long biological half-life matches with mAbs' half-lives. In addition, ^{89}Zr also shows high sensitivity

and long resolution in PET. However, it has also some disadvantages such as high gamma energy and limited availability (Table 2.4) (12, 40).

While ^{89}Zr is getting more attention as a research field; purification methods after its production and the properties as bifunctional chelating agents for radiolabelling are under investigation with increasing interest (39). In this field, the most important thing is the stability of ^{89}Zr radiolabelled molecules, and of course, the chelating agent. Among many chelating agents used in other radiolabelling processes with other radionuclides, ^{89}Zr has some differences due to its structure. ^{89}Zr shows stability at +4 oxidation state. If all the studies about the chelating agents are taken into consideration for ^{89}Zr radiolabelling, p-isothiocyanatobenzyl-desferrioxamine (DFO-p-Bz-NCS) is the most popular and stable bifunctional agent. The other advantage of this agent is the availability on the market. It provides high stability and efficiency in addition to the easy labelling methods and commercial availability (41, 42).

Table 2.4. Advantages and disadvantages of ^{89}Zr (10).

Advantages	Disadvantages
Long half-life (3.3 days) (which is suitable with molecules with long biological half-life)	Limited availability
High sensitivity	High gamma energy
High resolution	-

2.5. Cancer and Lymphoma

Cancer is a life-threatening disease characterized by abnormal and uncontrolled cell growth. Cancer has a great potential to metastases in the body via the lymph or bloodstream to many organs such as the breast, liver, brain, bone etc. The ranks of cancer causing death is an important health problem all around the world. World Health Organization (WHO), mentioned that in 2019, cancer ranks 2nd in the list of causes of death before the age of 70 in the world. The cancer incidence and mortality is growing day by day. 19.3 million new cases and 10 million death caused by cancer, were estimated by GLOBOCAN 2020 (43).

Lymphoma is a type of cancer in which tumour cells originate from lymphocyte cells and are classified depending on which of the B and T lymphocytes are affected (1). Stashenko et al. firstly identified CD20 in 1980 as a B-cell marker. CD20 antigen is expressed on most of the B-cell lymphomas (3). CD20, the transmembrane protein, is 33-35 kDa in size and is expressed in normal and malignant B lymphocytes. This transmembrane protein is used for targeting and therapeutic purposes in diagnosis and/or treatment of NHL and many autoimmune diseases (2). The high expression level and presence of this membrane protein on the cell surface provides a high level of recognition by mAbs while also allowing it to bind to Fc-dependent effector mechanisms (3, 44).

NHL presented in 544,000 new cases and 260,000 deaths in 2020. Many countries have showed increasing incidence rates between 1980-1990, however it does not increase in these days (43). According to the UK Cancer Research Institute, 14,100 new NHL patients are diagnosed every year in the UK. Burkitt's lymphoma, the NHL type in children, is the most common type of cancer in children in the UK (45). According to the Turkey cancer statistics in 2016, NHL is the 6th most common cancer type in Turkey (46).

2.5.1. Lymphoma Types

Lymphomas are mainly categorized in two groups: NHL and Hodgkin's Lymphoma (HL) and all of these originate from two types of white blood cells which are B cells and T cells (47) (Figure 2.5).

HL is the uncommon type of lymphoma. In this type, large abnormal tumour cells which called Hodgkin Reed Sternberg cells, are the noticeable cells to diagnose HL. Basically, HL consists of 4 main subtypes; nodular sclerosis, mixed cellularity, lymphocyte-rich and lymphocyte-depleted HL (47).

On the other hand, NHL is the most common type of lymphoma. All the subtypes of NHL are divided in B and T cell lymphoma. However, B cell types are more common and it is about the 80% of all NHL events (47).

Burkitt's lymphoma is one of the three most common NHL subtypes in children (48). Burkitt's Lymphoma, known as a childhood NHL, accounts for 40% of lymphoma in children. Burkitt's lymphoma is a type of cancer that progresses rapidly,

and therefore early diagnosis is important (49). Pediatric lymphomas are more aggressive and fast-growing than lymphomas in adults (47, 50).

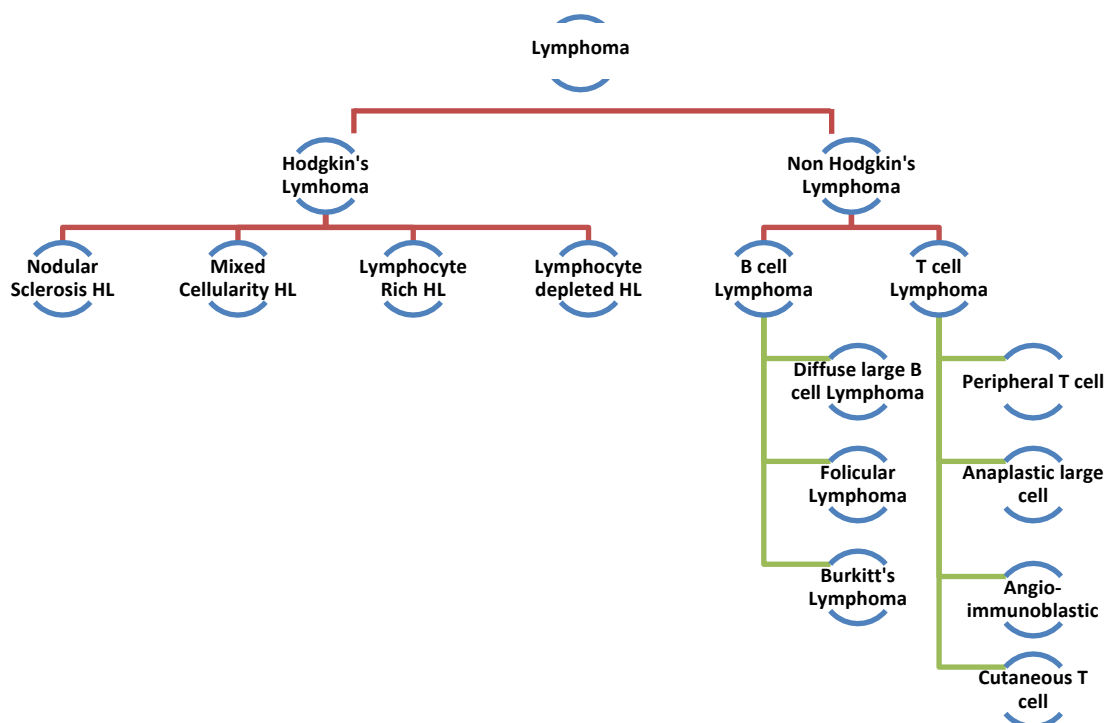


Figure 2.5. Lymphoma types and classification schema.

2.5.2. Diagnosis and Imaging of Lymphoma

^{67}Ga is one of the radionuclide which can be used in imaging of lymphoma. ^{67}Ga scintigraphy is based on the ^{67}Ga accumulation in the lymphoma cells by binding to transferrin receptors. This radionuclide improves the specificity for the diagnosis of lymphoma. However, scans with ^{67}Ga taken 7 to 14 days and the high doses of ^{67}Ga radioactivity are the limitations of ^{67}Ga diagnosis and imaging of lymphoma. Also, PET shows higher specificity and sensitivity in NHL and HL compared with ^{67}Ga scanning (51, 52).

Thallium-201 (^{201}Tl) is another radionuclide used in lymphoma for detecting the active tumour rather than thymic rebound over the decade, although it has been

mainly used in myocardial perfusion. However, it was found that ^{67}Ga shows better sensitivity than ^{201}Tl (53, 54).

^{18}F - Fluorodeoxyglucose (FDG) is one of the most effective radiopharmaceuticals to diagnose the lymphoma as well as other cancer types. This metabolic imaging technique target the glucose metabolism and affect the transferring radiolabelled FDG into the cells (53, 55).

^{11}C -methionine, ^{11}C -choline, ^{18}F -fluorocholine are the other radiopharmaceuticals considered for lymphoma diagnosis and imaging, however, they have not been used due to their widespread use and advantages of the ^{18}F -FDG PET (53).

2.5.3. Immuno-PET Imaging of Lymphoma

Most of the radiopharmaceuticals for imaging of lymphoma are focused on CD20 surface antigen. These radiopharmaceuticals consist of radiometals and mAbs which are used as targeting part. Rituximab, cetuximab, ibritumomab tiuxetan, tositumomab etc. have been radiolabelled with several radionuclides for decades to use as CD20 over expressed lymphoma imaging agents. It is followed by other mAbs for the lymphoma such as CD30, CD38 overexpressed types etc. (56).

2.6. Monoclonal Antibodies

mAb production studies started due to the hybridoma technology discovered by Kohler and Milstein in 1975. According to this method, hybridomas formed by combining B cells of mice immunized with antigen and myeloma cancer cells are obtained (5).

mAbs have an average molecular weight of 150 kDa, contain 2 heavy and 2 light chains, and these two chains stay together with disulfide bonds (44, 57). In every chain, there are fixed and variable regions (57). The Fab part (the part containing the heavy and light chain) is the region where the antigen binds, while the Fc part is the fixed fragment and the region where the receptors bind (Figure 2.6) (58).

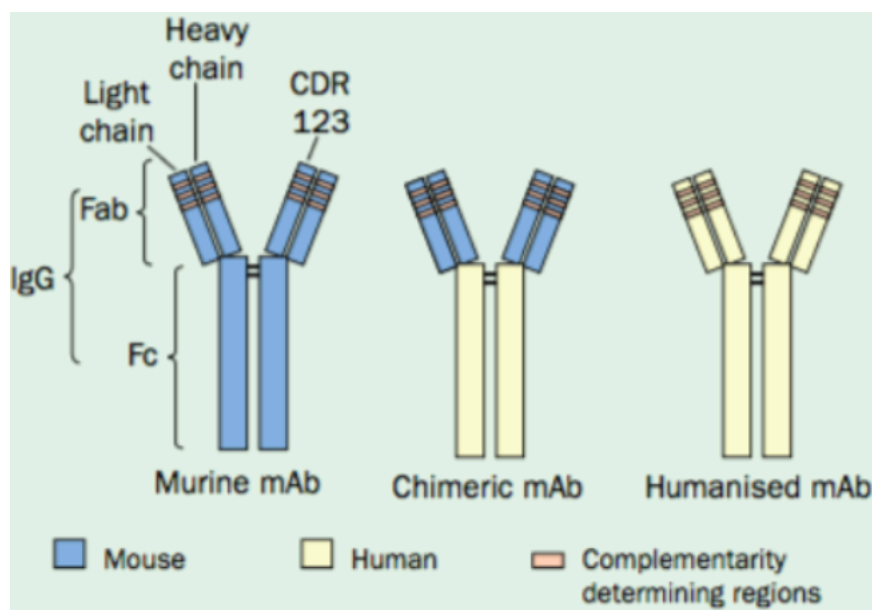


Figure 2.6. mAb types (59).

Their clinical use has been limited due to the high immunogenicity of the first generation mAbs related to their murine origin (6). Basically, three problems have been encountered with murine mAbs. These are; 1) Interaction of the mouse Fc part with the human Fc part; 2) Short half-life in serum; 3) Development of human anti-mouse antibodies (59).

Chimeric, humanized and fully human mAbs have been produced with developing technologies and as a result, immune response has decreased as can be seen in Figure 2.6 (6).

The first chimeric antibodies were produced in 1980s and one of the chimeric antibody, rituximab, was approved by Food and Drug Administration (FDA) for the treatment purpose of B-cell originated NHL in 1997 (13). After that, the usage areas of mAb and mAb-related products increased day by day. In addition to their use for the treatment, they can also be used for targeting purposes due to their target specificity (Table 2.5) (7).

Currently, there are around 300 mAbs in clinical research for more than 200 cancer types, 34 of which have been approved by the FDA and the European Medicines Agency (EMA) (44, 60). Until now, around 20 mAbs have been labelled with various radionuclides, and most of them are under the early clinical trials (15).

Table 2.5. Several mAbs approved by FDA initially (13, 61).

mAb	Type	Target	FDA Approval Year
Rituximab	Chimeric	CD 20	1997
Trastuzumab	Humanized	HER2	1998
Alemtuzumab	Humanized	CD 52	2001
Ibritumomab Tiuxetan	Murine	CD 20	2002
Tositumomab	Murine	CD20	2003
Bevacizumab	Humanized	VEGF	2004
Cetuximab	Chimeric	EGF	2004

Rituximab is the first chimeric mAb with proven therapeutic efficacy for NHL and approved by the FDA. It followed by humanized mAbs such as Trastuzumab, Alemtuzumab, and Bevacizumab and were approved to treat different types of cancer (13). Besides using antibodies for NHL treatment, Ibritumomab Tiuxetan and Tositumomab can also be used for radionuclidic therapy by labelling with a radionuclide. (13, 14). Developing technology provided the human and humanized mAbs such as "Ofatumumab", which received FDA approval in 2009 and "Obinutuzumab", which received FDA approval in 2013 and were produced to use in NHL treatment (62).

Although the purpose of these mAbs, conjugated with several molecules or unconjugated, for cancer is primarily therapeutic (Figure 2.7) (63), they can also be used for the diagnosis by radiolabeling and fluorescent agent labelling with PET, SPECT and optic imaging methods (8).

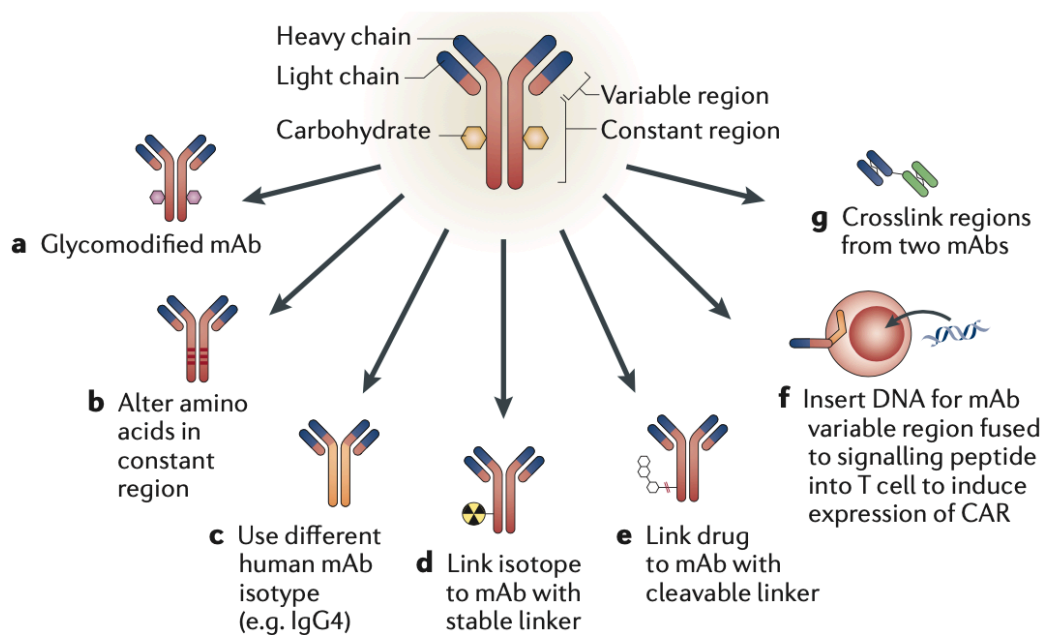


Figure 2.7. Different types of conjugated mAbs (63).

2.6.1. mAbs Used in Lymphoma

CD20 antigen is specific to B cell which is expressed in mature B cells and most of the NHL. Rituximab, tositumomab, obinutuzumab, ofatumumab are the mAbs are specific to B cells and recognize the CD20 antigen in the surface of B cells. Rituximab, ocrelizumab, ofatumumab are Type 1 CD20 antibodies while obinutuzumab and tositumomab are Type 2 CD20 antibodies (64). Their binding and death mechanisms in CD 20 are different (Figure 2.8).

These mAbs bind the small loop of the CD20 antigen on the cell surface of B cells. The way antibodies bind to this antigen can be divided into two main groups. First group, ofatumumab and rituximab, causes complement-dependent cytotoxicity and antibody-dependent cell mediated cytotoxicity by inducing the redistribution of CD20 in the plasma membrane. Second group, tositumomab and obinutuzumab, show minimal complement-dependent cytotoxicity and strong antibody-dependent cell mediated cytotoxicity. They show increasing direct antitumour effect on CD20 in B cell surface. (65). Obinutuzumab binds to the CD20 at lower density than rituximab (64).

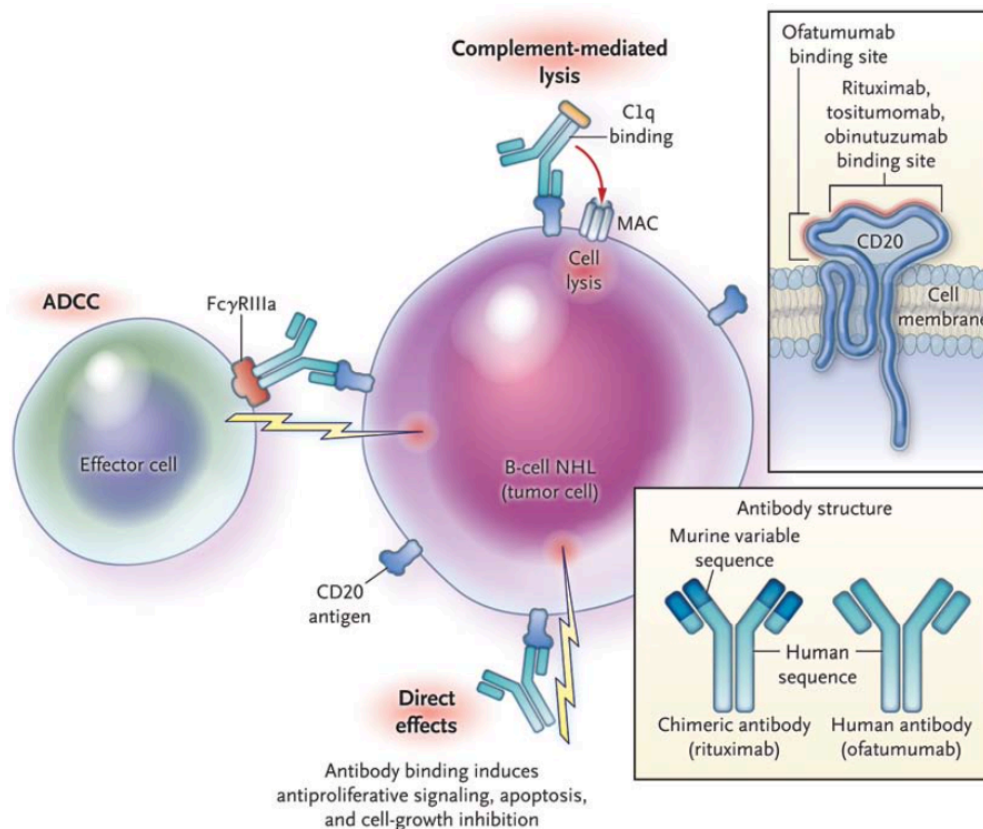


Figure 2.8. Anti CD20 mAbs (Rituximab, Tositumomab, Obinutuzumab and Ofatumumab) activation mechanism (65).

2.7. ^{89}Zr Radiolabelled mAbs

^{89}Zr is the ideal radionuclide for mAbs due to long half-life and it is also labelled with high yield and purity with low production costs (37, 66). ^{89}Zr labelled mAbs show high stability as long as bifunctional chelator is conjugated to mAbs, in this purpose DFO is the most common chelating agent for ^{89}Zr labelled mAbs (Figure 2.9) (19).

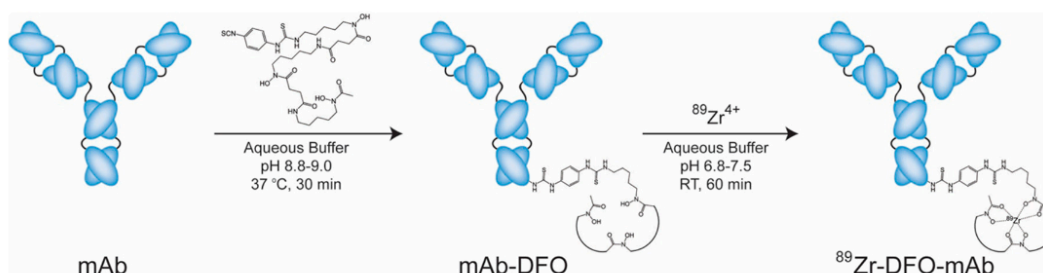


Figure 2.9. Schema of ^{89}Zr radiolabelling of mAb (67).

Chelators and their coordination properties, linkers and the conjugation reactions may be/present as highly effective parameters on labelling efficiency, stability and biodistribution of ^{89}Zr labelled mAbs (68). Different kinds of chelating agents have been under investigation for ^{89}Zr radiolabelling. The most used bifunctional chelating agents are Desferrioxamine (DFO) (Figure 2.10) and DFO derivatives (Table 2.6). The other popular chelators such as DTPA, DOTA etc. are not suitable for ^{89}Zr radiolabelling due to +4 oxidation state of ^{89}Zr (68).

Table 2.6. Different derivatives of DFO used in ^{89}Zr -radiolabelling.

Chelators	References
DFO-1-hydroxy-2-pyridone (HOPO)	(69)
p-SCN-Bn-DFO	(70)
DFO-Suc-N	(37)
DFO-AHA	(42)
DFO-Sq	(71)
Bromoacetyl-DFO	(72)

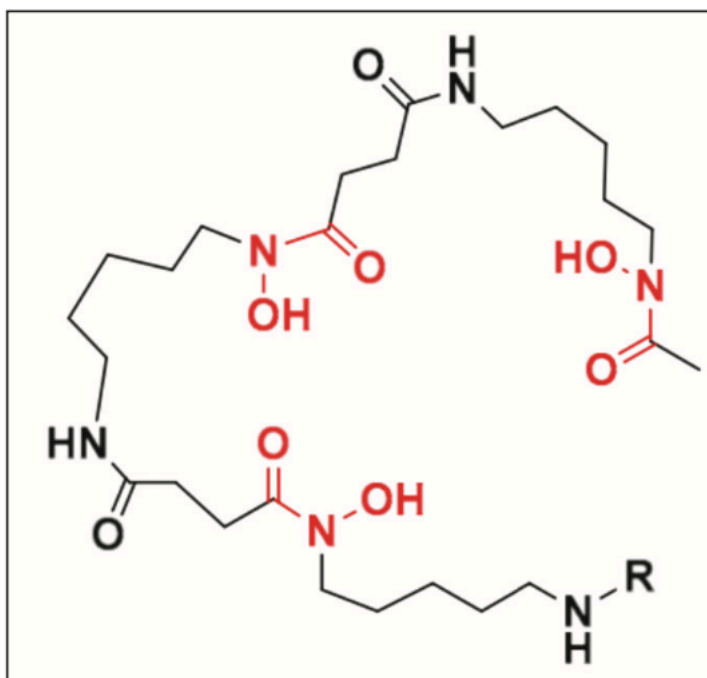


Figure 2.10. DFO schematic representation (73).

The first animal study was reported in 1997 by Meijs et al. (74). The first clinical study was done by Börjesson et al. In this study, ^{89}Zr radiolabelled c-mAb U36 was studied to detect head and neck cancer patients (66). It is followed by many studies which carried out on the ^{89}Zr radiolabelled mAbs in preclinical and clinical with great success (68). Several preclinical and clinical studies of ^{89}Zr -mAbs such as ^{89}Zr -cetuximab (33); ^{89}Zr -ibritumomab tiuxetan (34); ^{89}Zr -rituximab (35); ^{89}Zr trastuzumab (36); ^{89}Zr -J591; ^{89}Zr -c-mAb U36 (37) are ongoing (Table 2.7).

Table 2.7. ^{89}Zr -radiolabelled mAbs in preclinical and clinical stages (27, 28).

Products	Trade name of mAb	Cancer type	Reference
^{89}Zr - cetuximab	Erbitux	NHL	(75)
^{89}Zr - ibritumomab tiuxetan	Zevalin	NHL	(34)
^{89}Zr -rituximab	Rituxan	NHL	(76)
^{89}Zr trastuzumab	Herceptin	Breast cancer	(77)
^{89}Zr -huJ591	-	Prostate cancer	(75)
^{89}Zr -c-mAb U36	cmAb U36	Head and neck squamous cell carcinoma	(66)
^{89}Zr - tositumomab	Bexxar	NHL	(17)
^{89}Zr -pertuzumab	Omnitarg	Breast cancer	(78)

2.8. ^{89}Zr Radiolabelled mAbs and Non Hodgkin's Lymphoma

Various CD20 targeted and FDA approved mAbs are used in the treatment of NHL and five of them have been tried to be labelled with ^{89}Zr . First of them was ibritumomab tiuxetan radiolabelled with ^{89}Zr . (34, 73).

Perk et al. (2006), studied ^{89}Zr -ibritumomab tiuxetan (Zevalin) to evaluate the ^{89}Zr for labelling procedures and future radiopharmaceuticals and to compare with ^{90}Y -Zevalin. It is provided that ^{89}Zr -Zevalin was labelled with high yield and purity. When the distribution of ^{89}Zr -Zevalin and ^{90}Y -Zevalin compared, ^{89}Zr showed highly similar biodistribution with ^{90}Y -Zevalin (34).

^{89}Zr -rituximab is popular to use for the diagnosis of lymphoma. Natarajan et al. (2012), worked with ^{89}Zr radiolabelled rituximab to image the tumour model for longer period. This study showed that ^{89}Zr -rituximab is a promising radiopharmaceutical for lymphoma, especially NHL imaging due to high specific activity, purity and stability for 5 days in human serum. According to the result obtained from this study, ^{89}Zr -rituximab can be used to diagnose of NHL. ^{89}Zr -rituximab is in the clinical stage for FDA approval (79). This study followed by radiation dosimetry study of ^{89}Zr -rituximab by Natarajan et al. (2015) as a supporting evidence for potency for NHL imaging (80).

Yoon et al. (2018), worked on CD20 antibodies by radiolabelling with ^{89}Zr . Rituximab (chimeric) and tositumumab (murine) antibodies are the CD20 site specific mAbs as previous generation while obinutuzumab and ofatumumab are the newest CD20 specific mAbs for lymphoma. In this study, those mAbs were radiolabelled with ^{89}Zr and then evaluated by PET/CT imaging and biodistribution studies. As a result of this study, researchers mentioned that all ^{89}Zr radiolabelled anti CD20 mAbs have a great potential for lymphoma diagnosis, and especially new generation of mAbs which are ofatumumab and obinutuzumab have a great potential for lymphoma diagnosis and imaging (17).

3. MATERIALS and METHODS

3.1. Materials and Equipment

All materials, chemicals and instruments used in this research have been listed in Table 3.8 and Table 3.1.

Table 3.1. Chemicals.

Absolute Ethanol	Sigma-Aldrich
Acetonitril	Sigma-Aldrich
Desferrioxamine (DFO)-p-Bz-NCS	Macrocyclic
DiMethyl Sulfoxide (DMSO)	Sigma-Aldrich
Fetal Bovine Serum (FBS)	Gibco
Formaldehyde	Sigma-Aldrich
Hydrochloric Acid (HCl)	Sigma-Aldrich
HL 60 Cells (ATTC, CCL-240)	American Type Culture Collection
L-Glutamine 200 mM (x100)	Gibco
Methanol	Sigma-Aldrich
Phosphate-Buffered Solution Tablets	Sigma-Aldrich
Penicillin/Streptomycin (10,000 Unit.ml⁻¹ / 10,000 µg.ml⁻¹)	Gibco
Ramos Cells (RA 1) (ATTC, CRL-1596)	American Type Culture Collection
Resin Hydroxamate	Sigma-Aldrich
Roswell Park Memorial Institute (RPMI) 1640 Medium	Gibco
Saline (Sodium Chloride 0.9%)	B - Braun
Sodium Carbonate (Na₂CO₃)	Sigma-Aldrich
Sodium Bicarbonate (NaHCO₃)	Sigma-Aldrich
Tocilizumab (RoActemra)	Roche
Obinutuzumab (Gazyva)	Roche, Basel
Oxalic Acid	Sigma-Aldrich

Table 3.2. Equipments and softwares.

Biorender	
Cell Counter	Luna II Automated Cell Counter
Cell Counter Slide	Luna Cell Counter Slides
Centrifuge	Thermo Scientific Espresso
Class II Cabinet	MicroFlow Peroxide Advanced Bio Safety Cabinet-Class II
Dose Calculator	Capintec, INC CRC-25 PET
Gamma-Counter	Perkin Elmer Wizard 3
Geiger Müller	Berthold LB 124
ITLC SG Paper	Agilent
Laura Chromatography Software v5.0.7.56	
Nano Drop	Devonix DS-II Spectrophotometer
Nano Positron Emission Tomography/Computed Tomography (PET/CT)	Mediso
Nano Positron Emission Tomography/Computed Tomography (PET/CT) Imaging Chamber (Three Mice Chamber)	Mediso Multicell
pH-Meter	Mettler Toledo
Prism	
Radio High Pressure Liquid Chromatography (RHPLC)	Agilent 1200 Series with Lab Logic Gamma-Ram-4
Radio Thin Layer Chromatography (RTLCL)	Lab Logic Scan-RAM Experience&Expertise
Superdex 200 10/300 GL Size Exclusion Chromatography Column	GE, USA
Thermo Mixer	Eppendorf Thermomixer C

3.2. Characterization Studies on mAbs

In order to determine Toc and Obi amounts, enzyme linked immunosorbent assay (ELISA) and sodium dodecyl sulphate polyacrylamide gel electrophoresis (SDS PAGE) tests were aimed to use. But, due to the confidentiality agreement between Roche and Singleton Hospital Nuclear Medicine Department/Swansea and University

Hospital of Wales PETIC /Cardiff, tests could not be performed in this research. Only the general methods were given in the following paragraphs.

3.2.1. ELISA

ELISA is the biological assay used commonly for the detection and quantification of peptides, proteins, Abs and mAbs. It is mainly based on the interactions between antibodies and antigens and it depends on their affinity and specificity. Direct, indirect and sandwich capture are several detection methods used in ELISA. Sandwich ELISA assay is the most commonly used type due to the high sensitivity and specificity.

96 well plates are coated with CD20 antigen in buffer solution, containing BSA and the antigens are incubated overnight. Then, Abs at different concentrations diluted in BSA/TBS are added to the plates and incubated for 2-3 hours. It is followed by incubation of Horse Radish Peroxide (HRP) conjugated anti-human IgG for an hour and after that, plates are washed and incubated with tetramethyl benzidine (TMB) at room temperature (25°C) for 30 min. Measurements are completed at 450 nm with the ELISA plate reader (81, 82).

3.2.2. SDS PAGE

Abs are analyzed in SDS-PAGE consisting of 3-8% Tris-Acetate gel. Molecular weights of Abs are determined by SDS PAGE before radiolabelling process.

3.3. ^{89}Zr Production and Purification

^{89}Zr was produced on cyclotron by the bombarding (p,n) of target yttrium foil, and it was sent via transfer tunnel as a solid disc into the hot cell. The solid disc includes different metals in addition to the ^{89}Zr and the concentration of ^{89}Zr is generally in between 0,1-1%. Therefore, ^{89}Zr should be purified from the foil.

Before the separation and purification processes of ^{89}Zr , the key point is washing all of the materials which will be used, with 6 M 37% HCl and water, respectively. The reason was the importance of the washing process, i.e: it blocks the binding of metals to the ions and other substances.

Several different chemicals were prepared for using at purification process:

- Deionised water (15,5 ml) (a)
- 1 M oxalic acid (320 mg oxalic acid: 4 ml water) (3 ml) (b)
- 30% H₂O₂ (0,1 ml) (c)
- 2 M HCl (6 ml) (d)
- 2 M HCl (12 ml) (g)
- Ion exchange cartridge column (resin hydroxamate) (f),

Ion exchange cartridge column preparation:

- 1250 mg resin was weighed out and poured into the cartridge.
- The cotton was put on top of the powder, and the cartridge lid was closed.
- After the lid closure, the column was washed by
 - 1) 75 ml acetonitrile
 - 2) 10 ml (0,9%) saline
 - 3) 2 ml HCl (2M), respectively.
- Finally air was pumped with a syringe several times.

⁸⁹Zr was separated from yttrium disc by using a resin hydroxamate column and washing with HCl and oxalic acid. The purpose of using oxalic acid was obtaining ⁸⁹Zr-oxalate. 2 M HCl and H₂O₂ solutions were used to collect the last remaining ⁸⁹Zr in the column.

After all items were prepared, they were placed on cassette systems in the hot cell for ⁸⁹Zr purification (Figure 3.1). Finally, the hot cell was closed for the solid disc placing into the reaction vial by using a hot cell handle, and the system was ready to start by software.

After the completion of this purification process, ⁸⁹Zr-oxalic acid solution needs to be neutralized for radiolabelling of mAbs.



Figure 3.1. The cassette system which is used ^{89}Zr purification in hot cell.

((a) Water, (b) Oxalic acid, (c) H_2O_2 , (d) HCl , (e) Empty vial, (f) Resin hydroxamate column, (g) HCl , (h) Reaction vial, (i) Yttrium waste vial, (j) ^{89}Zr vial-1, (k) ^{89}Zr vial-2, (l) ^{89}Zr vial-3) (Cardiff University, Positron Emission Tomography Imaging Centre).

3.4. ^{89}Zr Formulation Studies

7 different formulations were prepared. The main formulation was ^{89}Zr -Obi; but, in order to obtain the optimum molar ratio of (mAb:DFO-p-Bz-NCS: ^{89}Zr) and consequently the highest radiolabelling efficiency, 5 different ^{89}Zr -Obi formulations

were prepared (Table 3.3). In addition to ^{89}Zr -Obi formulations, ^{89}Zr -Toc formulation was also prepared as a control formulation for in-vitro and in-vivo studies.

Table 3.3. Molar ratio and composition of prepared formulations.

	Formulation Codes	Antibody	Formulation	(mAb:DFO-p-Bz-NCS:^{89}Zr) (Molar Ratio)
Formulation 1	^{89}Zr -Obi	Obinutuzumab	^{89}Zr - Obinutuzumab	$1:10:10^{-1}$
Formulation 2	^{89}Zr -Obi (DFO 1)	Obinutuzumab	^{89}Zr - Obinutuzumab	$1:1:10^{-1}$
Formulation 3	^{89}Zr -Obi (DFO 2)	Obinutuzumab	^{89}Zr - Obinutuzumab	$1:15:10^{-1}$
Formulation 4	^{89}Zr -Obi (^{89}Zr 1)	Obinutuzumab	^{89}Zr - Obinutuzumab	$1:10:2.10^{-1}$
Formulation 5	^{89}Zr -Obi (^{89}Zr 2)	Obinutuzumab	^{89}Zr - Obinutuzumab	$1:10:1.4.10^{-1}$
Formulation 6	^{89}Zr -Obi (^{89}Zr 3)	Obinutuzumab	^{89}Zr - Obinutuzumab	$1:10:0.6.10^{-1}$
Formulation 7 (Control)	^{89}Zr -Toc	Tocilizumab	^{89}Zr - Tocilizumab	$1:10:10^{-1}$

3.5. ^{89}Zr Radiolabelling Process

^{89}Zr antibody labelling with ^{89}Zr process was carried out in two steps which are 1) DFO-p-Bz-NCS and antibody conjugation (Figure 3.2 and Figure 3.3), 2) ^{89}Zr incubation of DFO-p-Bz-NCS-antibody conjugate (Figure 3.4). The amounts of the antibodies and other chemicals were calculated according to the Vosjan et al. labelling protocols (83) shown in Table 3.10. Briefly, mAb solutions between 2-10 mg.ml⁻¹ were used in 1 ml volume and pH were adjusted to 8.9-9.1 by exchanging solution for DFO-p-Bz-NCS (in DMSO)-mAb conjugation were carried out at 550 rpm for 30 min. It was followed by ^{89}Zr incubation for 1 hour by gently shaking. (83).

3.5.1. DFO-p-Bz-NCS -Antibody Conjugation

Before conjugation process, mAb's pH should be adjusted to pH 9 (pH 8.9 - 9.1). Vosjan et al. (2010) stated that pH has great importance at every step (83). For

the conjugation of mAbs and DFO-p-Bz-NCS at the highest rate, the medium must be alkaline and the pH must be adjusted to 9 and at the same time buffer solution was used for solvent exchange. At this point, the buffer solution use is important. NaHCO_3 should be used as a buffer solution for labelling because precipitate may form after pH adjustment if Na_2CO_3 was used (84). After the Obi- DFO-p-Bz-NCS and Toc- DFO-p-Bz-NCS conjugations were completed [in (1:10) (mAb: DFO-p-Bz-NCS) ratio], the PD-10 column was prepared and used to remove the free DFO-p-Bz-NCS. After that, DFO-p-Bz-NCS -Obi conjugates were measured by nanodrop to determine the mAb concentration spectrophotometrically and DFO-p-Bz-NCS-Obi samples were collected and mixed to label with ^{89}Zr .

25 μl Obi stock solution (25 mg. ml^{-1}) and 10 μl of Toc solution (20 mg. ml^{-1}) were prepared separately and adjusted to pH 8.9-9.1 with 100 μl NaHCO_3 buffer.

Solutions were measured in nanodrop to find the concentrations of mAbs after this process. Then DFO-p-Bz-NCS amount could be calculated according to the Obi and Toc concentrations depending on the pH adjustment.

- DFO-p-Bz-NCS was solved in DMSO with 0.005 M concentration.
- DFO-p-Bz-NCS in DMSO was added to Obi and Toc solutions, and incubated at 37°C and stirred at 550 rpm for 1 hour.
- After the completion of the reaction, the PD-10 column was used for the separation of unconjugated DFO-p-Bz-NCS. Several washings were done, and all eluates were collected to measure conjugated mAbs (DFO-p-Bz-NCS-Obi and DFO-p-Bz-NCS-Toc) by nanodrop and the pure eluates were mixed for ^{89}Zr labelling. This mixed solution was measured mAb conjugates by nanodrop once more for the calculation of ^{89}Zr activity.

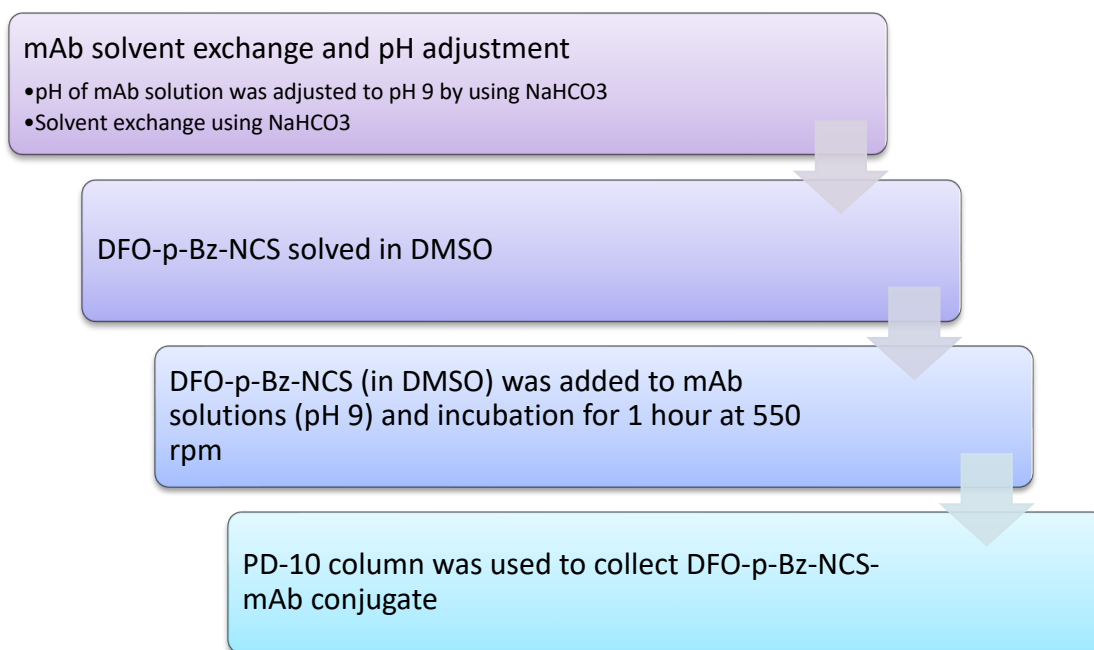


Figure 3.2. Preparation Flow-chart for DFO-p-Bz-NCS and mAbs (Obi and Toc) conjugation.

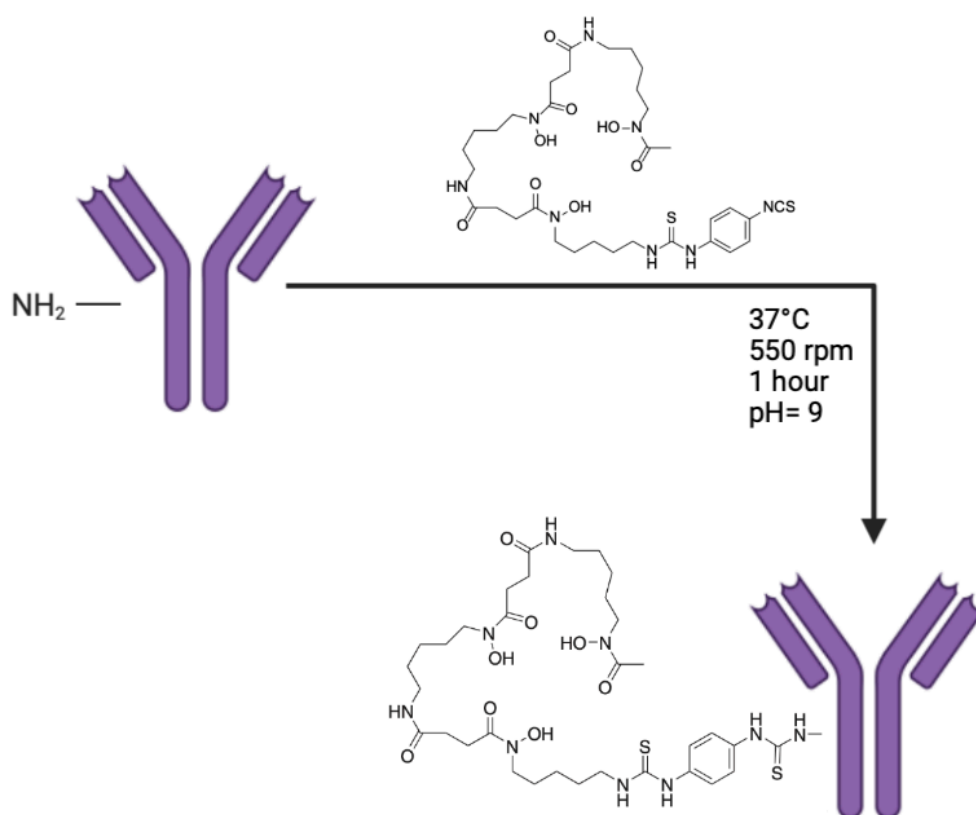


Figure 3.3. DFO-p-Bz-NCS and mAb conjugation.

3.5.2. ^{89}Zr Radiolabelling

[Antibody molarity: ^{89}Zr activity (MBq)] ratio should be (10:1) according to the several studies (83, 84). ^{89}Zr production and purification processes were explained in Section 3.3. After that, ^{89}Zr should be neutralized with Na_2CO_3 for radiolabelling of mAbs.

0.5 M Na_2CO_3 was used for neutralization of ^{89}Zr in oxalic acid and pH should be adjusted to 7 (between 6.8 and 7.2). 0.5 M Na_2CO_3 was pipetted drop by drop and mixed until pH reaches 7. Neutralized ^{89}Zr was used for Toc and Obi radiolabelling. Required volumes were used according to the Toc and Obi amount. The ratio was always kept in molar ratio of (1:10) (^{89}Zr :mAb).

^{89}Zr (in Na_2CO_3) and Obi and Toc solutions were incubated for 1 hour at room temperature (25 °C) (RT) by gently shaking in the reaction vial.

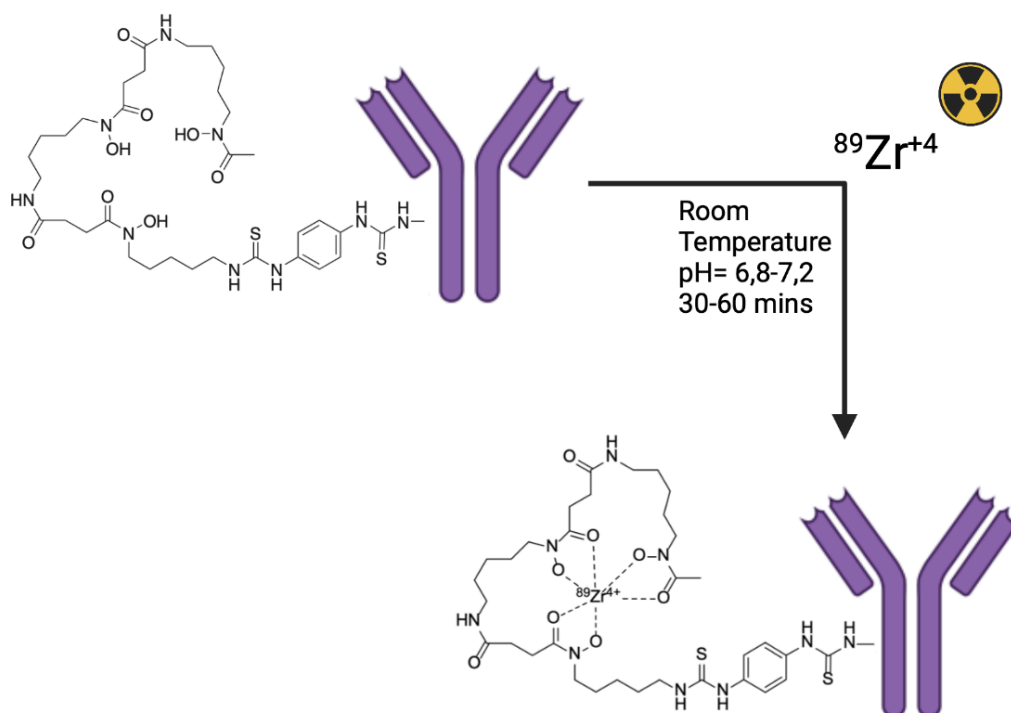


Figure 3.4. ^{89}Zr radiolabelling of mAb schema.

3.6. Quality Control Tests

Radiochemical purity (by RTLC, RHPLC) and stability tests were carried out as quality control tests as follows:

3.6.1. Radiochemical Purity

The ^{89}Zr -Obi and ^{89}Zr -Toc should not contain free ^{89}Zr or ^{89}Zr - DFO-p-Bz-NCS more than 5%. These impurities were detected by RTLC and RHPLC analysis (85).

Radio-TLC

RTLC analyzes were carried out with SG (covered with silica gel) chromatography papers. ^{89}Zr -Obi, ^{89}Zr -Toc and free ^{89}Zr were applied to SG papers and then, they were placed into a tank containing the DMSO solution. After the development time, chromatography papers were removed and measured by gamma-scintillation. ^{89}Zr -Obi, ^{89}Zr -Toc and if exist ^{89}Zr - DFO-p-Bz-NCS and free ^{89}Zr were detected (85).

Radio-HPLC

Size exclusion chromatography was performed size exclusion column. pH 7.4 phosphate buffer was used as mobile phase and each samples were analyzed for 60 min. These analyzes were performed by HPLC with a radioactivity detector running with Laura chromatography software v5.0.7.56 (84).

3.7. Stability

9.25 MBq ^{89}Zr -Obi was incubated in 5 ml saline solution (NaCl 0.9%) at 37°C and samples were withdrawn at 4th, 24th, 48th, 60th, 72th and 90th hours (86). Samples were analyzed by RHPLC using size exclusion column. RHPLC chromatograms, ^{89}Zr bound Obi and free ^{89}Zr were reported by using Graph Prism.

3.8. In-vitro Cell Culture Studies

In vitro cell culture studies were carried out with at CD20 (+) Ramos cells (Burkitt's Lymphoma/ NHL) and CD20 (-) HL 60 cells (leukemia). These two cell cultures were suspension cell type.

Ramos cells were grown in Roswell Park Memorial Institute (RPMI)-1640 medium containing 1% Penisillin-Streptomisin, 20% Fetal Bovine Serum (FBS) and

1% glutamine while HL 60 cells were grown in RPMI-1640 medium containing 1% Penicillin-Streptomisin, 10% FBS and 1% Glutamine.

Immuno-reactivity, binding assay studies were carried out for both cell types and results were compared with each other (78, 86, 87).

3.8.1. Immuno-reactivity Studies

Immuno-reactivity studies were carried out depending on the studies of Lindmo et al,1984 and Natarajan et al, 2012 (79, 87). Six different concentrations (5.10^6 ; 4.10^6 ; 3.10^6 ; 2.10^6 ; $1.5.10^6$; $0.5.10^6$ cells.ml⁻¹) of cells were prepared for both Ramos and HL 60 cells (n:3). 50 µl of ⁸⁹Zr labelled Obi in 1kBq (10 ng of Obi) radioactive concentration was added to each samples and incubated at 37°C, 300 rpm for 2 h (Figure 3.5). After incubation, samples were centrifuged and washed with PBS, two times. Cell pellets and supernatants were measured by gamma-counter and immuno-reactive fractions were determined by linear regression analyzes by plotting of (total/specific) activity versus inverse cell concentration (1/ cell concentration) and 1/y intercept was calculated.

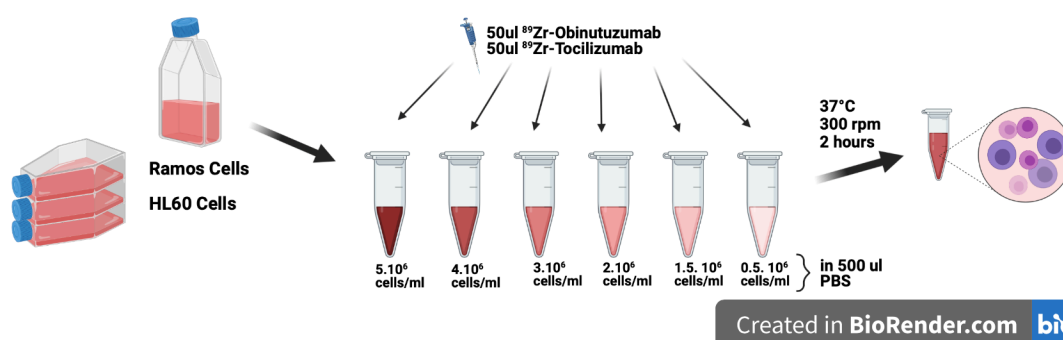


Figure 3.5. Immuno-reactivity study schema (created in BioRender.com).

3.8.2. Binding Assay Studies

Competitive binding assay was employed on Ramos cells. Cells were incubated with $6.16. 10^{-9}$ M ⁸⁹Zr-Obi solution (Table 3.11) in the presence of different concentrations ($6.16. 10^{-6}$ – $6.16. 10^{-11}$ M) (Table 3.12) of unlabelled Obi as competitor at 4 °C for 1.5 h. The cells were washed with PBS twice and the supernatant was removed; pellets were assayed in a gamma-counter. The percentage of ⁸⁹Zr-Obi bound

in the presence of competitor/non-competitor (B/Bo .100) was plotted against the log concentration of added competitor (79). Dissociation constant (Kd), and median effective concentration (EC₅₀) were determined by GraphPad Prism.

Table 3.4. Obi molarity calculation.

Sample	Measured (mg.ml ⁻¹)	Vol (µl)	Antibody Mass (Dalton)	Molarity (M)	Moles (n)
Obi Pure	25	20	146064,72	0,00017116	3,42E-09
Obi Measured on nanodrop in (Na ₂ CO ₃)	2	100	146064,72	1,37E-05	1,37E-09
Obi measured on nanodrop	0.9	100	146064,72	6,16E-06	6,16E-10

Table 3.5. Obi concentration calculation.

Samples	Concentration (mg.ml ⁻¹)	Antibody Mass (Dalton)	Molarity (M)
1	0.9	146064,72	6,16E-06
2	0.09	146064,72	6,16E-07
3	0.009	146064,72	6,16E-08
4	0.0009	146064,72	6,16E-09
5	0.00009	146064,72	6,16E-10
6	0.000009	146064,72	6,16E-11

3.9. In-vivo Animal Studies

In-vivo animal studies were carried out at the Cardiff University, University Hospital Wales (UHW), Radioactivity Animal Laboratory under Martin Ruthardt's Project Licence (P1DDB264F, 28 Sep 2017-26 Sep 2022).

In order to carry out these studies, I attended the animal handling course in Turkey under the training of *Ankara University (ANKUSEM)* and received the certificate number "ANK. S. 17. BR. 05. 0193" (Attachement-1). Also, in order to carry out the same studies in the UK, I attended another animal handling course under the training of *Charles River UK Ltd in the UK*, achieved the exam and received the

certificate from the *Royal Society of Biology* with the number of “BIO/2020/725” (Attachment-2).

Studies were performed on 15 female SCID mice and they were divided into three groups and 5 mice were used in each group. 2 million Ramos live cells per mice were injected intravenously by tail vein in the first group; 2 million live HL 60 cells per mice were injected intravenously by tail vein in the second group, and the last group was the control group without any cell injection. Animals were checked daily, and after 1 week, ^{89}Zr -Obi was injected into the mice (Table 3.5).

3.9.1. PET/CT Imaging Studies

Nano PET/CT images were taken at the most appropriate time for image acquisition, and then biodistribution studies were performed. PET/CT images were taken after 6 days of ^{89}Zr -Obi injection.

3.9.2. Biodistribution Studies

Biodistribution studies were performed immediately after the obtaining of PET/CT images. Biodistribution studies were carried out by removing organs (skeleton, lung, spleen, heart, liver, knees, hips, shoulders, brain, kidney) from the animals in each group and measuring them with a gamma-counter.

Table 3.6. Summary of the ^{89}Zr -Obi injections into animals with different cancer models.

Mouse Details	Tracer	Injected Cells	Syringe Activity (MBq)	Injection Volume (μl)	Injection Time (p.m)	Remaining Syringe Activity (MBq)
Mice 1	^{89}Zr -Obi	Ramos	1.93 (at 16:39)	65	16:45	0.38 (at 16:46)
Mice 2	^{89}Zr -Obi	Ramos	2.09 (at 16:11)	65	16:15	0.31 (at 16:16)
Mice 3	^{89}Zr -Obi	Ramos	1.99 (at 16:18)	65	16:23	0.30 (at 16:24)
Mice 4	^{89}Zr -Obi	Ramos	1.85 (at 16:25)	65	16:28	0.35 (at 16:29)
Mice 5	^{89}Zr -Obi	Ramos	1.99 (at 16:32)	65	16:37	0.37 (at 16:38)
Mice 1	^{89}Zr -Obi	HL 60	1.96 (at 16:50)	65	16:52	0.30 (at 16:52)
Mice 2	^{89}Zr -Obi	HL 60	1.82 (at 16:54)	65	17:01	0.30 (at 17:01)
Mice 3	^{89}Zr -Obi	HL 60	1.69 (at 17:03)	65	17:05	0.34 (at 17:06)
Mice 4	^{89}Zr -Obi	HL 60	1.84 (at 17:08)	65	17:10	0.50 (at 17:11)
Mice 5	^{89}Zr -Obi	HL 60	1.53 (at 17:13)	65	17:27	0.29 (at 17:28)
Mice 1	^{89}Zr -Obi	Control	1.97 (at 15:45)	65	15:52	0.52 (at 15:54)
Mice 2	^{89}Zr -Obi	Control	2.03 (at 15:58)	65	16:00	0.38 (at 16:02)
Mice 3	^{89}Zr -Obi	Control	2.06 (at 16:05)	65	16:07	0.56 (at 16:08)
Mice 4	^{89}Zr -Obi	Control	1.83 (at 17:26)	65	17:31	0.21 (at 17:32)
Mice 5	^{89}Zr -Obi	Control	0.99 (at 17:26)	65	17:27	0.29 (at 17:28)

3.10. Statistical Analyzes

Statistical analyzes were performed to evaluate whether there is a statistical difference between the results obtained or not. Since the number of data obtained from the experiments was less than 30, non-parametric test methods were applied in the evaluations. According to the number of groups compared; Mann Whitney U-test was used to compare two groups, and Kruskal Wallis Analysis of Variance was used to compare three or more groups. To express the differences within the same group, standard error (SE) was used in the results of cell culture and in-vitro studies, and standard deviation (SD) was used in the results of other studies. When comparing the differences between the groups, $p < 0.05$ was considered statistically significant.

4. RESULTS

4.1. Characterization Studies on mAbs

4.1.1. ELISA

The ELISA test, which was performed by following the procedures as described in Section 3.2.1, is one of the antibody recognition tests. Although it is one of the tests planned to be carried out within the scope of the thesis, this test could not be performed due to agreement between F. Hoffman-Roche Company and Nuclear Medicine Department/Singleton Hospital and PETIC/University Hospital of Wales. In the confidentiality agreement signed, it was agreed not to carry out analysis on the "Obi" antibody, which was found under the name of "Gazyva" on the market and not to give any knowledge to the third parties. Therefore, this analysis could not be performed.

4.1.2. SDS-PAGE

The SDS-PAGE test, which was performed by following the procedures as described in Section 3.2.2, is one of the antibody recognition tests. Although it is one of the tests planned to be carried out within the scope of the thesis, this test could not be performed due to agreement between F. Hoffman-Roche Company and Nuclear Medicine Department/Singleton Hospital and PETIC/University Hospital of Wales. In the agreement signed, it was agreed not to carry out analysis on the "Obi" antibody, which was found under the name of "Gazyva" on the market and not to give any knowledge to the third parties. Therefore, this analysis could not be performed.

4.2. ^{89}Zr Production and Purification

Initially, solid target activity was measured, and it was found as 1669 MBq at 12:59 pm. Radionuclide ^{89}Zr was obtained in 3 different vials in oxalate form with different doses and afterwards, the highest dose was chosen for use (Table 4.1). In this process, adjusted doses and volumes were crucial for the labelling process. After the separation process, those 3 different vials (1000 μl each) were measured to calculate ^{89}Zr activity to be used in radiolabelling. 3rd reaction vial was used (because of the highest concentration requirement) and from this vial 200 μl solution was taken and

used for neutralization. Activity and volumes of ^{89}Zr before and after neutralization are shown in Table 4.2.

Table 4.1. Reaction vials and their activity/time (MBq).

Sample	Radioactivity (MBq)	Time (p.m)
Solid Target	1669	12:59
1.Rxn Vial	0,02	14:47
2.Rxn Vial	390	14:47
3.Rxn Vial	560	14:47
^{90}Y Waste Vial	76	14:54

Table 4.2. ^{89}Zr activity before and after neutralization.

	Radioactivity (MBq)	Volume (μl)	Specific Activity ($\mu\text{l.MBq}^{-1}$)
^{89}Zr (Before neutralization)	38.9	200	5.1413
^{89}Zr (After neutralization)	33.5	446	13.3134

4.3. ^{89}Zr Formulation Studies

The optimum molar ratio of the composition of (mAb:DFO-p-Bz-NCS: ^{89}Zr) and the obtained highest radio-efficient formulation was Formulation 2 with (1:10:10⁻¹) molar ratio.

4.4. ^{89}Zr Radiolabelling Process

4.4.1. DFO-p-Bz-NCS -Antibody Conjugation

Obi- DFO-p-Bz-NCS and Toc- DFO-p-Bz-NCS conjugations were performed as explained in Section 3.5.1. Obi and Toc concentrations before and after pH adjustment/solvent exchange and necessary DFO-p-Bz-NCS volumes were summarized in Table 4.3. After DFO-p-Bz-NCS-Obi and DFO-p-Bz-NCS-Toc conjugation, nanodrop measurements (for concentration calculation) were done and results are shown in Table 4.4.

Table 4.3. Formulations of mAbs and total volume measurements before and after pH adjustment and solvent exchange.

Formulation	(mAb:DFO-p-Bz-NCS:⁸⁹Zr) (Molar Ratio)	mAbs in solution	Measured (mg.ml⁻¹)	Vol (μl)
Formulation 1	1:10:10 ⁻¹	Original calculated amount of Obi Pure (P1AD3543-002-05)	25	20
		measured on nanodrop (in NaHCO ₃)	8.26	100
Formulation 2	1:1:10 ⁻¹	Original calculated amount of Obi Pure (P1AD3543-002-05)	25	16
		measured on nanodrop (in NaHCO ₃)	4.21	100
Formulation 3	1:15:10 ⁻¹	Original calculated amount of Obi Pure (P1AD3543-002-05)	25	16
		measured on nanodrop (in NaHCO ₃)	4.17	100
Formulation 4	1:10:2.10 ⁻¹	Original calculated amount of Obi Pure (P1AD3543-002-05)	25	16
		measured on nanodrop (in NaHCO ₃)	4.32	100
Formulation 5	1:10:1.4.10 ⁻¹	Original calculated amount of Obi Pure (P1AD3543-002-05)	25	16
		measured on nanodrop (in NaHCO ₃)	3.89	100
Formulation 6	1:10:0.6.10 ⁻¹	Original calculated amount of Obi Pure (P1AD3543-002-05)	25	16
		measured on nanodrop (in NaHCO ₃)	4.06	100
Formulation 7 (Control)	1:10:10 ⁻¹	Original calculated amount of Toc Pure	20	10
		measured on nanodrop (in NaHCO ₃)	4.05	100

Table 4.4. Obi and Toc amounts for pH adjustment and DFO-p-Bz-NCS conjugation.

Formulation (*)	Sample	Measured (mg.ml⁻¹)	Vol (μl)	Antibody mass (Dalton)	Molarity (M)	Moles (n)	DFO-p-Bz-NCS (M)	DFO-p-Bz-NCS (ml)	DFO-p-Bz-NCS (μl)
Formulation 1 (Obi)	Measured on nanodrop (in Na ₂ CO ₃)	8.26	100	146064.72	5.65503 .10 ⁻⁵	5.65503 .10 ⁻⁹	5.65503 .10 ⁻⁸	0.011310055	11.31005
	Measured on nanodrop	4.08	50	146064.72	2.79328 .10 ⁻⁵	1.39664 .10 ⁻⁹	1.39664.10 ⁻⁸	0.0002793282	2.793282
Formulation 2 (Obi)	Measured on nanodrop (in Na ₂ CO ₃)	4.21	100	146064.72	2.88 .10 ⁻⁵	2.88 .10 ⁻⁹	2.88228 .10 ⁻⁹	0.000576	0.576456793
	Measured on nanodrop	2.05	100	146064.72	1.40 .10 ⁻⁵	1.40 .10 ⁻⁹	1.40349 .10 ⁻⁹	0.000281	0.280697488
Formulation 3 (Obi)	Measured on nanodrop (in Na ₂ CO ₃)	4.17	100	146064.72	2.85 .10 ⁻⁵	2.85 .10 ⁻⁹	4.28235 .10 ⁻⁸	0.008565	8.564697
	Measured on nanodrop	2.32	100	146064.72	1.59 .10 ⁻⁵	1.59 .10 ⁻⁹	2.38251 .10 ⁻⁸	0,004765	4.765011
Formulation 4 (Obi)	Measured on nanodrop (in Na ₂ CO ₃)	4.32	100	146064.72	2.96 .10 ⁻⁵	2.96 .10 ⁻⁹	2,95759. 10 ⁻⁸	0,005915	5,915186
	Measured on nanodrop	2.32	100	146064.72	1.59 .10 ⁻⁵	1.59 .10 ⁻⁹	1,59. 10 ⁻⁸	0,003177	3,176674
Formulation 5 (Obi)	Measured on nanodrop (in Na ₂ CO ₃)	3.89	100	146064.72	2.66 .10 ⁻⁵	2.96 .10 ⁻⁹	2.66 .10 ⁻⁸	0,005326406	5,326406
	Measured on nanodrop	2.32	100	146064.72	1.59 .10 ⁻⁵	1.59 .10 ⁻⁹	1.59 .10 ⁻⁸	0,003176674	3,176674
Formulation 6 (Obi)	Measured on nanodrop (in Na ₂ CO ₃)	4.06	100	146064.72	2.78 .10 ⁻⁵	1.2 .10 ⁻⁹	2.78 .10 ⁻⁸	0,00555918	5,55918
	Measured on nanodrop	2.32	100	146064.72	1.59 .10 ⁻⁵	1.59 .10 ⁻⁹	1.59 .10 ⁻⁸	0,003176674	3,176674

Table 4.4. Obi and Toc amounts for pH adjustment and DFO-p-Bz-NCS conjugation (**continued**).

Formulation (*)	Sample	Measured (mg.ml⁻¹)	Vol (μl)	Antibody mass (Dalton)	Molarity (M)	Moles (n)	DFO-p-Bz-NCS (M)	DFO-p-Bz-NCS (ml)	DFO-p-Bz-NCS (μl)
Control Formulation (Toc)	Measured on nanodrop (in Na ₂ CO ₃)	4.05	100	144987.06	2.79335.10 ⁻⁵	2.79335.10 ⁻⁹	2.79335 .10 ⁻⁸	0.005586705	5.586705
	Measured on nanodrop	1.62	80	144987.06	1.11734.10 ⁻⁵	0.89387.10 ⁻⁹	0.89387.10 ⁻⁸	0.001787746	1.787746

(* : Formulation ingredients were given in Table 3.10).

4.4.2. ⁸⁹Zr Radiolabelling

⁸⁹Zr radiolabelling of Obi and Toc were performed according to the method explained in Section 3.5.2. ⁸⁹Zr activity was measured after total amount of Obi- DFO-p-Bz-NCS and Toc- DFO-p-Bz-NCS determinations. The amounts of Obi and Toc and required ⁸⁹Zr volumes are shown in Table 4.5.

Table 4.5. ⁸⁹Zr and mAb amounts for radiolabelling.

Formulation	Measured mAbs (mg.ml ⁻¹)	Vol mAbs (μl)	Total Amount mAbs (μg)	DFO-p-Bz-NCS (nMoles)	Required ⁸⁹ Zr activity (MBq)	Molar Composition (mAb: DFO-p-Bz-NCS: ⁸⁹ Zr)
Formulation 1	4,08	50	204	13.7	20,4	1:10:10 ⁻¹
Formulation 2	2.05	100	205	1.4	20.5	1:1:10 ⁻¹
Formulation 3	2.32	100	232	23.8	23.2	1:15:10 ⁻¹
Formulation 4	2.32	100	232	15.9	46.4	1:10: 2. 10 ⁻¹
Formulation 5	2.32	100	232	15.9	33.1	1:10: 1.4 .10 ⁻¹
Formulation 6	2.32	100	232	15.9	15.5	1:10: 0.7 .10 ⁻¹
Formulation 7 (Control)	1.62	80	129.6	13.0	13.0	1:10:10 ⁻¹

4.5. Quality Control Results

4.5.1. Radiochemical Purity

Radio-TLC

RTLC analyzes were done as explained in the Section 3.6. RTLC results showed that ⁸⁹Zr-Obi and ⁸⁹Zr-Toc formulations could be radiolabelled with the yield of 100%. Free ⁸⁹Zr, ⁸⁹Zr-Obi and ⁸⁹Zr- Toc RTLC results are shown in Figure 4.1, Figure 4.2 and Figure 4.3.

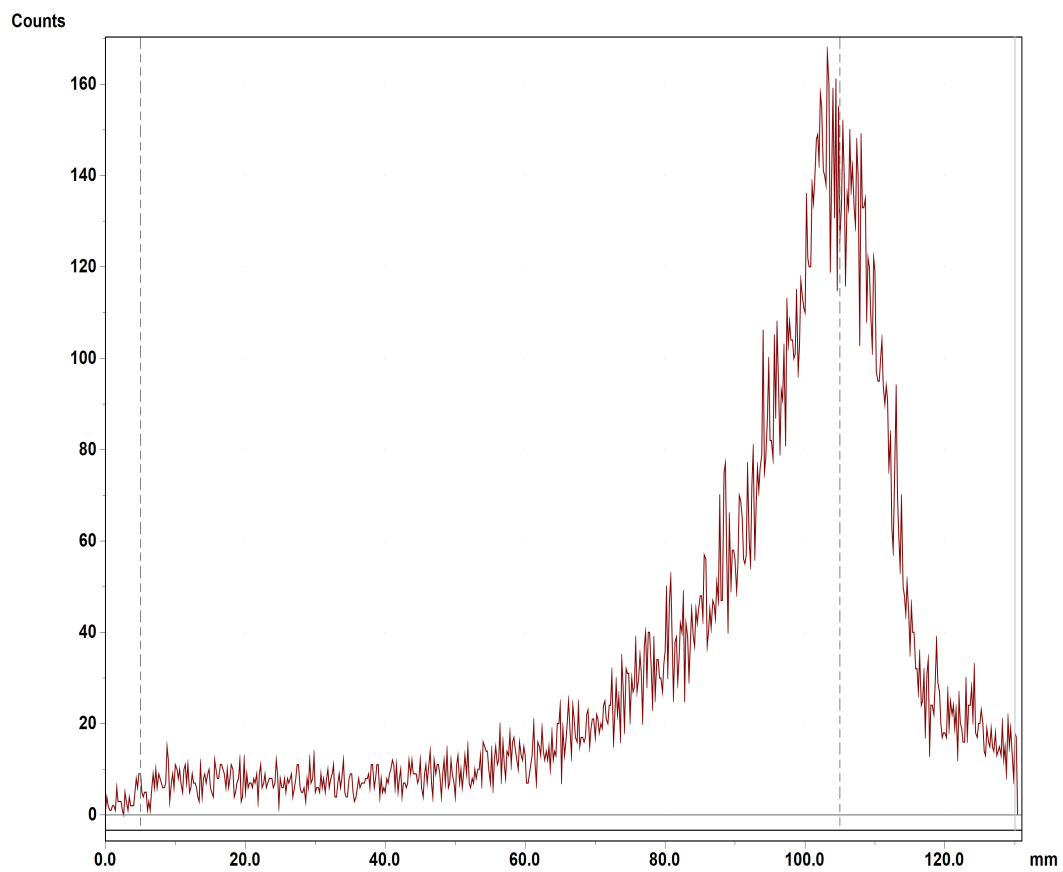


Figure 4.1. Free ^{89}Zr RTLC chromatogram.

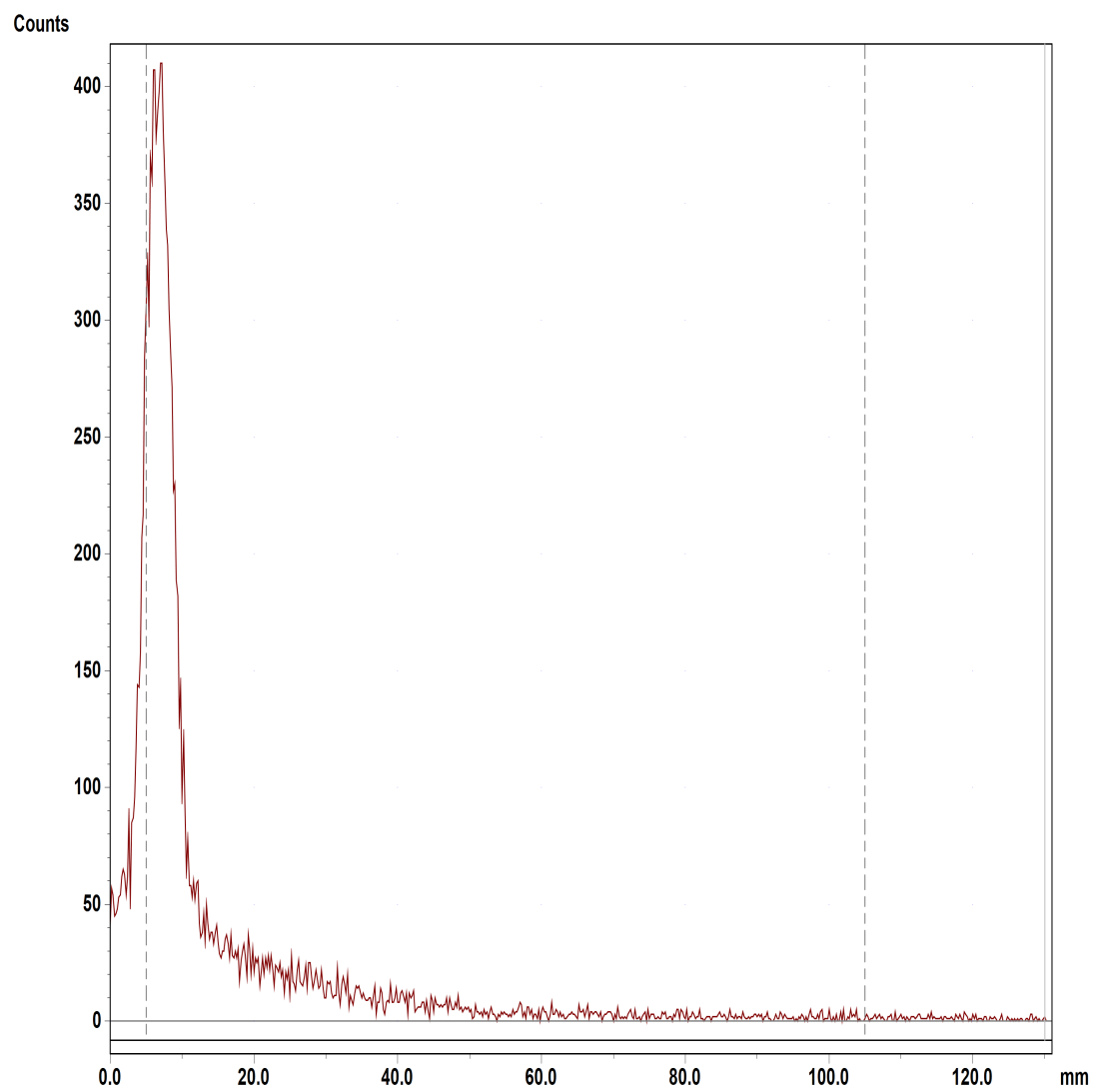


Figure 4.2. ^{89}Zr -Obi RTLC chromatogram.

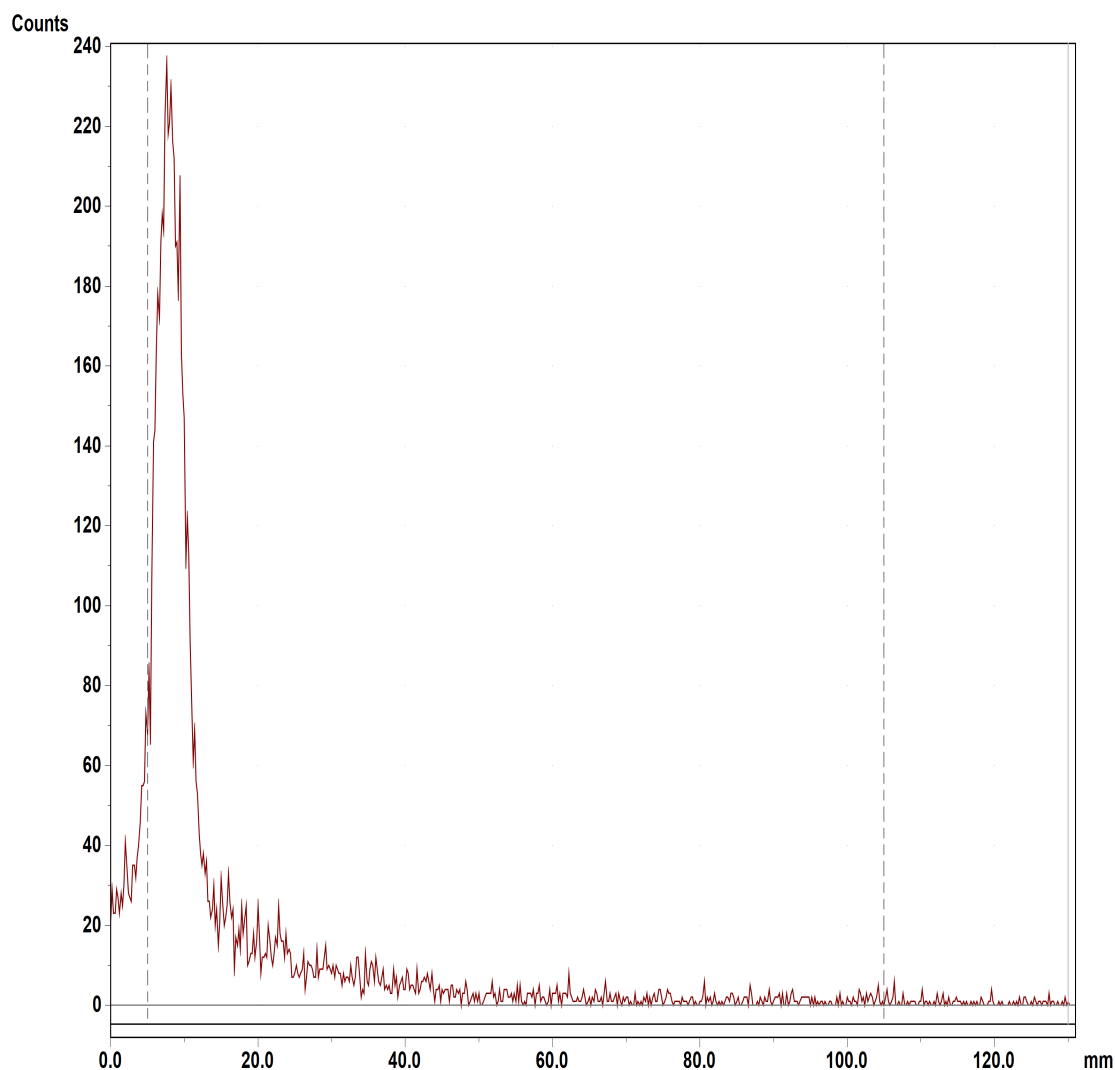


Figure 4.3. ^{89}Zr -Toc RTLC chromatogram.

Radio-HPLC

RHPLC analyzes were done as explained in the Section 3.6. RHPLC results were shown in Figure 4.4. Results showed that ^{89}Zr -Obi and ^{89}Zr -Toc were radiolabelled successfully, and also their labelling yields (ROI%) were found within the limits (Table 4.6). Our results are found parallel to the previous studies (88). Free ^{89}Zr , Obi-stock and Toc-stock solutions also were analyzed to provide a better understanding of the ^{89}Zr -Obi and ^{89}Zr -Toc peaks. The chromatograms showed free ^{89}Zr peak observed around 40th min whereas ^{89}Zr labelled antibodies, proteins etc., peaks were generally obtained in between 20th and 30th min (83, 84, 89).

Our results were also in good agreement with this data: ^{89}Zr -Obi and ^{89}Zr -Toc peaks were found around the 25th min while free ^{89}Zr was obtained at the 40th min.

Table 4.6. ROI (%) values of each formulations.

Formulation	mAb:DFO-p-Bz- NCS: ^{89}Zr (Molar Ratio)	Impurity (*)	ROI (%)	
			^{89}Zr -mAb	Free ^{89}Zr
Formulation 1	1:10:10 ⁻¹	2.27	97.73	0
Formulation 2	1:1:10 ⁻¹		87.28	12.72
Formulation 3	1:15:10 ⁻¹	5.47	94.53	0
Formulation 4	1:10:2.10 ⁻¹		91.2	8.2
Formulation 5	1:10:1.410 ⁻¹		94.70	2.50
Formulation 6	1:10: 0.6. 10 ⁻¹		100	0
Formulation 7 (Control)	1:10:10 ⁻¹		100	0

(*) The impurities are thought to come from the ingredients of commercial product (from other excipients etc.).

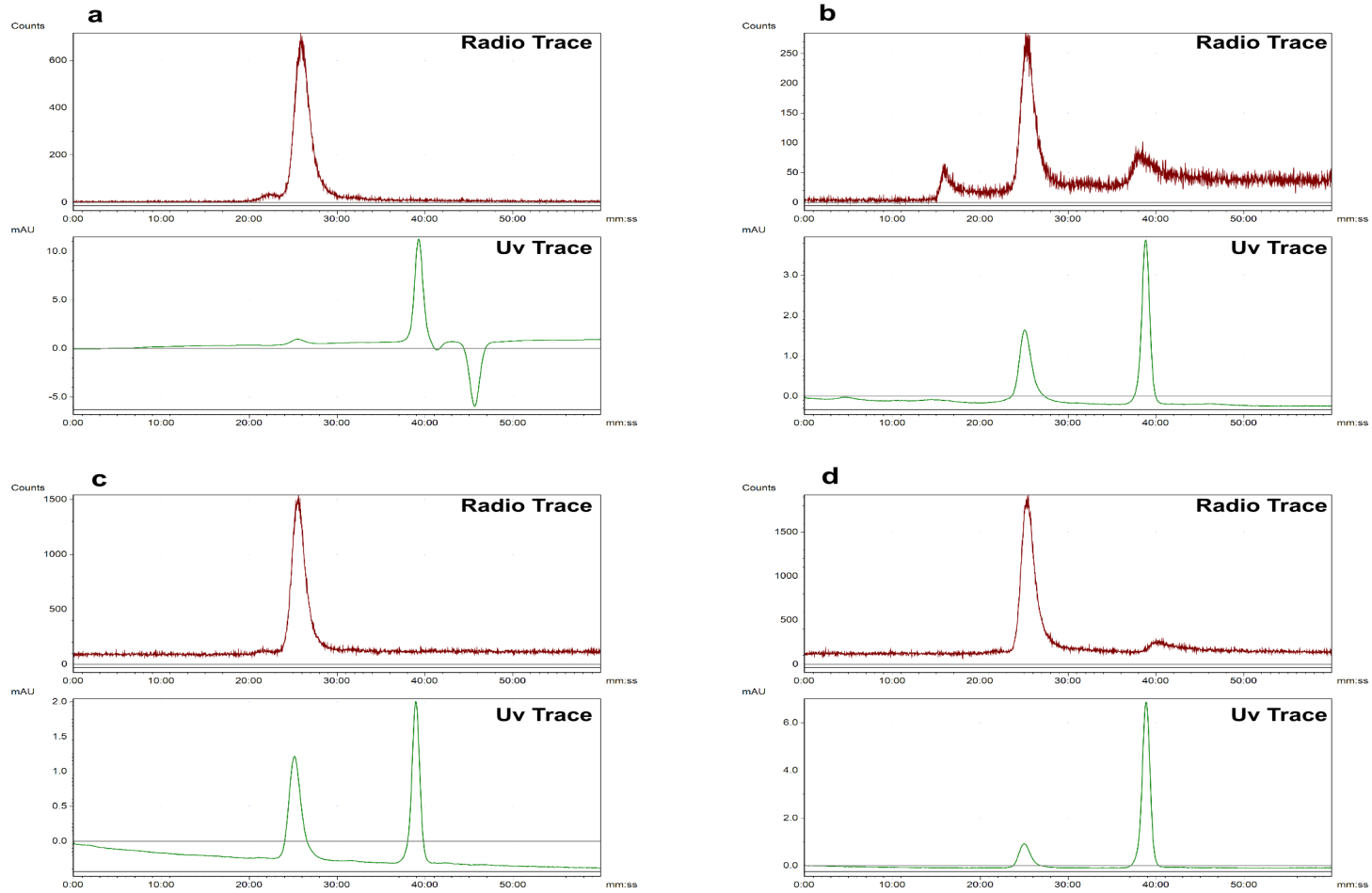


Figure 4.4. RHPLC chromatograms of formulations.

a) Formulation 1 b) Formulation 2 c) Formulation 3 d) Formulation 4 e) Formulation 5 f) Formulation 6 g) Free ^{89}Zr h) Formulation 7.

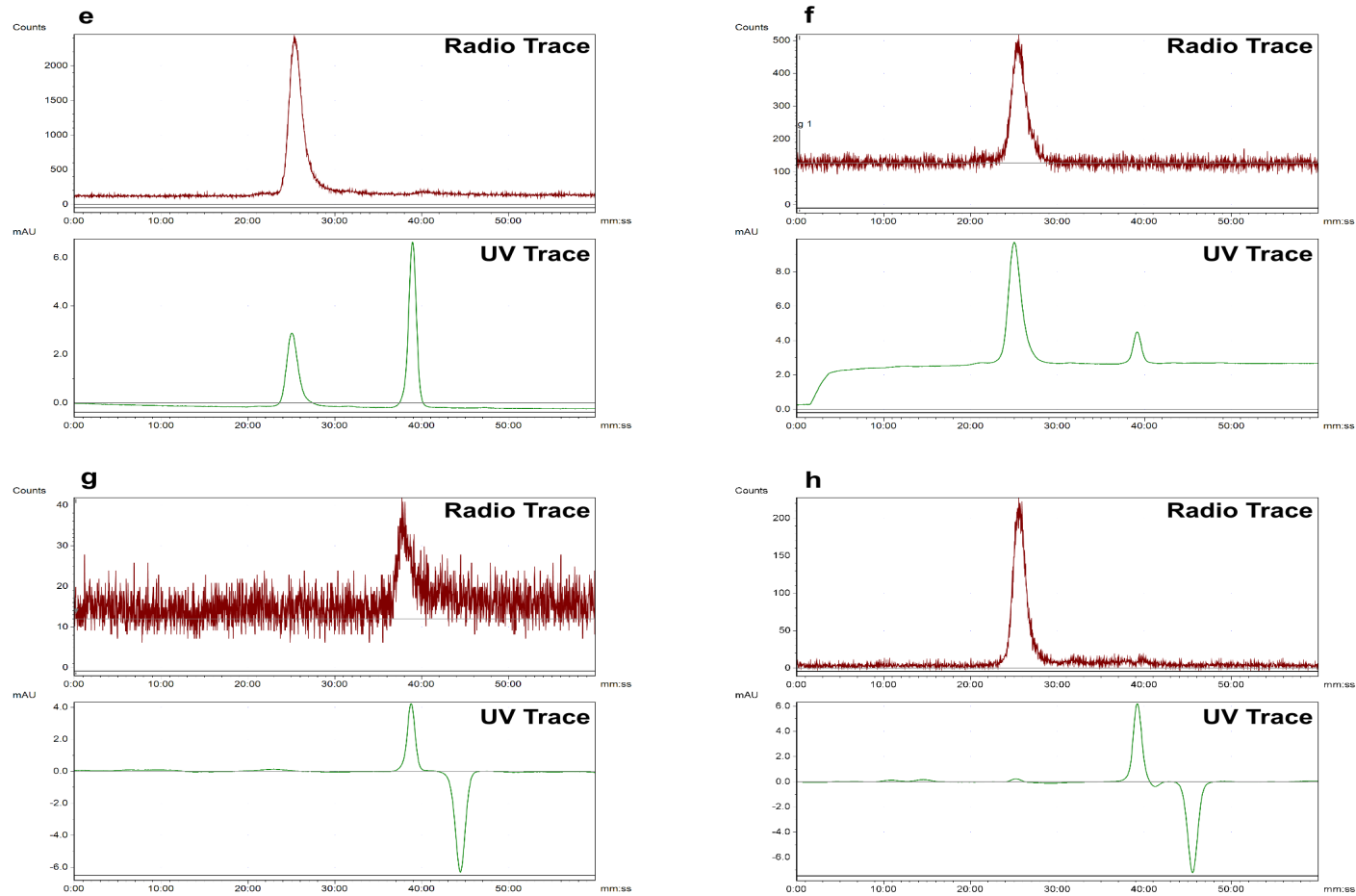


Figure 4.4. RHPLC chromatograms of formulations (Continued).

a) Formulation 1 b) Formulation 2 c) Formulation 3 d) Formulation 4 e) Formulation 5 f) Formulation 6 g) Free ^{89}Zr h) Formulation 7

4.6. Stability

Stability tests were performed as explained in section 3.7. ROI values are given at Table 4.7 and Figure 4.6; stability results of ^{89}Zr -Obi are given at Figure 4.7 and RHPLC peaks are shown at Figure 4.8.

Table 4.7. Stability test results of ^{89}Zr -Obi formulation by RHPLC.

Time (h)	ROI (%)			
	Impurity	Free ^{89}Zr	^{89}Zr -mAb	^{89}Zr -mAb/Total
0	3.76	0	96.24	96.24
4	3.68	0	96.32	96.32
24	3.87	5.64	90.49	94.13
48	5.20	14.96	79.84	84.21
60	3.54	28.98	67.48	69.95
72	4.87	42.62	52.51	55.19
90	4.53	48.98	46.50	48.70

After 4 h incubation, ROI (%) of ^{89}Zr -Obi was observed in 96.32% while free ^{89}Zr was not observed. However, (^{89}Zr -Obi/total) activity ratio was found 94.13% at 24th h which meant a minimal decomposition of ^{89}Zr -Obi found around 24th. The ratio decreased each time point after 24th h and 84.21% was found at 48th h. A significant difference was found among 69.95 %, 55.19 % and 48.4% at the time points of 60th, 72th and 90th h, respectively ($p < 0.05$).

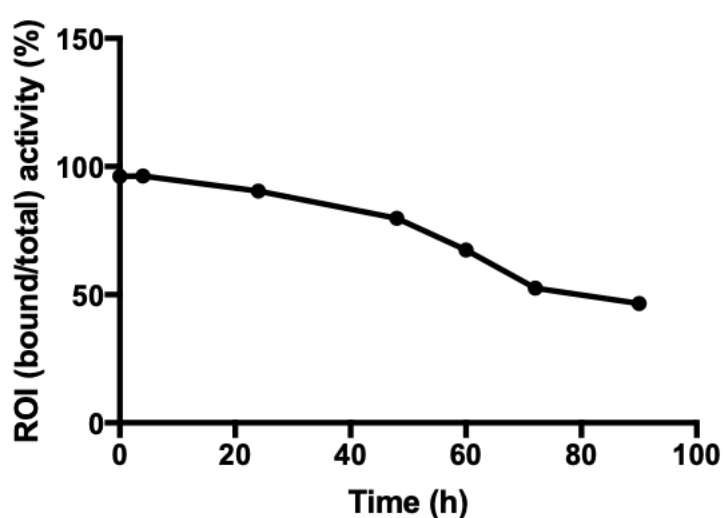


Figure 4.5. Stability results in saline (0.9% NaCl) after 96 h incubation at 37°C (n:3).

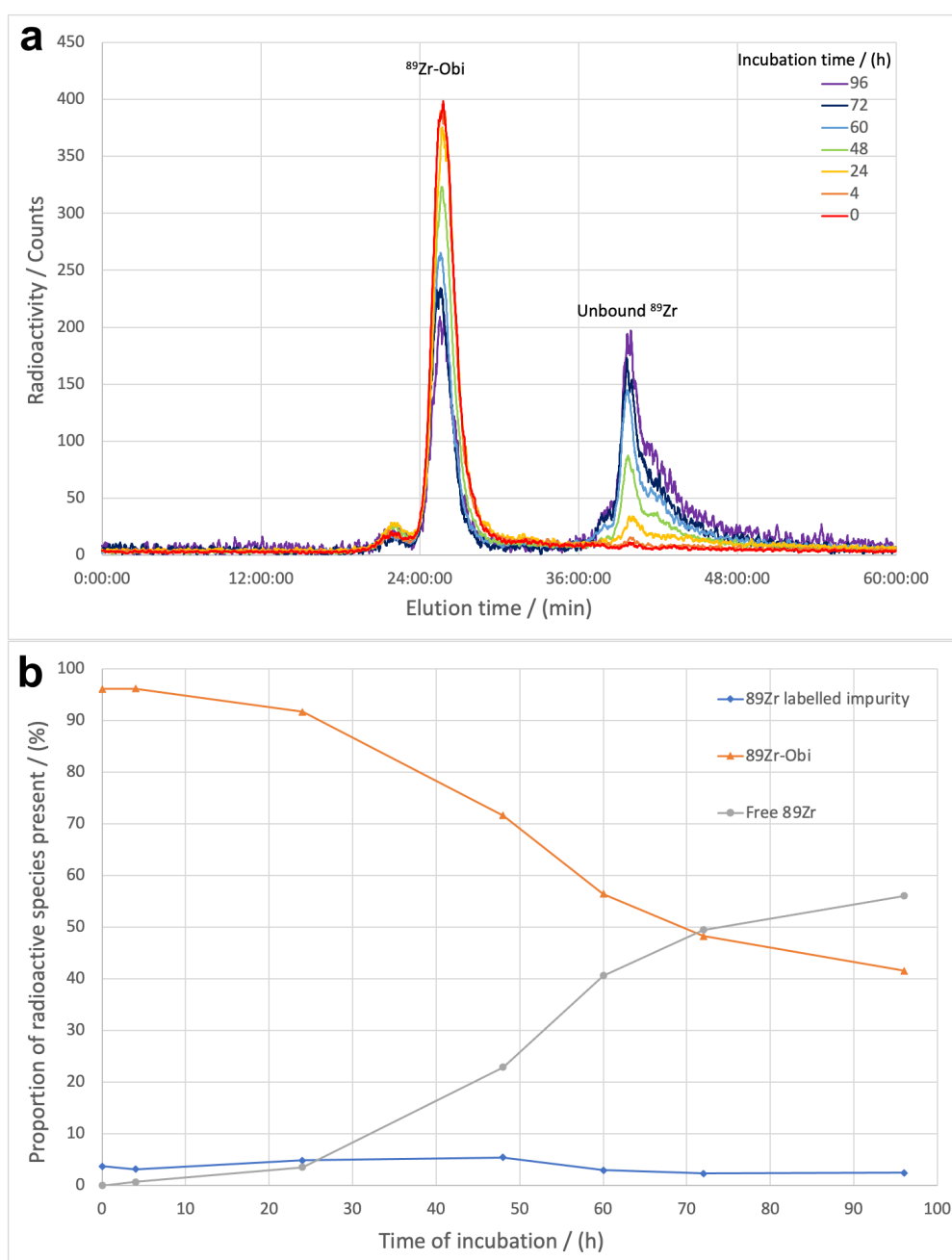


Figure 4.6. Stability results of ^{89}Zr -Obi incubated at 37°C in saline (0.9% NaCl) between 0-96 hours.

a) Radio-HPLC traces. b) Integrated ROIs from Radio-HPLC traces expressed as % of total ROI area.

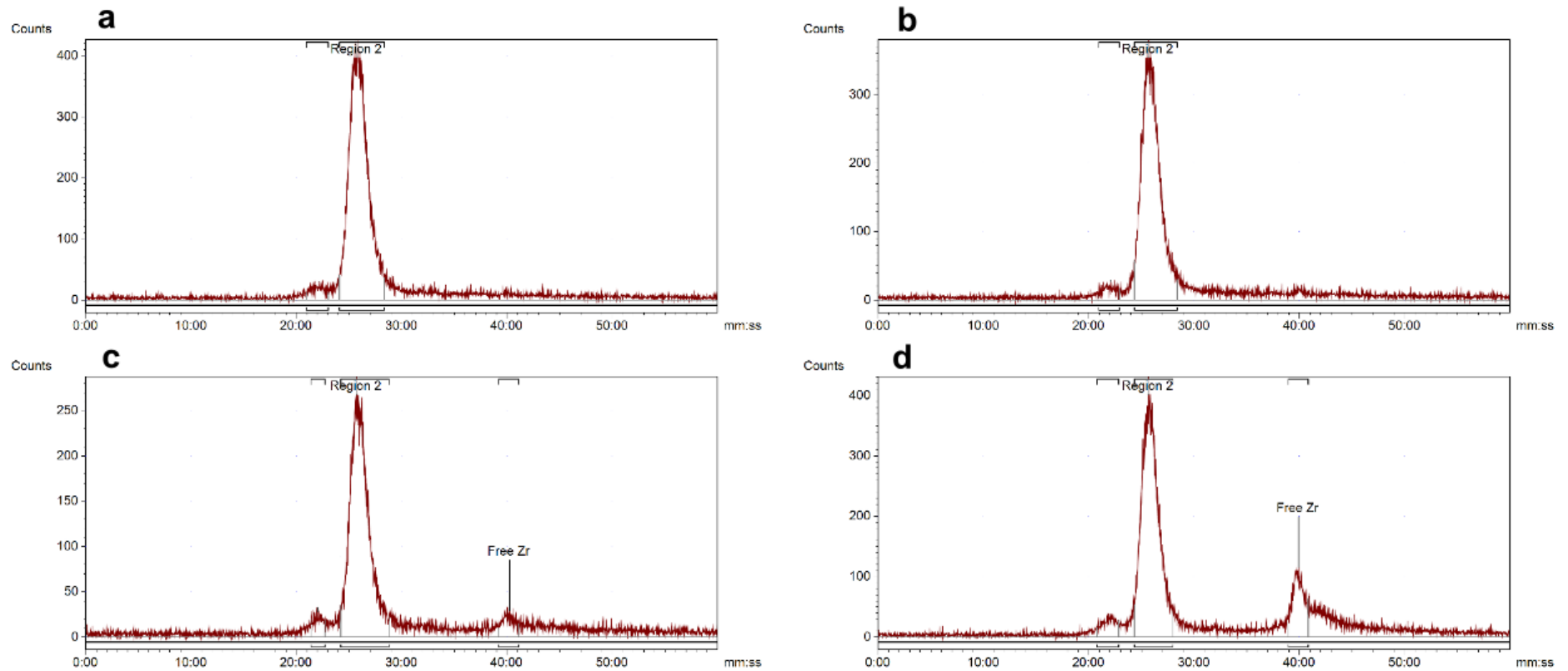


Figure 4.7. RHPLC peaks of ^{89}Zr -Obi stability tests.

a) 0 h b) 4 h c) 24 h d) 48 h e) 60 h f) 72 h g) 96 h of incubations (* Region 2 : ^{89}Zr -mAb peak).

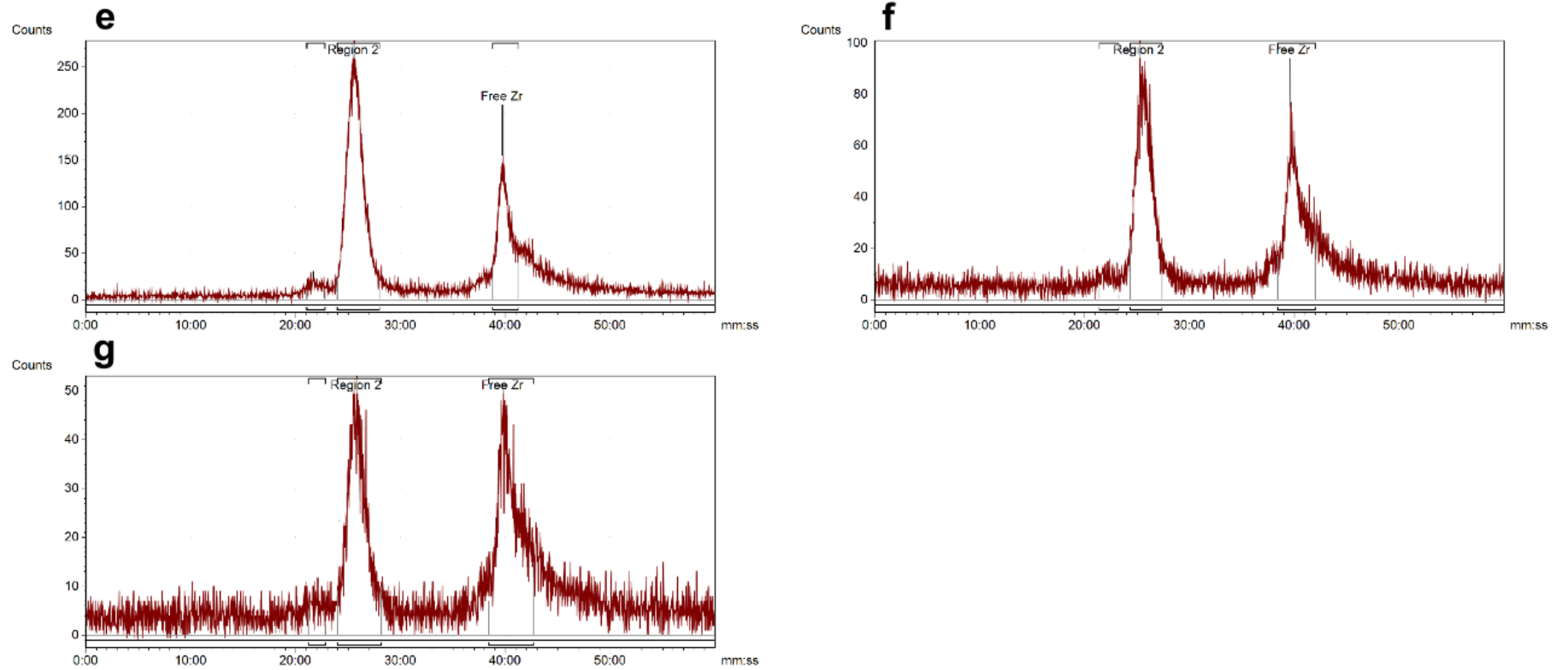


Figure 4.7. RHPLC peaks of ^{89}Zr -Obi stability tests (continued).

a) 0 h b) 4 h c) 24 h d) 48 h e) 60 h f) 72 h g) 96 h of incubations (* Region 2 : ^{89}Zr -mAb peak).

4.7. In-vitro Cell Culture Study Results

4.7.1. Immuno-reactivity Studies

Immuno-reactivity studies were performed as described in Section 3.8.1. Results are summarized in Table 4.8 and Table 4.9. Immuno-reactivity graphs were depicted at Figure 4.8, Figure 4.9 and Figure 4.10, showing the binding fraction of ^{89}Zr -Obi and ^{89}Zr -Toc with CD20 (+) Ramos cells and ^{89}Zr -Obi with HL 60 cells. According to the results, ^{89}Zr -Obi with Ramos cells showed high immuno-reactivity (60.9161%) as expected; however, ^{89}Zr -Toc with Ramos cell did not exhibit any significant immuno-reactivity (2.3806%). On the other hand, when ^{89}Zr -Obi with Ramos cells (CD20 (+)) and ^{89}Zr -Obi with HL 60 cells (CD20 (-)) were compared with each other, the data proved that Obi has specificity only for the CD 20 (+) cells (Table 4.11).

Table 4.8. Immuno-reactivity results of ^{89}Zr -Obi and ^{89}Zr -Toc in Ramos and HL 60 cells (mi: million).

Cell Type	Formulation	Cell Concentration (mi cell.ml ⁻¹)	Inverse Cell Concentration (ml.mi cell ⁻¹)	Activity (Total/Specific) (kBq)
Ramos Cells	^{89}Zr -Obi	10	1	2.254040
		8	0.125	2.295126
		6	0.166	2.624033
		4	0.25	4.614268
		3	0.333	3.948665
		1	0.1	9.188495
Ramos Cells	^{89}Zr -Toc	10	1	44.479363
		8	0.125	55.061930
		6	0.166	43.267151
		4	0.25	49.475844
		3	0.333	36.084956
		1	0.1	34.811948
HL 60 cells	^{89}Zr -Obi	10	1	10.541530
		8	0.125	17.609610
		6	0.166	17.343640
		4	0.25	15.190360
		3	0.333	25.774940
		1	0.1	18.193060

Table 4.9. Immuno-reactivity values of studied formulations.

Formulation	r	1/r	Immuno-reactivity (%)
^{89}Zr -Obi – Ramos Cells	1.6416	0.609116	60.9161
^{89}Zr -Toc – Ramos Cells	42.005	0.023806	2.3806
^{89}Zr -Obi – HL 60 Cells	16.141	0.061954	6.1954

(r: correlation coefficient).

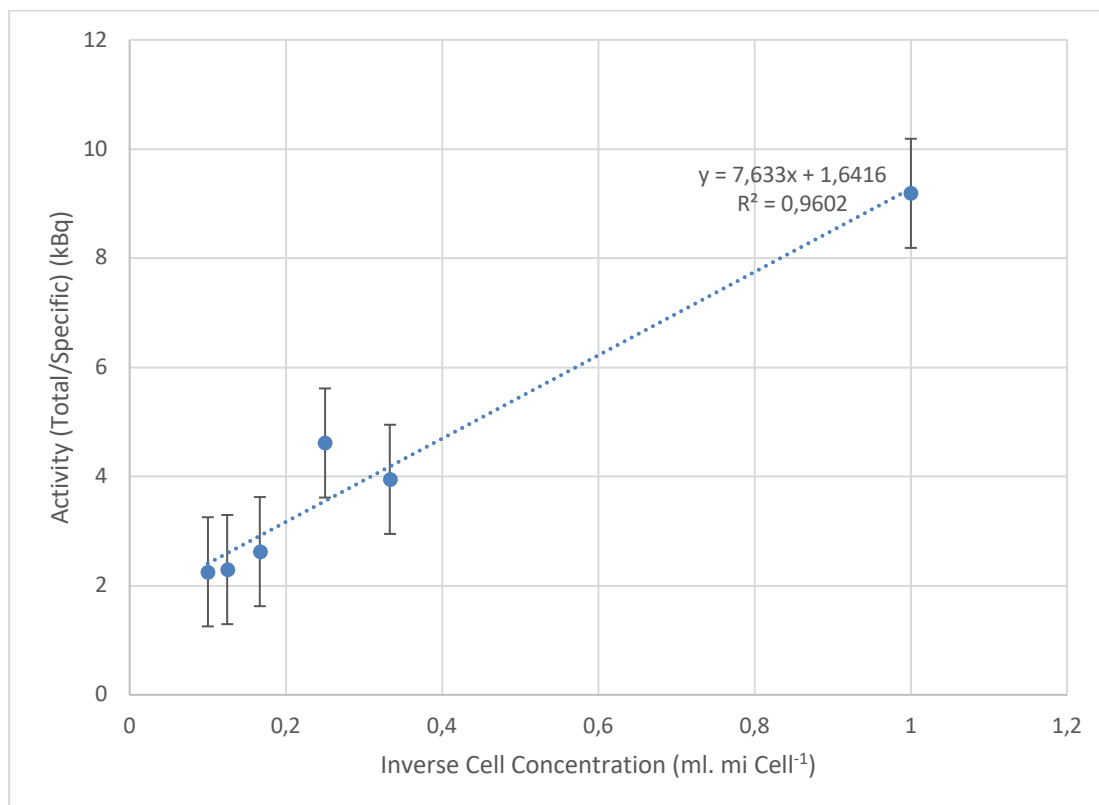


Figure 4.8. Immuno-reactivity determination of ⁸⁹Zr-Obi with Ramos cells (n:3).

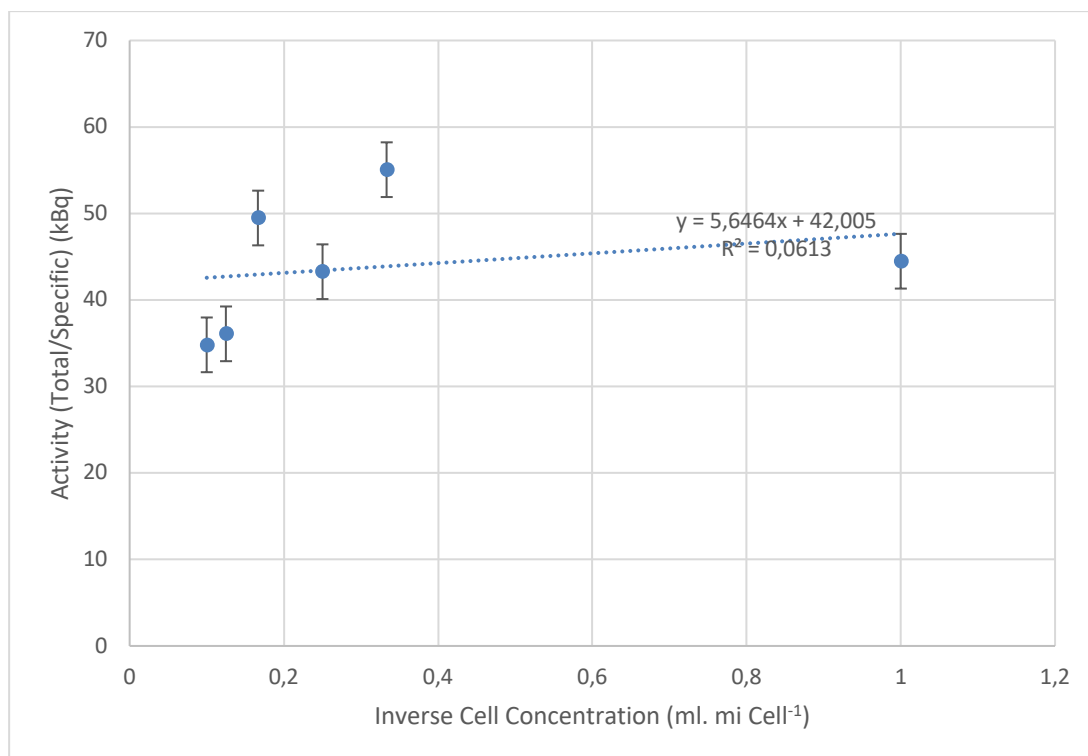


Figure 4.9. Immuno-reactivity determination of ⁸⁹Zr-Toc with Ramos cells (n:3)

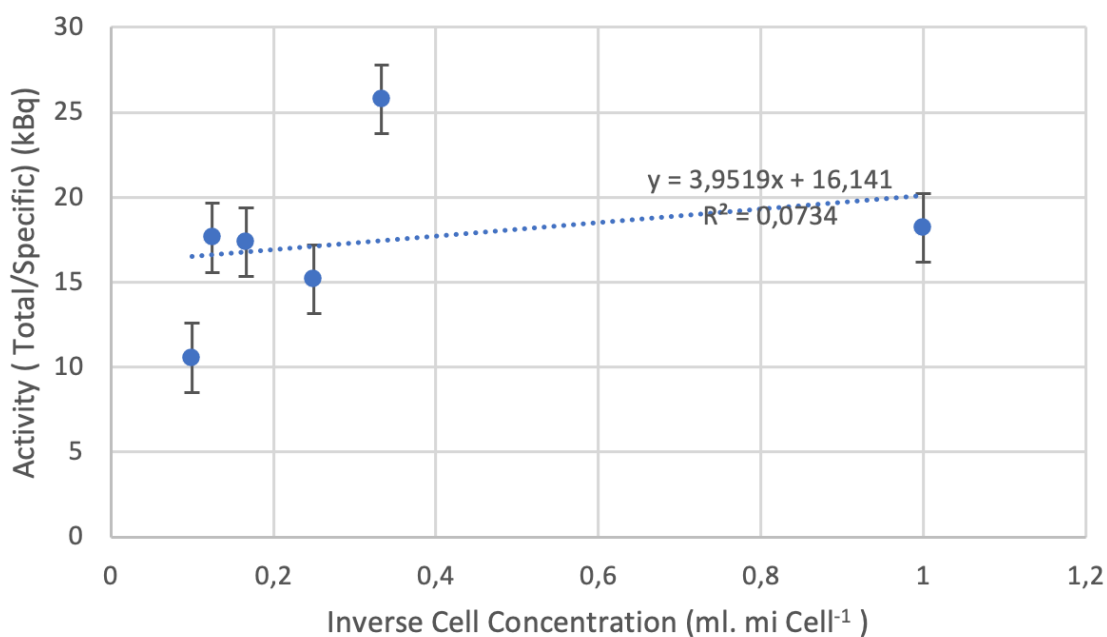


Figure 4.10. Immuno-reactivity determination of ⁸⁹Zr-Obi with HL 60 cells (n:3).

4.7.2. Binding Assay Studies

The binding assay was only performed for ⁸⁹Zr-Obi on Ramos cells to show its affinity to CD 20 (+) Ramos cells. Binding assay results are summarized in Table 4.10 and Table 4.11. According to the results, it was observed that the binding increased with the increasing concentration, with EC₅₀ 16.1 μM, but there was a threshold value. On the other hand, the K_d value was found to be 27.3 nM. When this limit value was reached, the percentage of binding did not increase despite the increasing concentration (Figure 4.12).

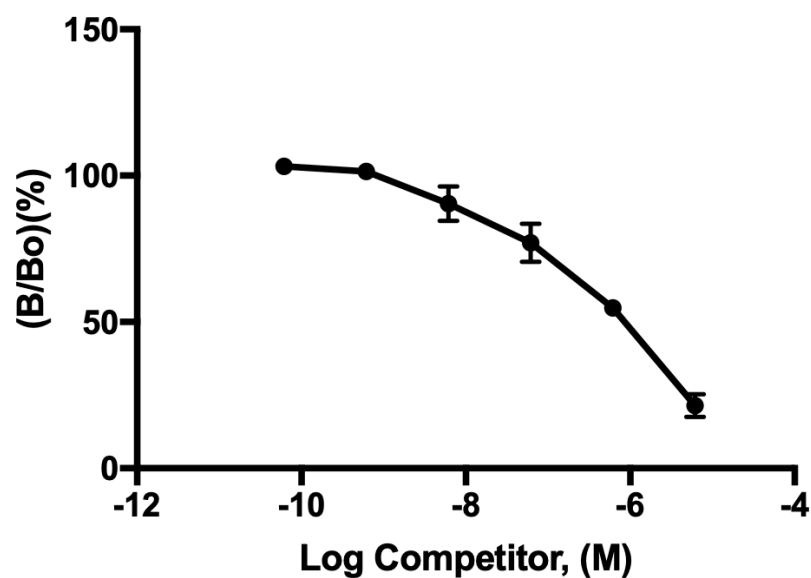
Table 4.10. Obi concentration and competitor values.

Samples	Concentration (mg.ml ⁻¹)	Antibody Mass (kDa)	Molarity (mol. L ⁻¹)	Log (B)
1	0.9	146064,72	6,16E-06	-5,210302975
2	0.09	146064,72	6,16E-07	-6,210302975
3	0.009	146064,72	6,16E-08	-7,210302975
4	0.0009	146064,72	6,16E-09	-8,210302975
5	0.00009	146064,72	6,16E-10	-9,210302975
6	0.000009	146064,72	6,16E-11	-10,21030297

Table 4.11. Binding assay results of ⁸⁹Zr-Obi with Ramos cells.

Concentration (mg.ml ⁻¹)	Log (B)	(B/Bo) (%)
0.9	-10,210419	103,641224
0.09	-9,2104193	101,248923
0.009	-8,2104193	94,563705
0.0009	-7,2104193	72,4955277
0.00009	-6,2104193	56,7730074
0.000009	-5,2104193	24,203273

(B:Competitor, Bo:Non-competitor).

**Figure 4.11.** Binding activity of ⁸⁹Zr-Obi with Ramos cells

(B:Competitor, Bo:Non-competitor) (n:3).

4.8. In-Vivo Animal Study Results

4.8.1. PET/CT Imaging Studies

Animal studies were performed as explained in Section 3.9.1. Nano PET/CT images of ^{89}Zr -Obi for Ramos and HL 60 cells and control group are shown in Figure 4.12 and Figure 4.13 and Figure 4.14. Images showed that ^{89}Zr -Obi was uptaken primarily in the spleen, as expected because of lymphoma cells. However, the interesting part of these images was spleen uptake found for all mice, although spleen uptake was expected only for Ramos cell injected mice. Both control and HL 60 cells injected mice have also shown spleen uptake, although the same uptake amount was not observed for Ramos cell injected mice.

^{89}Zr -Obi, injected dose per gram (ID/g) % values per organs were calculated (Figure 4.15). The only significant differences have been observed in between livers of Ramos injected mice and control group, and HL60 injected mice and control group ($p < 0.05$). However, there was no difference observed in liver uptake between Ramos cell injected mice and HL60 cell injected mice ($p > 0.05$) (Figure 4.16). Finally, there was no significant difference observed in other organs between groups ($p > 0.05$).

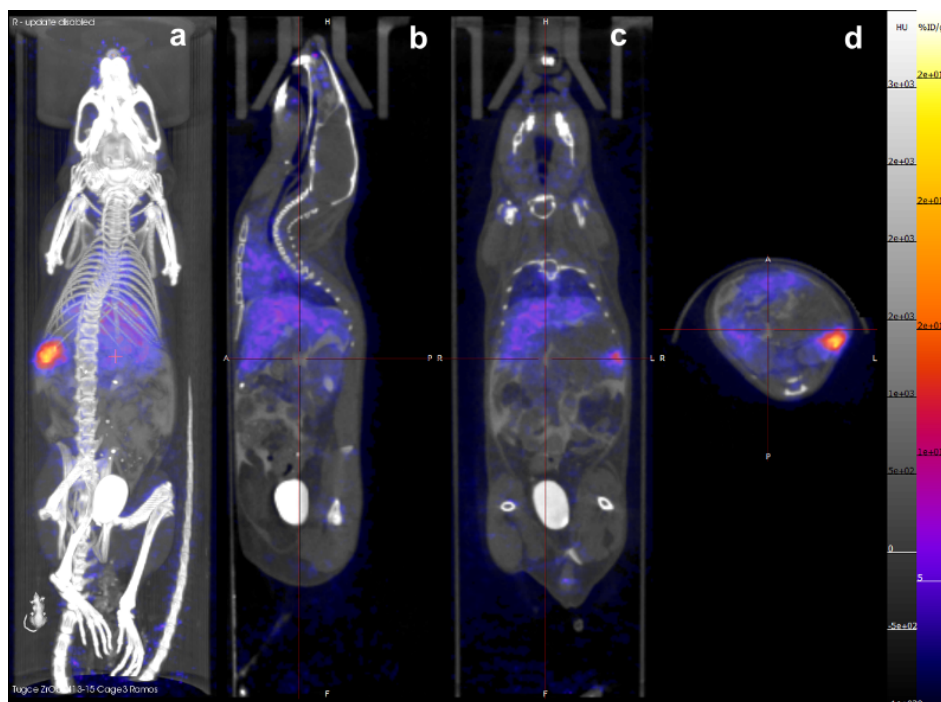


Figure 4.12. Nano PET/CT images of Ramos cell injected mice six days after ^{89}Zr -Obi injection

(a: coronal b: right c: left d: transaxial images).

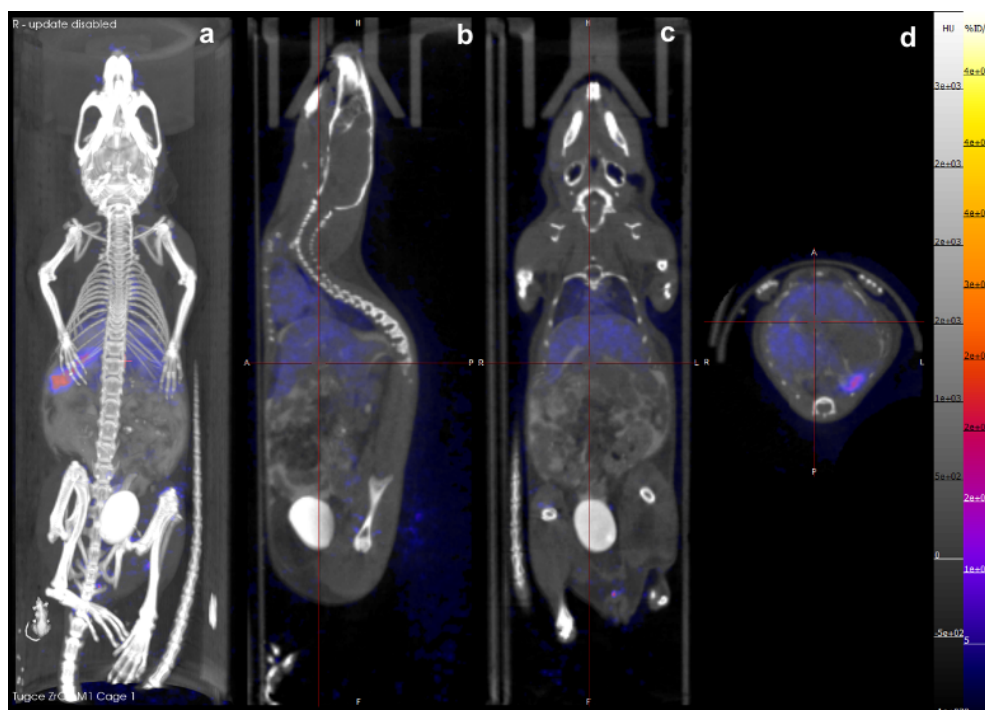


Figure 4.13. Nano PET/CT images of HL 60 cell injected mice six days after ^{89}Zr -Obi injection

(a: coronal b: right c: left d: transaxial images).

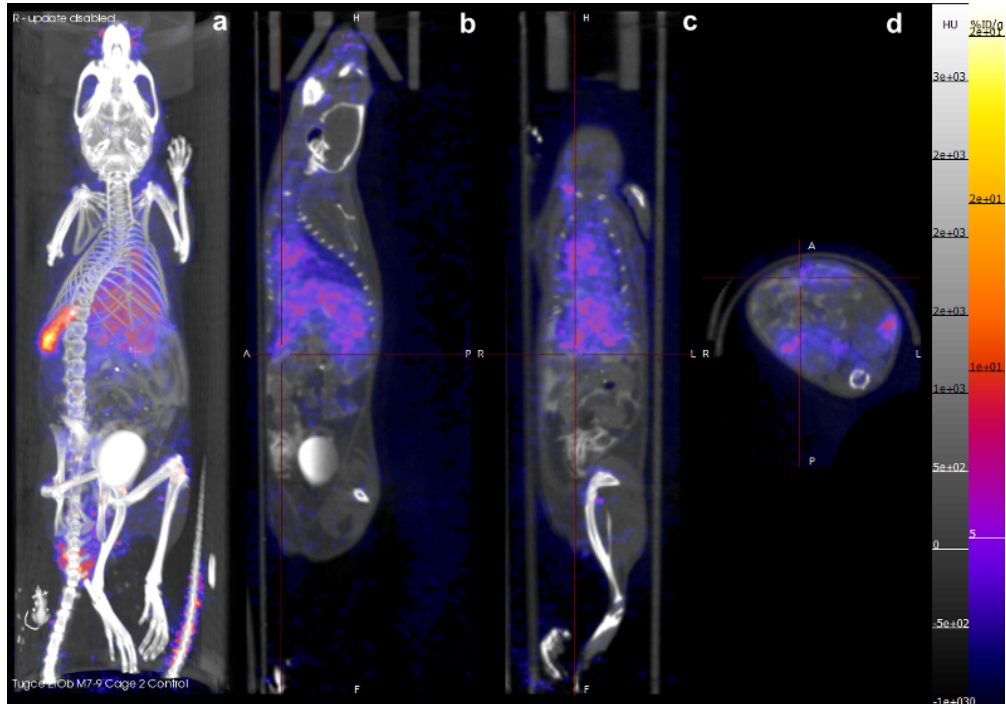


Figure 4.14. Nano PET/CT images of control mice six days after ^{89}Zr -Obi injection

(a: coronal b: right c: left d: transaxial images).

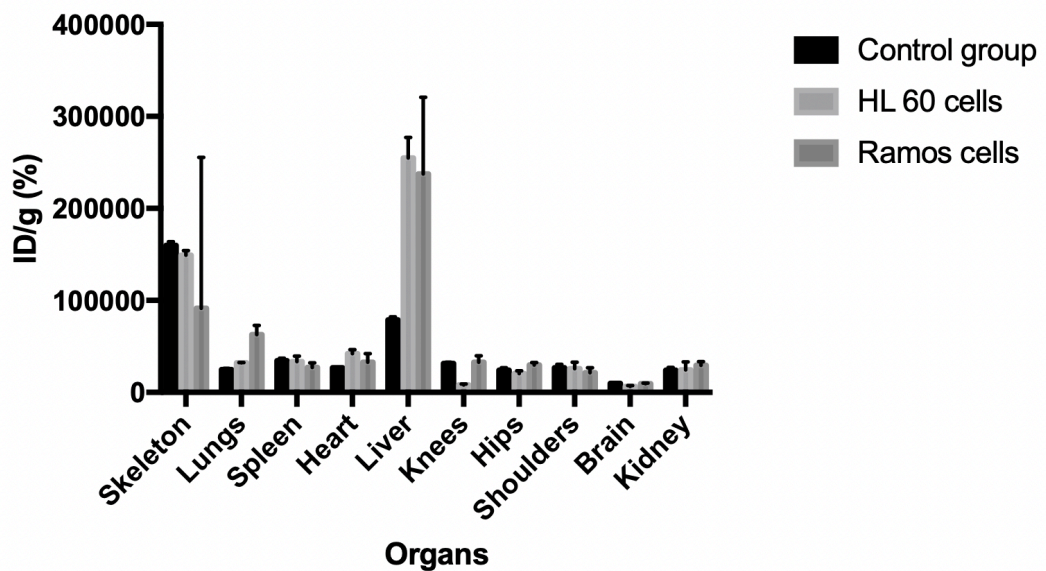


Figure 4.15. Percentage of ID/g value for each organ of each group of female SCID mice.

4.8.2. Biodistribution Studies

Biodistribution studies were performed as described in Section 3.9.2. and results are given in Figure 4.17 and Table 4.12. The uptake of ^{89}Zr -Obi/Ramos cells injected animals were not significantly different from animals injected with HL 60 cells and designated as the control group (Figure 4.30) ($p>0.05$).

Table 4.12. Biodistribution results of ^{89}Zr -Obi injected mice in different animal groups.

Mouse	Injected Cells	Weight (g)	Injected Activity (mBq)	Whole Mouse Activity (mBq)	InjectionTime 21.04.21 (p.m)	Measured Activity (CPS)						
						Spleen	Liver	Kidney	Lung	Brain	Femur	Heart
Mouse 1	Ramos	18.82	1.62	0.44	16:14	2391.4	16617.4	2571.4	1100.6	208.2	1468.6	1272.8
Mouse 2	Ramos	20.54	1.69	0.45	16:14	2409.6	15865.9	2478.4	1760.4	232.1	1975.6	952.5
Mouse 3	Ramos	19.68	1.55	0.41	17:30	2570.2	14772.7	2503.9	1376.7	283.5	1844.4	1081.0
Mouse 4	Ramos	18	1.71	0.46	17:30	2968.3	16995.1	2548.8	1773.3	215.4	2021.6	1009.1
Mouse 5	Ramos	19.59	1.5	0.41	17:30	1963.8	14471.1	2287.8	1700.3	235.8	1800.6	950.7
Average						2460.6	15744.4	2470.1	1542.2	235.0	1822.1	1053.2
Mouse 1	HL 60	19.15	1.66	0.44	12:35	2555.0	16654.7	2065.3	1250.2	206.7	2314.9	1025.6
Mouse 2	HL 60	21.1	1.34	0.36	12:55	2331.3	14577.8	2335.3	1569.8	163.9	1527.7	508.5
Mouse 3	HL 60	18.23	1.19	0.37	12:05	2731.7	13714.1	2360.2	2088.1	174.6	1834.8	799.4
Mouse 4	HL 60	17.63	1.35	0.38	13:20	2734.8	15562.0	2719.0	1273.9	211.4	1794.3	469.7
Mouse 5	HL 60	20.18	1.32	0.42	13:20	3093.1	16608.1	2301.9	901.7	250.7	1953.5	1268.9
Average						2689.1	15423.3	2356.3	1416.7	201.4	1885.0	814.4

Table 4.12. Biodistribution results of ^{89}Zr -Obi injected mice in different animal groups (**continued**).

Mouse	Injected Cells	Weight (g)	Injected Activity (mBq)	Whole Mouse Activity (mBq)	InjectionTime 21.04.21 (p.m)	Measured Activity (CPS)						
						Spleen	Liver	Kidney	Lung	Brain	Femur	Heart
Mouse 1	Control	17.1	1.65	0.46	13:20	3259.4	17048.5	2757.8	1875.4	242.0	2108.1	1239.2
Mouse 2	Control	20.52	0.7	0.2	14:58	1297.5	7075.5	1211.7	621.9	75.7	793.5	552.0
Mouse 3	Control	19.46	1.45	0.4	14:58	2489.1	14140.4	2296.2	1070.2	306.2	1758.6	1840.3
Mouse 4	Control	18.67	1.62	0.44	14:48	2657.5	17235.4	2643.6	1631.3	150.2	1869.8	1411.2
Mouse 5	Control	18.28	1.5	0.39	16:14	2244.9	12755.8	2028.6	1516.4	253.2	1594.3	1334.3
Average						2389.6	13651.1	2187.5	1343.0	205.4	1624.8	1275.4

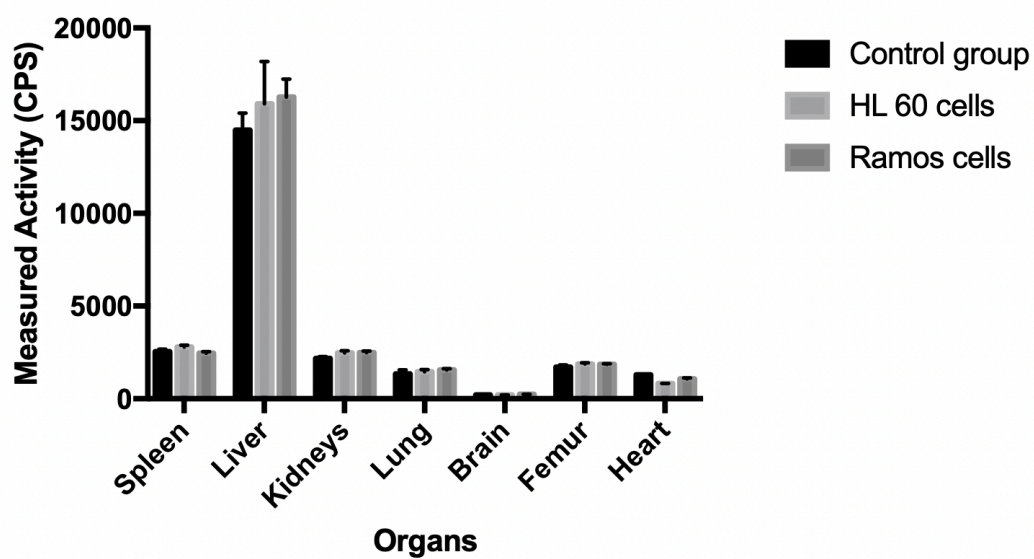


Figure 4.16. Biodistribution results of ^{89}Zr -Obi in different animal models (HL60 cells, Ramos cells and control groups).

5. DISCUSSION

Cancer is one of the diseases that occurs due to uncontrollable cell division and causes deaths at the highest numbers worldwide. Lymphoma is a type of cancer frequently encountered in adults and childhood, originates from lymphocyte cells, and is classified according to whether B or T type depending on the affected cells. NHL, the most common subtype, showed an increasing incidence, especially between 1980-1990, and it is still the most common type of lymphoma today. According to 2020 data, 544,000 new NHL cases were detected, while 260,000 deaths occurred. Burkitt's lymphoma is the most common subtype of NHL in children in the world and the most common subtype in children in the UK (45). In Turkey, according to 2016 statistics, NHL is the 6th most common cancer type (46). Considering all these reasons and the fact that early diagnosis makes a significant difference, within the scope of this thesis, it is aimed to develop mAb type radiopharmaceutical formulations to be used in the early diagnosis of NHL.

Immuno-PET, developed in the 1990s, is one of the detection methods for imaging radiopharmaceutical biodistribution with PET, obtained as a result of labelling of bioactive molecules with radionuclides. Combining mAbs, the most commonly used bioactive molecules with PET radionuclides, is a fascinating research field because of its high sensitivity and resolution. In addition, mAbs can rather easily be labelled with radionuclides and have appropriate emissions for optimum resolution. In addition, the radionuclide ^{89}Zr has been used for labelling of mAbs, which has a favourable half-life and has therefore gained increasing popularity (38, 90) recently. Therefore, it is planned to label mAbs in this study.

CD20 antigen-specific mAbs used in the diagnosis/treatment of lymphoma; rituximab, tositumomab, obinutuzumab, ofatumumab etc., have clinical therapeutic uses. Among all these used mAbs, "Obi", which is relatively new in the market, has very limited studies on it and is still being done, has been chosen in this research. Unlike rituximab, which is available in the market and has radionuclidic labelling property, obinutuzumab shows high antibody-dependent cell-mediated cytotoxicity and can bind to CD20 antigen at a lower density than rituximab.

Among the limited studies on obinutuzumab, only one study has recently been reported on labelling with ^{89}Zr radionuclide. Yoon et al. (2018), in this study, labelled

obinutuzumab and ofatumumab (new generation), rituximab and tositumomab (previous generation) mAbs, and compared with the Raji cells. Additionally, in-vivo studies have been performed on tumours created by subcutaneous injection of Raji cells. In this research, Obi, approved by the FDA 3 years ago for the use in the treatment of lymphoma, was used for the early diagnosis of Burkitt's lymphoma, a subclass of NHL. CD20 (+) and Ramos cells forming Burkitt's lymphoma and CD20 (-) HL60 cells were used as the control group to evaluate the efficacy of the radiopharmaceutical formulation developed as a result of labelling obinutuzumab with ^{89}Zr . To prove the effect of ^{89}Zr -Obinutuzumab formulation on Burkitt's lymphoma, tocilizumab, showing no CD20 specificity, was also labelled with ^{89}Zr .

In this section, several identification tests SDS-PAGE, ELISA, UV spectrophotometry analyze should be performed on Obi and Toc, as pharmaceutical part of the radiopharmaceutical formulations, before the production of ^{89}Zr and the labelling of antibodies. However, the product of Obi, which is available in the market under the name of "Gazyva", was given as a gift by the "Roche" company, for only this thesis studies. A mutual agreement was signed promising that no analysis that would fall within the scope of reverse engineering should not be performed on the "Gazyva". For this reason, recognition tests necessarily carried out on pharmaceutical parts (mAbs and conjugates) could not be included in this thesis.

5.1. ^{89}Zr Production and Purification

^{89}Zr production was carried out in cyclotron using the ^{89}Y solid target by Cardiff PET Research and Imaging Centre, University Hospital of Wales. After (p,n) bombardment of the solid target, the extraction and purification of ^{89}Zr from the solid target were carried out. The most important part before extraction was acid wash of all materials used in extraction process. It is important in terms of preventing of ^{89}Zr , as a radio-metal, from binding to possible metal ions and other substances remaining in the materials.

The materials to be used in the production of ^{89}Zr in oxalic acid were carefully prepared and ^{89}Zr was obtained in cassette system set up in the hot-cell as shown in Figure 3.11. Finally, ^{89}Zr was neutralized and its pH was adjusted to pH 7 to label mAbs. Neutralization of ^{89}Zr was done as described in Section 3.5.2.

Lin et al. (2016), compared the both form of ^{89}Zr -oxalate and ^{89}Zr -chloride for mAb labelling (91). As stated in this study, ^{89}Zr is widely produced from yttrium foil target with $^{89}\text{Y}(\text{p},\text{n})^{89}\text{Zr}$ reaction which was used in our ^{89}Zr production. As mentioned in many studies, ^{89}Zr -oxalate is successfully produced with this reaction and target type (91-93). ^{89}Zr -oxalate form is frequently used in mAb labelling (84). Therefore, ^{89}Zr -oxalate has been used in this research, also.

5.2. ^{89}Zr Formulation Studies

^{89}Zr radiolabelling of mAb process was basically carried out in 2 steps. The first step is the conjugation of mAb and DFO-p-Bz-NCS, bifunctional chelating agent. The second step consists of adding ^{89}Zr to the DFO-p-Bz-NCS -mAb conjugate solution and then radiolabelling occurs. The reason for being a 2-step process is primarily to increase the binding rate by providing mAb-chelating agent conjugation.

Formulation studies were carried out as described in Section 3.4. Based on the (mAb: DFO-p-Bz-NCS: ^{89}Zr) ratios used in literature (83, 84), formulations were prepared in different ratios of DFO-p-Bz-NCS and ^{89}Zr in order to determine the main ^{89}Zr -Obi formulation and to observe the effects of these ratios on the labelling efficiency. In addition, ^{89}Zr -Toc was specified as the control formulation and was compared with ^{89}Zr -Obi formulation for in-vitro and in-vivo studies.

5.3. ^{89}Zr Radiolabelling Process

The prepared formulations and their ratios (mAb: DFO-p-Bz-NCS: ^{89}Zr) were given in Table 3.10. The first important point in this step is the adjustment of the pH of the mAbs. At this point, the unknown ingredients of the commercial preparation "Gazyva-Roche" solution were changed to NaHCO_3 and its pH was adjusted to 8.9-9.1; otherwise the conjugation could not be achieved and the labelling with ^{89}Zr would not be successful. If Na_2CO_3 has been used instead of NaHCO_3 as a buffer solution, precipitation would be observed. Depending on all these data, the prepared formulations were not studied at different pHs. Instead, it was aimed to determine the results of different molar ratios of formulations prepared with only one (mAb: DFO-p-Bz-NCS: ^{89}Zr) composition obtained from the literature, which was also referred as the radiochemistry of the labelling. In this purpose, 7 different formulations (one of

them was control formulation) were prepared and different DFO amounts were used in Formulation 1, Formulation 2 and Formulation 3. Table 4.17 shows formulation amounts before and after pH change and purification process. After pH adjustment, purification was carried out to obtain conjugated DFO-p-Bz-NCS-mAb only, thereby removing unconjugated DFO-p-Bz-NCS, unconjugated antibodies, etc., and in this way, undesirable impurities coming from Gazyva were removed.

Among the others, there were several reasons for choosing the formulation of ^{89}Zr -Obi in the ratios of (mAb: DFO-p-Bz-NCS: ^{89}Zr) (1:10:10⁻¹) as the main formulation. The most important reason was the labelling efficiency. This radiolabelling efficiency was determined with radiochemistry studies. In addition, Vosjan et al. published the radiolabelling process in the same ratio of ^{89}Zr -mAb formulation with the high radiolabelling efficiency in the “Nature Protocol” in 2010 (83). Knight et al. also reported a study about ^{89}Zr -mAb radiolabelling and it has also been shown that by reducing the amount of radionuclide (micro level), the highest radioactivity can be achieved at the same ratio and with the high efficiency (84). Our results were found parallel to both literature (17, 20).

In this study, 6 different formulations of ^{89}Zr -Obi were prepared in different ratios of (mAb: DFO-p-Bz-NCS: ^{89}Zr). ^{89}Zr -Obi and ^{89}Zr -Toc were also prepared as the main and control formulations. As it was mentioned previously, the optimum ratio of (mAb: DFO-p-Bz-NCS: ^{89}Zr) was determined as (1:10:10⁻¹), however we prepared different ratios of them to verify this data. These results are discussed at the Section 5.4.1. in RHPLC results part. Our results were in good agreement with previous findings (83).

5.4. Quality Control Tests

5.4.1. Radiochemical Purity

Free ^{89}Zr can be found as a radiochemical impurity showing the labelling insufficiency in different Obi and Toc formulations. RHPLC analyzes determines the free ^{89}Zr (radiochemical impurity) while RTLC shows the free ^{89}Zr .

In order to determine the optimum ratio of (mAb: DFO-p-Bz-NCS: ^{89}Zr) in ^{89}Zr labelling of Obi, 6 different ratios of (mAb:DFO-p-Bz-NCS: ^{89}Zr) were prepared and RHPLC analyzes were carried out. In addition, free ^{89}Zr was determined for ^{89}Zr -

Obi and ^{89}Zr -Toc formulations in the same ratio of (mAb: DFO-p-Bz-NCS: ^{89}Zr) by using RTLC and RHPLC.

Radio-TLC

After the formulation preparations stated in the Section 3.6.1, the optimum ^{89}Zr -Obi and ^{89}Zr -Toc formulations were chosen and RTLC analyzes were performed as described in Section 3.6. To obtain better understanding of the differences between free ^{89}Zr ; ^{89}Zr -Obi and ^{89}Zr -Toc, RTLC analyzes of them were performed and the results were given in Section 4.5. The results showed that ^{89}Zr -Obi (main formulation) and ^{89}Zr -Toc (control formulation) do not have any ^{89}Zr impurities, that means our formulations, in the common ratio obtained from literature, showed 100% labelling yields. In order to verify these data, RHPLC analyzes were also carried out.

Radio-HPLC

RHPLC analyzes were performed on the formulations prepared in different (mAb: DFO-p-Bz-NCS: ^{89}Zr) ratios of main and control formulations were specified in Section 3.6. RHPLC analyzes for main and control formulations were performed to confirm the obtained RTLC results and to obtain more detailed and quantitative data. Whereas, the reason for the other formulations was to determine the effect of different (mAb:DFO: ^{89}Zr) ratios on the labelling efficiency.

RHPLC analyzes were performed as stated in Section 3.6. and the results obtained are given in Section 4.5. Comparison of labelling efficiency (%) of formulations prepared using different ratios (mAb: DFO-p-Bz-NCS: ^{89}Zr) are given in Figure 4.18. As observed, no free ^{89}Zr was observed in the ratio (1:10:10⁻¹) (mAb: DFO-p-Bz-NCS: ^{89}Zr) of Formulation 1 like the frequently used molar composition in the literature (83) and molar ratio used by the R&D laboratory of Wales PET and Imaging Research Center in UHW.

Whereas, 12.72% free ^{89}Zr was found in Formulation 2 which has (1:1:10⁻¹) ratio of (mAb: DFO-p-Bz-NCS: ^{89}Zr) (the free ^{89}Zr ratio obtained was not in acceptable limit (5%) (83)). This result may be a proof of the importance of the ratio of DFO-p-Bz-NCS used as a bifunctional chelating agent in the labelling of mAb and

^{89}Zr . We concluded that ^{89}Zr could not bind at the desired ratio in the absence of sufficient chelating agent and would remain in the form of free ^{89}Zr .

Free ^{89}Zr was not detected in Formulation 3 which was in the ratio of (1:15:10⁻¹) (mAb: DFO-p-Bz-NCS: ^{89}Zr). Considering that, there were no factors affecting the labelling efficiency from other parameters, this amount of free ^{89}Zr might have occurred as a result of the labelling of the unconjugated DFO-p-Bz-NCS with a certain amount of ^{89}Zr due to the excess amount of DFO-p-Bz-NCS in mAb:DFO conjugate. These results showed the importance of the ratio of DFO-p-Bz-NCS and the bifunctional chelators, to mAb- ^{89}Zr .

Additionally, Formulations 4, 5, 6 were prepared with ^{89}Zr amount necessary for ^{89}Zr labelling efficiency and were detected. When the ratio was (1:10:2.10⁻¹) (mAb: DFO-p-Bz-NCS: ^{89}Zr), 8.2 % of free ^{89}Zr was observed; while 2.5% of free ^{89}Zr was determined with (1:10:1.4 .10⁻¹) ratio of (mAb: DFO-p-Bz-NCS: ^{89}Zr). In formulation 4 and 5, more ^{89}Zr volume (and so the activity) was used in labelling than the routine method. It showed the overused ^{89}Zr amount depleted the DFO-p-Bz-NCS sites to be bound, causing the presence of free ^{89}Zr .

In the last formulation of ^{89}Zr -Obi, Formulation 6, with (1:10: 0.7 .10⁻¹) ratio of (mAb: DFO-p-Bz-NCS: ^{89}Zr), less ^{89}Zr amount was added for labelling and no free ^{89}Zr was found in RHPLC. It was observed that, all ^{89}Zr was bound to DFO-p-Bz-NCS and also less ^{89}Zr bound to the DFO-p-Bz-NCS than the routine formulation ratio. Depending on the data obtained from above mentioned determinations; optimum saturation could be achieved with the ratio of (1:10:10⁻¹) for (mAb: DFO-p-Bz-NCS: ^{89}Zr) composition.

Obi stock solution, Toc stock solution, ^{89}Zr -Obi and ^{89}Zr -Toc formulations were analyzed in order to get better understanding of the difference in the RHPLC results of the prepared main, other and control formulations. Accordingly, the peak observed in the Obi solution and forming at the 21st minute was determined and this peak was interpreted originating from Obi solution as impurity. Since the “Gazyva” preparation was used (available on the market and used in the clinic), the peak observed at the 21st minute was interpreted could be from the other excipients in this product. In addition, the place of this peak overlapped with the expected peak of mAb. It is known that peak at the 40th minute is the mAb Obi peak. This information was

obtained by comparing the Obi stock sample with the ^{89}Zr -Obi solution peak. 2% impurity from Gazyva solution was also observed in the main formulation but it remained within the acceptable limits (35).

5.5. Stability Studies

Stability studies were carried out on the optimum Formulation 2 obtained after the formulation studies mentioned in the Section 3.4. and specified in Section 4.3. Stability studies were performed as specified in Section 3.7. and the results obtained were indicated in Section 4.6. In the stability tests, saline (0.9% NaCl) solution was used and samples were withdrawn between 0-96th h and analyzed by RHPLC. Although the impurity (mentioned in the results) might be the other substances coming from the “Gazyva” preparation, they were taken into account in the quantitative analysis. While there was no free ^{89}Zr at 0th and 4th h; the ^{89}Zr -Obi ROI % values at the 0th and 4th h were 96.24 % and 96.32 %, respectively. The difference between 0th and 4th h of samples taken from ^{89}Zr -Obi, was found to be statistically insignificant ($p < 0.05$).

In the analysis performed at 24th h, the ROI value of free ^{89}Zr was found to be 5.64 %, while ^{89}Zr -Obi ROI decreased to 90.49%. At the end of the 24th h, minimal degradation has been observed to start ($p > 0.05$).

The degradation rate of free ^{89}Zr at the end of the 48th and 60th h were 14.96% and 28.98%, respectively. It was followed by 42.62 % and 48.98 % of free ^{89}Zr ratio at 72th and 90th h.

As can be seen in the results, ^{89}Zr -Obi started to exhibit serious degradation at the end of 24th h and the degradation increased gradually. In literature, only one study exists evaluating the stability of ^{89}Zr -Obi in similar conditions. Yoon et al. (2018) studied on ^{89}Zr radiolabelled different mAbs, and one of them was Obi. The ^{89}Zr -Obi stability test was performed in human serum, which was a different solution from our experiments, and incubated at 4 °C and 37 °C after 24, 48, 72, 120 and 168 hs. Samples were taken and incubated for 5 min, at 23 °C in 10 mM diethylenetriamepentaacetic acid (DTPA) and analyzed by TLC. After that, samples were analyzed after 5th and 7th days and results showed that ^{89}Zr -Obi radiochemical purity of ^{89}Zr -Obi was higher than 95% at 37 °C for 5 days. The ratio decreased at the day 7 as 91% radiochemical

purity. On the other hand, ^{89}Zr -Obi showed better stability at 4°C, and radiochemical purity was found more than 95% for 7 days (17).

A different protocol was used in that study compared with our stability test protocol. However, differences between the studies are significant. In our research, ^{89}Zr -Obi showed only 24 h stability and after that minimal degradation started although Yoon et al. found different results and 5 days stability. These differences might come from the usage of different procedures for stability studies or the labelling procedure. For example, in our study, NaHCO_3 was used as a buffer solution, while Yoon et al. used HEPES solution. In our research, the Vosjan et al. (2010) method published at “Nature Protocol” was followed for the labelling procedure (83).

Due to the limited studies on ^{89}Zr -Obi, we also evaluated other studies related with the stability of ^{89}Zr radiolabelled mAbs. White et al. (2020) studied on another mAb, ^{89}Zr -Bistrongomab (Bsg). In this study, stability tests were also performed in saline at 37 °C for 144 h. Minimal degradation of ^{89}Zr -Bsg started after 48 h (free ^{89}Zr : 4.8%) (86).

Perk et al. (2006) also studied on the ^{89}Zr radiolabelled mAb, Zevalin, and evaluated stability in saline for 48 h at room temperature. Radiochemical purity was found as 95.6%, and it showed that ^{89}Zr -Zevalin is stable for 48 h (34).

5.6. In-vitro Cell Culture Studies

In-vitro studies were carried out in two main steps; while Ramos cell line was used as the main group causing Burkitt’s Lymphoma; HL 60 cell line was used as the control group. Since, Obi is the pharmaceutical part of the formulation and has CD 20 affinity therefore, its main target was CD 20 (+) Ramos cells. CD 20 (-) HL 60 cells were selected as the control group. Measurements of the affinity of ^{89}Zr -Obi to Ramos cell culture was compared with ^{89}Zr -Toc formulation.

5.6.1. Immuno-reactivity Studies

Immuno-reactivity studies were performed as described in Section 3.8.1. and the results are shown in Section 4.7.1. Using the ^{89}Zr -Obi and ^{89}Zr -Toc formulations at the same concentration and activity, Ramos and HL 60 cells were prepared at six different concentrations. Affinity of ^{89}Zr -Obi to cells, was measured and its affinity

was interpreted by comparing it with ^{89}Zr -Toc (control) formulation which has no affinity to the cells.

In this study, the immuno-reactivity of ^{89}Zr -Obi (main formulation), was found to be 60.9161% on CD20 (+) Ramos cells and 6.1954% on CD20 (-) HL 60 cells. The value of 60.9161% obtained here was a desirable high value indicating the high affinity of Obi to CD20 (+) cells considering the overall high percentage value of immuno-reactivity compared to the literature (78, 79, 86). Likewise, the value of 6.1954% found in CD20 (-) cells proved that Obi did not show any affinity for HL 60 cells and exhibited low immuno-reactivity on CD 20 (-) cells.

In addition, the immuno-reactivity of ^{89}Zr -Toc (control formulation) and ^{89}Zr - Obi (main formulation) on Ramos cells were compared to prove that the Obi's affinity observed on Ramos cells was not due to non-specific binding. While ^{89}Zr -Obi showed 60.9161% immuno-reactivity value; the ^{89}Zr -Toc formulation had 2.386% immuno-reactivity. The results showed that the immuno-reactivity value obtained on Ramos cells of ^{89}Zr -Obi was not a non-specific binding. While the immuno-reactivity of ^{89}Zr -Obi and ^{89}Zr -Toc were compared for Ramos cells, ^{89}Zr -Obi's affinity was also compared in different cell lines which were HL 60 and Ramos. The results obtained from these data proved that ^{89}Zr -Obi showed affinity to CD20 (+) Ramos cells, while it had no affinity to HL 60 cells which was CD 20 (-).

Yoon et al. (2018)'s report supported our immuno-reactivity results. In their study, the immuno-reactivity assay was performed for anti CD20 mAbs such as Obi, ofatumumab, rituximab, tositumomab on Raji cells which have also CD20 (+) cells like Ramos cells (17, 94). In this study, 67% immuno-reactivity was found for ^{89}Zr -Obi, and 76%, 40% and 79% immuno-reactivities were detected for Zr-ofatumumab, rituximab and tositumomab, respectively (17). In our study, ^{89}Zr -Obi's immuno-reactivity to Ramos cells was found 60.61%, which is close to Yoon et al.'s results. The differences between the immuno-reactivity values might be related with different cell lines even if they are both CD20 (+) type, they might have different CD20 epitopes.

As a result of these data, immuno-reactivity results are good enough to continue to the next step which is binding assay. Therefore, binding assay of ^{89}Zr -Obi formulation on Ramos cells could also be carried out.

5.6.2. Binding Assay

As described in Section 3.8.2, it was aimed to find the binding constant and to obtain the binding graph by applying to the Zr^{89} -Obi formulation in the Ramos cell line. Obtained results are given in Section 4.7.2. Competitor binding assay was used in this section, and K_d and EC_{50} values were determined by competitor (B) binding assay. In this part, competitor assay was important due to avoiding from nonspecific binding of Obi to Ramos cells. Therefore, different concentrations of unlabelled Obi were incubated in 6 samples of the same concentrations of Ramos cells and after that the same concentration of ^{89}Zr -Obi was added and determination were carried out. So, in this part the unlabelled Obi was competitor (B) whilst the non-competitor (Bo) was ^{89}Zr -Obi. Competitive binding occurs with the addition of non-competitor after primarily incubating cells of competitive ones. Thus, the binding constant was calculated by excluding specific binding.

In the light of the data, the EC_{50} value was found to be 16.1 μM . This value, showed the Obi could bind to target only 50%. The effects of drug/antibodies etc. are the fraction of drug-receptor relation, and when all receptors bind drug/antibody caused the maximal effect (95). This EC_{50} value showed the mild concentration which produced the biological effects of drugs/antibodies etc. (96, 97). EC_{50} value also showed the potency, and it meant potent drugs have lower EC_{50} value. These data are generally used for in-vitro or in-vivo measurement of cells or animals (98).

Additionally, the other determined parameter was the K_d value, states the binding affinity between the small or macro molecule and the receptor (98). Therefore, this value is generally used to compare different pharmaceuticals conducted in the same experimental setup. (96). The K_d value, obtained in the same way, was 27.3 nM. Although the obtained graph was not an ideal one, it showed the increased binding with the increasing ^{89}Zr -Obi concentration. According to the obtained graph, it can be said that Zr^{89} -Obi at the concentration of 0.9 $mg.ml^{-1}$ reached approximately the maximum binding and a slight plateau line was obtained. In an ideal graph, it is expected that the maximum and minimum binding concentrations can be determined and the plateau line can clearly be observed. The ideal graph could not be observed in our experiments although they were repeated two times at different concentrations, and the graph approaching to the ideal graph is given in Figure 4.26.

The same method was performed by Marquez et al. (2014) for the binding study. But, the similar results could not be obtained in our study (78). What we expected with this study was to be able to see the slow increasing in binding with the increasing concentration at the beginning in the graph. In the final, there would be no change in binding even if the residual concentration increased and, it would be detected clearly by seeing the plateau lines on the graph. Whereas, in the graph obtained, binding increased depending on the increasing ^{89}Zr -Obi concentration, although we could not clearly see the plateau line at the beginning and at the saturation stage.

Accordingly, EC_{50} value could not be calculated exactly. There might be various reasons for this. Although the experiments were repeated several times, expected graph could not be obtained. One of the reasons for this might be an insufficient choice of concentration points. In order to determine these values, 6 different concentrations were prepared according to the literature. The desired data was obtained by taking 6 sample points and the binding constant was determined. It was in agreement with the literature. The graph obtained clearly showed that the binding increased depending on the concentration, but unfortunately it did not clearly exhibit the limit values.

5.7. In-vivo Animal Studies

In-vivo animal studies were performed under two parts: PET/CT imaging and biodistribution, although planned as three parts. It was planned to continue in-vivo studies with histology part. However, histological studies could not be done due to the COVID-19 pandemic situation and radiation protection principles in the UK (i.e. radioactivity in organs should decay and become non-radioactive for histology experiments).

5.7.1. PET/CT Imaging

Nano PET/CT images of ^{89}Zr -Obi for Ramos and HL 60 cells and control group are shown in Figure 4.27, Figure 4.28 and Figure 4.29. Spleen uptake was shown in all groups although the spleen uptake was expected only for Ramos cell group. ID/g % value per each organ of each group are shown in Figure 4.30. Considering the organs ID/g % value compared between groups, differences were found in the livers of the

HL60 cell injected group and control group and, also, between Ramos cell injected group and control group.

In this study, Ramos cells injected into animals were expected to cause Burkitt's lymphoma, while mice injected with HL60 cells were expected to develop leukemia. Accordingly, cells were expected to proliferate in the spleen and subsequently in lymph nodes and bone marrows. Since the prepared formulation ^{89}Zr -Obi is a CD20 specific formulation, it was expected to be uptaken only by the group injected with CD20 over-expressed Ramos cells. However, the data obtained showed that there was no significant difference between the control group, the group injected with HL60 cells and the group injected with Ramos cells. At this point, two different possibilities were considered. The first was that the injected cancer cells did not cause the expected disease in mice and histological studies should be performed to clarify this situation. The second possibility was that Obi in the injected formulation demonstrated therapeutic efficacy on mice injected with Ramos cells and was thought to have developed Burkitt's lymphoma. On the contrary of this hypothesis, Zettlitz et al. (2017) mentioned that ^{89}Zr radiolabelled radiopharmaceuticals showed higher uptake in kidneys, liver and spleen which are clearance organs due to residualizing feature of ^{89}Zr . Additionally, it was also specified spleen uptake was observed only in SCID mice unlike the Balb/C mice due to abnormal structure and smaller size in SCID mice (99).

The main reason for these comments is the percentage of immuno-reactivity obtained in Ramos cells of the ^{89}Zr -Obi formulation in in-vitro studies and the absence of immuno-reactivity in HL60 cells.

5.7.2. Biodistribution Studies

Biodistribution analysis of ^{89}Zr -Obi formulation is given in Table 4.25. After the injection to the mice, the remaining activity in the injection and the total activity were calculated. Count per seconds (CPS) measurements of individual organs in the mice in each group were calculated by gamma-counter and is shown in Figure 4.31.

Lymphoma and leukemia tumour models, were expected to develop after injection of Ramos and HL 60 cells, in spleen and lymph nodes. However, as shown by the immuno-reactivity results in Section 4.7.1 after ^{89}Zr -Obi injection, an uptake was expected to be observed in only Ramos cell injected animal models. But,

biodistribution data obtained in both cells injected animals (Ramos and HL60 cells injected) and control group showed the same uptake. It was determined that there was no significant difference in between the groups ($p < 0.05$). This situation can be interpreted in several ways: The first hypothesis was systemically injected tumour cells (Ramos and HL 60) did not induce lymphoma cancer in animals. Because, if the injected cancer cells could form a cancer model in animals, it would be expected that the mice injected with Ramos cells will show a significant uptake, especially in the spleen and lymph nodes. However, the biodistribution results, obtained and calculated for each organ, did not show any significant difference among three different groups. In this part, expanded spleen was expected and also lymph nodes were expected to multiply in Ramos cell injected mice causing Burkitt's lymphoma. But, neither spleen expansion nor an increase in lymph nodes was observed. It is expected that this hypothesis will be clarified with the completion of histology studies. However, the situation during the pandemic and due to limited time in UK, histology studies could not be performed. As a continuation of these studies, histology studies are planned to perform when the suitable conditions are obtained.

6. CONCLUSION

The data obtained from ^{89}Zr labelled Obinutuzumab and in-vitro and in-vivo studies performed in this doctoral thesis are as follows:

- ^{89}Zr -Obi has been labelled by using the DFO-p-Bz-NCS chelating agent with high radiochemical purity and high stability,
- ^{89}Zr -Toc was prepared with high radiochemical purity, as a control formulation for in-vitro studies,
- RTLC and RHPLC results of ^{89}Zr -Obi and ^{89}Zr -Toc showed high radiochemical purity,
- Stability studies of ^{89}Zr -Obi showed that the formulation was stable for 24 h and (^{89}Zr /total) activity was determined as 94.13% at the end of 24th h. Degradation began to be observed after 24 hours.
- Immuno-reactivity and binding assay studies have been carried out by in-vitro studies.
- Immuno-reactivity of ^{89}Zr -Obi were found 60.95% and 6.14% in Ramos (CD20 +), and HL60 (CD20 -), respectively. Also, ^{89}Zr -Toc was evaluated in Ramos cells and its immuno-reactivity was found 2.38%.
- Comparative results of immuno-reactivity proved the high specificity of ^{89}Zr -Obi to CD20 (+) Ramos cells.
- Binding constant studies were performed on ^{89}Zr -Obi formulation. Ramos cells and the EC_{50} value was determined as $1.6 \cdot 10^{-2}$ μM .
- In-vivo studies were carried out with three groups of female SCID mice, and PET/CT images were obtained and followed by biodistribution studies.
- PET and biodistribution studies did not reveal a significant difference among three groups.

As a result, ^{89}Zr -Obi (Obi mAb:DFO-p-Bz-NCS: ^{89}Zr) ($1:10:10^{-1}$) was found to be a promising radiopharmaceutical for lymphoma diagnosis despite the in-vivo studies were not found as expected. Besides the formulation, it was also proven that ^{89}Zr is a promising radionuclide for immuno-PET imaging and further histopathological studies should be carried out in order to enlighten the uptake of cell culture mechanism related with the cancer type.

7. REFERENCES

1. LaFlamme M. Non Hodgkin's Lymphoma 2018 [Available from: <https://www.healthline.com/health/non-hodgkins-lymphoma#symptoms>].
2. Chen K, Page JG, Schwartz AM, Lee TN, DeWall SL, Sikkema DJ, et al. False-positive immunogenicity responses are caused by CD20+ B cell membrane fragments in an anti-ofatumumab antibody bridging assay. *J Immunol Methods*. 2013;394(1-2):22-31.
3. Beers SA, Chan CH, French RR, Cragg MS, Glennie MJ. CD20 as a target for therapeutic type I and II monoclonal antibodies. *Semin Hematol*. 2010;47(2):107-14.
4. Abbas A, Lichtman A, Pillai S. *Cellular and Molecular Immunology*. 7, editor. Philadelphia: Saunders: Elsevier; 2010.
5. Barbaros B, Dikmen M. Cancer Immunotherapy. *Erciyes University Journal of the Institute of Science and Technology*. 2015;31(4):177-81.
6. van Dongen GA, Vosjan MJ. Immuno-positron emission tomography: shedding light on clinical antibody therapy. *Cancer Biother Radiopharm*. 2010;25(4):375-85.
7. Ecker DM, Jones SD, Levine HL. The Therapeutic Monoclonal Antibody Market. *mAbs*. 2015;7(1):9-14.
8. Oliveira S, Heukers R, Sornkom J, Kok RJ, van Bergen En Henegouwen PM. Targeting tumours with nanobodies for cancer imaging and therapy. *J Control Release*. 2013;172(3):607-17.
9. Cutler CS, Hennkens HM, Sisay N, Huclier-Markai S, Jurisson SS. Radiometals for combined imaging and therapy. *Chem Rev*. 2013;113(2):858-83.
10. Sarcan ET, Silindir-Gunay M, Ozer AY, Hartman N. ⁸⁹Zr as a promising radionuclide and it's applications for effective cancer imaging. *Journal of Radioanalytical and Nuclear Chemistry*. 2021;330(1):15-28.
11. Saha GB. Radiopharmaceuticals and Methods of Radiolabelling. In: Saha GB, editor. *Fundamentals of Nuclear Pharmacy*. sixth ed: Springer; 2010. p. 83.
12. van Dongen GA, Visser GW, Lub-de Hooge MN, de Vries EG, Perk LR. Immuno-PET: a navigator in monoclonal antibody development and applications. *Oncologist*. 2007;12(12):1379-89.
13. Schrama D, Reisfeld RA, Becker JC. Antibody targeted drugs as cancer therapeutics. *Nat Rev Drug Discov*. 2006;5(2):147-59.
14. Sharkey RM, Goldenberg DM. Perspectives on cancer therapy with radiolabelled monoclonal antibodies. *J Nucl Med*. 2005;46 Suppl 1:115s-27s.
15. Bensch F, Smeenk MM, van Es SC, de Jong JR, Schroder CP, Oosting SF, et al. Comparative biodistribution analysis across four different (⁸⁹Zr)-monoclonal antibody tracers-The first step towards an imaging warehouse. *Theranostics*. 2018;8(16):4295-304.

16. Abou DS, Ku T, Smith-Jones PM. In vivo biodistribution and accumulation of ⁸⁹Zr in mice. *Nucl Med Biol.* 2011;38(5):675-81.
17. Yoon JT, Longtine MS, Marquez-Nostra BV, Wahl RL. Evaluation of Next-Generation Anti-CD20 Antibodies Labeled with (⁸⁹Zr) in Human Lymphoma Xenografts. *J Nucl Med.* 2018;59(8):1219-24.
18. Tipton TR, Roghanian A, Oldham RJ, Carter MJ, Cox KL, Mockridge CI, et al. Antigenic modulation limits the effector cell mechanisms employed by type I anti-CD20 monoclonal antibodies. *Blood.* 2015;125(12):1901-9.
19. Yoon JK, Park BN, Ryu EK, An YS, Lee SJ. Current Perspectives on (⁸⁹Zr)-PET Imaging. *Int J Mol Sci.* 2020;21(12).
20. Zettlitz KA, Tavaré R, Knowles SM, Steward KK, Timmerman JM, Wu AM. ImmunoPET of Malignant and Normal B Cells with (⁸⁹Zr)- and (¹²⁴I)-Labeled Obinutuzumab Antibody Fragments Reveals Differential CD20 Internalization In Vivo. *Clin Cancer Res.* 2017;23(23):7242-52.
21. Sheppard M, Laskou F, Stapleton PP, Hadavi S, Dasgupta B. Tocilizumab (Actemra). *Hum Vaccin Immunother.* 2017;13(9):1972-88.
22. Naki Sivri N. Radyonüklidik Tedavi. *Meslek İçi Sürekli Eğitim.* 2004;9:11-2.
23. Wadas TJ, Wong EH, Weisman GR, Anderson CJ. Coordinating radiometals of copper, gallium, indium, yttrium, and zirconium for PET and SPECT imaging of disease. *Chem Rev.* 2010;110(5):2858-902.
24. Kaur S, Venktaraman G, Jain M, Senapati S, Garg PK, Batra SK. Recent trends in antibody-based oncologic imaging. *Cancer Lett.* 2012;315(2):97-111.
25. van de Watering FC, Rijpkema M, Perk L, Brinkmann U, Oyen WJ, Boerman OC. Zirconium-89 labeled antibodies: a new tool for molecular imaging in cancer patients. *Biomed Res Int.* 2014;2014:203601.
26. Sharp PF, Welch A. Positron Emission Tomography. In: Murray AD, editor. *Practical Nuclear Medicine.* Oxford University: Springer; 2005. p. 35.
27. Jalilian AR, Osso JA. Production, applications and status of zirconium-89 immunoPET agents. *Journal of Radioanalytical and Nuclear Chemistry.* 2017;314(1):7-21.
28. Holland JP, Williamson MJ, Lewis JS. Unconventional nuclides for radiopharmaceuticals. *Mol Imaging.* 2010;9(1):1-20.
29. Teksöz S, Biber Müftüler FZ. Radioisotopes and Biomedical Applications in Nuclear Medicine. *Nuclear Medicine Seminars.* 2019;5(1):10-4.
30. Knowles SM, Wu AM. Advances in immuno-positron emission tomography: antibodies for molecular imaging in oncology. *J Clin Oncol.* 2012;30(31):3884-92.
31. Verel I, Visser GW, van Dongen GA. The promise of immuno-PET in radioimmunotherapy. *J Nucl Med.* 2005;46 Suppl 1:164s-71s.

32. Nayak TK, Brechbiel MW. Radioimmunoimaging with longer-lived positron-emitting radionuclides: potentials and challenges. *Bioconjug Chem.* 2009;20(5):825-41.
33. Perk LR, Visser GW, Vosjan MJ, Stigter-van Walsum M, Tijink BM, Leemans CR, et al. ⁸⁹Zr as a PET Surrogate Radioisotope for Scouting Biodistribution of the Therapeutic Radiometals ⁹⁰Y and ¹⁷⁷Lu in Tumour-Bearing Nude Mice After Coupling to the Internalizing Antibody Cetuximab. *J Nucl Med.* 2005;46:1898-906.
34. Perk LR, Visser OJ, Stigter-van Walsum M, Vosjan MJ, Visser GW, Zijlstra JM, et al. Preparation and evaluation of (⁸⁹Zr-Zevalin for monitoring of (⁹⁰Y-Zevalin biodistribution with positron emission tomography. *Eur J Nucl Med Mol Imaging.* 2006;33(11):1337-45.
35. Nagengast WB, de Vries EG, Hospers GA, Mulder NH, de Jong JR, Hollema H, et al. In vivo VEGF imaging with radiolabelled bevacizumab in a human ovarian tumour xenograft. *J Nucl Med.* 2007;48(8):1313-9.
36. Dijkers E, Hooge MNL-d, Kosterink JG, Jager PL, Brouwers AH, Perk LR, et al. Characterization of ⁸⁹Zr-trastuzumab for clinical HER2 immunoPET imaging. *Journal of Clinical Oncology.* 2007;25(18_suppl):3508-.
37. Verel I, Visser GW, Boellaard R, Stigter-van Walsum M, Snow GB, van Dongen GA. ⁸⁹Zr immuno-PET: comprehensive procedures for the production of ⁸⁹Zr-labeled monoclonal antibodies. *J Nucl Med.* 2003;44(8):1271-81.
38. Zhang Y, Hong H, Cai W. PET tracers based on Zirconium-89. *Curr Radiopharm.* 2011;4(2):131-9.
39. Bhatt NB, Pandya DN, Wadas TJ. Recent Advances in Zirconium-89 Chelator Development. *Molecules.* 2018;23(3).
40. Wei W, Rosenkrans ZT, Liu J, Huang G, Luo QY, Cai W. ImmunoPET: Concept, Design, and Applications. *Chem Rev.* 2020;120(8):3787-851.
41. Patra M, Bauman A, Mari C, Fischer CA, Blacque O, Haussinger D, et al. An octadentate bifunctional chelating agent for the development of stable zirconium-89 based molecular imaging probes. *Chem Commun (Camb).* 2014;50(78):11523-5.
42. Guerard F, Lee YS, Tripier R, Szajek LP, Deschamps JR, Brechbiel MW. Investigation of Zr(IV) and ⁸⁹Zr(IV) complexation with hydroxamates: progress towards designing a better chelator than desferrioxamine B for immuno-PET imaging. *Chem Commun (Camb).* 2013;49(10):1002-4.
43. Sung H, Ferlay J, Siegel RL, Laversanne M, Soerjomataram I, Jemal A, et al. Global Cancer Statistics 2020: GLOBOCAN Estimates of Incidence and Mortality Worldwide for 36 Cancers in 185 Countries. *CA Cancer J Clin.* 2021;71(3):209-49.
44. Ligiero TB, de Souza Albernaz M, de Carvalho SM, de Oliveira SM, Santos-Oliveira R. Monoclonal antibodies: application in radiopharmacy. *Curr Radiopharm.* 2013;6(4):231-48.

45. cancerresearchuk.org. Cancer Research UK; 2018 [Available from: <https://www.cancerresearchuk.org/health-professional/cancer-statistics/statistics-by-cancer-type/non-hodgkin-lymphoma#heading-Zero>.
46. hsgm.saglik.gov.tr. Turkish Cancer Statistic: Turkish Republic, General Directorate of Public; 2019 [Available from: https://hsgm.saglik.gov.tr/depo/birimler/kanser-db/istatistik/Turkiye_Kanser_Istatistikleri_2016.pdf.
47. Center MSKC. Lymphoma 2021 [Available from: <https://www.mskcc.org/cancer-care/types/lymphoma>.
48. who.int. Diffuse Large B-Cell Lymphoma: World Health Organisation 2018 [Available from: https://www.who.int/selection_medicines/committees/expert/20/applications/DiffuseLargeBCellLymphoma.pdf?ua=1&ua=1.
49. cancer.org. What is Non-Hodgkin's Lymphoma? : American Cancer Society; 2018 [Available from: https://www.cancer.org/cancer/non-hodgkin-lymphoma/about/what-is-non-hodgkin-lymphoma.html#written_by.
50. Molyneux EM, Rochford R, Griffin B, Newton R, Jackson G, Menon G, et al. Burkitt's lymphoma. *The Lancet*. 2012;379(9822):1234-44.
51. Vose JM, Bierman PJ, Anderson JR, Harrison KA, Dalrymple GV, Byar K, et al. Single-photon emission computed tomography gallium imaging versus computed tomography: predictive value in patients undergoing high-dose chemotherapy and autologous stem-cell transplantation for non-Hodgkin's lymphoma. *Journal of Clinical Oncology*. 1996;14(9):2473-9.
52. Kostakoglu L, Leonard JP, Kuji I, Coleman M, Vallabhajosula S, Goldsmith SJ. Comparison of fluorine-18 fluorodeoxyglucose positron emission tomography and Ga-67 scintigraphy in evaluation of lymphoma. *Cancer*. 2002;94(4):879-88.
53. Cheson BD. Role of functional imaging in the management of lymphoma. *J Clin Oncol*. 2011;29(14):1844-54.
54. Dadparvar S, Hussain R, Esteves F, Yu JQ, Grewal RK, Arif S, et al. Thallium-201 Imaging in Evaluation of Hodgkin's Disease. *The Cancer Journal*. 2002;8(6):469-75.
55. Burton C, Ell P, Linch D. The role of PET imaging in lymphoma. *Br J Haematol*. 2004;126(6):772-84.
56. Rylova SN, Del Pozzo L, Klingeberg C, Tonnesmann R, Illert AL, Meyer PT, et al. Immuno-PET Imaging of CD30-Positive Lymphoma Using 89Zr-Desferrioxamine-Labeled CD30-Specific AC-10 Antibody. *J Nucl Med*. 2016;57(1):96-102.
57. Shukla AA, Hubbard B, Tressel T, Guhan S, Low D. Downstream processing of monoclonal antibodies--application of platform approaches. *J Chromatogr B Analyt Technol Biomed Life Sci*. 2007;848(1):28-39.
58. Weiner LM, Surana R, Wang S. Monoclonal antibodies: versatile platforms for cancer immunotherapy. *Nat Rev Immunol*. 2010;10(5):317-27.

59. Breedveld FC. Therapeutic monoclonal antibodies. *Lancet*. 2000;355(9205):735-40.
60. Lamberts LE, Williams SP, Terwisscha van Scheltinga AG, Lub-de Hooge MN, Schröder CP, Gietema JA, et al. Antibody positron emission tomography imaging in anticancer drug development. *J Clin Oncol*. 2015;33(13):1491-504.
61. Wällberg H, Ståhl S. Design and evaluation of radiolabelled tracers for tumour imaging. *Biotechnol Appl Biochem*. 2013;60(4):365-83.
62. Cheson B. Ofatumumab, a novel anti-CD20 monoclonal antibody for the treatment of B-cell malignancies. *Journal of Clinical Oncology*. 2010;20(28):3525-30.
63. Weiner GJ. Building better monoclonal antibody-based therapeutics. *Nat Rev Cancer*. 2015;15(6):361-70.
64. Agez M, Mandon ED, Iwema T, Gianotti R, Limani F, Herter S, et al. Biochemical and biophysical characterization of purified native CD20 alone and in complex with rituximab and obinutuzumab. *Sci Rep*. 2019;9(1):13675.
65. Maloney DG. Anti-CD20 Antibody Therapy or B-cell Lymphomas. *N Engl J Med*. 2012;266:2006-16.
66. Borjesson PK, Jauw YW, Boellaard R, de Bree R, Comans EF, Roos JC, et al. Performance of immuno-positron emission tomography with zirconium-89-labeled chimeric monoclonal antibody U36 in the detection of lymph node metastases in head and neck cancer patients. *Clin Cancer Res*. 2006;12(7 Pt 1):2133-40.
67. Zeglis BM, Lewis JS. The bioconjugation and radiosynthesis of ⁸⁹Zr-DFO-labeled antibodies. *J Vis Exp*. 2015(96).
68. Heskamp S, Raave R, Boerman O, Rijpkema M, Goncalves V, Denat F. (89)Zr-Immuno-Positron Emission Tomography in Oncology: State-of-the-Art (89)Zr Radiochemistry. *Bioconjug Chem*. 2017;28(9):2211-23.
69. Allott L, Da Pieve C, Meyers J, Spinks T, Ciobota DM, Kramer-Marek G, et al. Evaluation of DFO-HOPO as an octadentate chelator for zirconium-89. *Chem Commun (Camb)*. 2017;53(61):8529-32.
70. Kristensen LK, Christensen C, Jensen MM, Agnew BJ, Schjöth-Frydendahl C, Kjaer A, et al. Site-specifically labeled (89)Zr-DFO-trastuzumab improves immuno-reactivity and tumour uptake for immuno-PET in a subcutaneous HER2-positive xenograft mouse model. *Theranostics*. 2019;9(15):4409-20.
71. Rudd SE, Roselt P, Cullinane C, Hicks RJ, Donnelly PS. A desferrioxamine B squaramide ester for the incorporation of zirconium-89 into antibodies. *Chem Commun (Camb)*. 2016;52(80):11889-92.
72. Tinianow JN, Gill HS, Ogasawara A, Flores JE, Vanderbilt AN, Luis E, et al. Site-specifically ⁸⁹Zr-labeled monoclonal antibodies for ImmunoPET. *Nucl Med Biol*. 2010;37(3):289-97.


73. Sarcan ET, Özer AY. Zirconium-89 Radiopharmaceuticals: Current Status and Future. In: Özer AY, editor. *New Trends in Radiopharmaceuticals*. Ankara: Türkiye Klinikleri; 2021. p. 16-22.
74. Meijs WE, Haisma HJ, Klok RP, van Gog FB, Kievit E, Pinedo HM, et al. Zirconium-labeled monoclonal antibodies and their distribution in tumour-bearing nude mice. *J Nucl Med*. 1997;38(1):112-8.
75. Pandit-Taskar N, O'Donoghue JA, Beylergil V, Lyashchenko S, Ruan S, Solomon SB, et al. (8)(9)Zr-huJ591 immuno-PET imaging in patients with advanced metastatic prostate cancer. *Eur J Nucl Med Mol Imaging*. 2014;41(11):2093-105.
76. Natarajan A, Habte F, Liu H, Sathirachinda A, Hu X, Cheng Z, et al. Evaluation of ⁸⁹Zr-rituximab tracer by Cerenkov luminescence imaging and correlation with PET in a humanized transgenic mouse model to image NHL. *Mol Imaging Biol*. 2013;15(4):468-75.
77. Laforest R, Lapi SE, Oyama R, Bose R, Tabchy A, Marquez-Nostra BV, et al. [(89)Zr]Trastuzumab: Evaluation of Radiation Dosimetry, Safety, and Optimal Imaging Parameters in Women with HER2-Positive Breast Cancer. *Mol Imaging Biol*. 2016;18(6):952-9.
78. Marquez BV, Ikotun OF, Zheleznyak A, Wright B, Hari-Raj A, Pierce RA, et al. Evaluation of (89)Zr-pertuzumab in Breast cancer xenografts. *Mol Pharm*. 2014;11(11):3988-95.
79. Natarajan A, Habte F, Gambhir SS. Development of a novel long-lived immunoPET tracer for monitoring lymphoma therapy in a humanized transgenic mouse model. *Bioconjug Chem*. 2012;23(6):1221-9.
80. Natarajan A, Gambhir SS. Radiation Dosimetry Study of [(89)Zr]rituximab Tracer for Clinical Translation of B cell NHL Imaging using Positron Emission Tomography. *Mol Imaging Biol*. 2015;17(4):539-47.
81. Busa LSA, Maeki M, Ishida A, Tani H, Tokeshi M. Simple and sensitive colorimetric assay system for horseradish peroxidase using microfluidic paper-based devices. *Sensors and Actuators B: Chemical*. 2016;236:433-41.
82. Trabik YA, Moenes EM, Al-Ghobashy MA, Nebsen M, Ayad MF. Analytical comparability study of anti-CD20 monoclonal antibodies rituximab and obinutuzumab using a stability-indicating orthogonal testing protocol: Effect of structural optimization and glycoengineering. *J Chromatogr B Analyt Technol Biomed Life Sci*. 2020;1159:122359.
83. Vosjan MJ, Perk LR, Visser GW, Budde M, Jurek P, Kiefer GE, et al. Conjugation and radiolabeling of monoclonal antibodies with zirconium-89 for PET imaging using the bifunctional chelate p-isothiocyanatobenzyl-desferrioxamine. *Nat Protoc*. 2010;5(4):739-43.
84. Knight JC, Paisey SJ, Dabkowski AM, Marculescu C, Williams AS, Marshall C, et al. Scaling-down antibody radiolabeling reactions with zirconium-89. *Dalton Trans*. 2016;45(15):6343-7.

85. Vugts DJ, Visser GW, van Dongen GA. ⁸⁹Zr-PET radiochemistry in the development and application of therapeutic monoclonal antibodies and other biologicals. *Curr Top Med Chem*. 2013;13(4):446-57.
86. White JM, Kuda-Wedagedara AN, Wicker MN, Spratt DE, Schopperle WM, Heath E, et al. Detecting TRA-1-60 in Cancer via a Novel Zr-89 Labeled ImmunoPET Imaging Agent. *Mol Pharm*. 2020;17(4):1139-47.
87. Lindmo T, Boven E, Cuttitta F, Fedorko J, Bunn PA. Determination of the Immunoreactive Fraction of Radiolabelled Monoclonal Antibodies by Linear Extrapolation to Binding at Infinite Antigen Excess. *Journal of Immunological Methods*. 1984;72:77-89.
88. Chekol R, Raja Solomon V, Alizadeh E, Bernhard W, Fisher D, Hill W, et al. ⁸⁹Zr-nimotuzumab for immunoPET imaging of epidermal growth factor receptor I. *Oncotarget*. 2018;9(24).
89. Poot AJ, Adamzek KWA, Windhorst AD, Vosjan M, Kropf S, Wester HJ, et al. Fully Automated (⁸⁹Zr) Labeling and Purification of Antibodies. *J Nucl Med*. 2019;60(5):691-5.
90. Larenkov A, Bubenschikov V, Makichyan A, Zhukova M, Krasnoperova A, Kodina G. Preparation of Zirconium-89 Solutions for Radiopharmaceutical Purposes: Interrelation Between Formulation, Radiochemical Purity, Stability and Biodistribution. *Molecules*. 2019;24(8).
91. Lin M, Mukhopadhyay U, Waligorski GJ, Balatoni JA, Gonzalez-Lepera C. Semi-automated production of (⁸)(⁹)Zr-oxalate/(⁸)(⁹)Zr-chloride and the potential of (⁸)(⁹)Zr-chloride in radiopharmaceutical compounding. *Appl Radiat Isot*. 2016;107:317-22.
92. Wooten A, Madrid E, Schweitzer G, Lawrence L, Mebrahtu E, Lewis B, et al. Routine Production of ⁸⁹Zr Using an Automated Module. *Applied Sciences*. 2013;3(3):593-613.
93. Holland JP, Sheh Y, Lewis JS. Standardized methods for the production of high specific-activity zirconium-89. *Nucl Med Biol*. 2009;36(7):729-39.
94. Tsai PC, Hernandez-Ilizaliturri FJ, Bangia N, Olejniczak SH, Czuczman MS. Regulation of CD20 in rituximab-resistant cell lines and B-cell non-Hodgkin lymphoma. *Clin Cancer Res*. 2012;18(4):1039-50.
95. Dose-Effect Relationship
https://www.chem.uwec.edu/chem491_w01/Pharmacognosy%20491/dose%20effect%20receptor%20intro.pdf2009 [
96. Ferguson DC. Principles of Pharmacodynamics and Toxicodynamics. Haschek and Rousseaux's Handbook of Toxicologic Pathology 2013. p. 61-76.
97. Holford N. Holford NHG and Sheiner LB "Understanding the Dose-Effect Relationship-Clinical Application of Pharmacokinetic-Pharmacodynamic Models", *Clin Pharmacokin* 6:429-453 (1981)-The Backstory. *AAPS J*. 2011;13(4):662-4.

98. The Difference between K_i , K_d , IC_{50} , and EC_{50} values <https://www.sciencesnail.com/science/the-difference-between-ki-kd-ic50-and-ec50-values2019> [
99. Economopoulos V, Noad JC, Krishnamoorthy S, Rutt BK, Foster PJ. Comparing the MRI appearance of the lymph nodes and spleen in wild-type and immunodeficient mouse strains. *PLoS One*. 2011;6(11):e27508.

8. SUPPLEMENTS

Supplement 1. Certificates for animal studies.



This is to certify that

Elif Tugce Sarcan


has successfully achieved the learning outcomes of the following modules as required under UK and EU training frameworks:

E1/L
 National Legislation (EU 1)
 Ethics, Animal Welfare, and the 3Rs – level 1 (EU 2)
 PIL A
 Basic and Appropriate Biology Theory/Skills (EU 3.1/3.2)
 Animal Care, Health and Management (EU 4)
 Recognition of Pain, Suffering and Distress (EU 5)
 Humane Methods of Killing Theory/Skills (EU 6.1/6.2)
 Minimally Invasive Procedures Without Anaesthesia Theory (EU 7)
 Minimally Invasive Procedures Without Anaesthesia Skills (EU 8)
 PIL B
 Anaesthesia for Minor Procedures (EU 20)
 PIL C
 Advanced Anaesthesia (EU 21)
 Principles of Surgery (EU 22)


Species covered: **Mouse**

Training organised by: **Charles River UK Ltd**

Certificate Number: **BIO/2020/725** Date: **16th November 2020**



Course Organiser




For the Royal Society of Biology

Please note, this Certificate allows you to apply for a Licence, but it is not a licence to perform procedures under the *Animals (Scientific Procedures) Act 1986*.

In the UK, competence in procedures, including euthanasia, using live animals, which could cause pain, suffering, distress or lasting harm, will only be achieved, under supervision, when a person begins their work.

Reference to EU Modules relates to requirements arising from Directive 2010/63/EU
http://ec.europa.eu/environment/chemicals/lab_animals/pdf/Endorsed_E-T.pdf



Incorporated by Royal Charter
 Registered Charity No: 277981



TÜRKİYE CUMHURİYETİ
ANKARA ÜNİVERSİTESİ SÜREKLİ EĞİTİM MERKEZİ

ANKÜSEM

DENEY HAYVANLARI KULLANIM SERTİFİKASI

ELİF TUĞÇE SARCAN

Ankara Üniversitesi Sürekli Eğitim Merkezi (ANKÜSEM) ve Hayvan Deneyleri Yerel Etik Kurulu işbirliği çerçevesinde 18 - 27 Eylül 2017 tarihleri arasında düzenlenen "Deneysel Hayvanları Kullanım Sertifikası" eğitimini başarı ile tamamlayarak bu belgeyi almaya hak kazanmıştır.

Prof. Dr. Erkan İbiş
Rektör

Prof. Dr. Taner KARAOĞLU
Hayvan Deneyleri Yerel Etik Kurulu Başkanı
Eğitim Programının Kategorisi: B Kategorisi
Belge No: ANK.S.17.BR.05.0193

Prof. Dr. Mualla SELÇUK
ANKÜSEM Müdürü

Supplement 2. Ethics Committee Approval/ Project Licence.

In-vivo animal studies were carried out at the Cardiff University, University Hospital Wales (UHW), Radioactivity Animal Laboratory under the Martin Ruthardt's Project Licence (P1DDB264F, 28 Sep 2017-26 Sep 2022). Since the project license is a personal document, it could not be attached here, however, the mentioned project number of the project license under which the studied are carried out were shared.

Supplement 3: Dissertation originality report, Turnitin

TITLE of THESIS: Development of Radiopharmaceutical Formulations for Imaging of non Hodgkin's Lymphoma

NAME of STUDENT: Elif Tuğçe Sarcan Bozkır

PAGE: 88

Development of Radiopharmaceutical Formulations for Imaging of Non Hodgkin's Lymphoma, Elif Tuğçe, Sarcan Bozkır

ORIGINALITY REPORT

9%	7%	7%	2%
SIMILARITY INDEX	INTERNET SOURCES	PUBLICATIONS	STUDENT PAPERS

PRIMARY SOURCES

1	E. Tugce Sarcan, Mine Silindir-Gunay, A. Yekta Ozer, Neil Hartman. "89Zr as a promising radionuclide and it's applications for effective cancer imaging", Journal of Radioanalytical and Nuclear Chemistry, 2021 Publication	<1%
2	www.ncbi.nlm.nih.gov Internet Source	<1%
3	link.springer.com Internet Source	<1%
4	openaccess.hacettepe.edu.tr:8080 Internet Source	<1%
5	aut.researchgateway.ac.nz Internet Source	<1%
6	www.mdpi.com Internet Source	<1%
7	jnm.snmjournals.org Internet Source	<1%

Supplement 4: Turnitin Digital Receipt

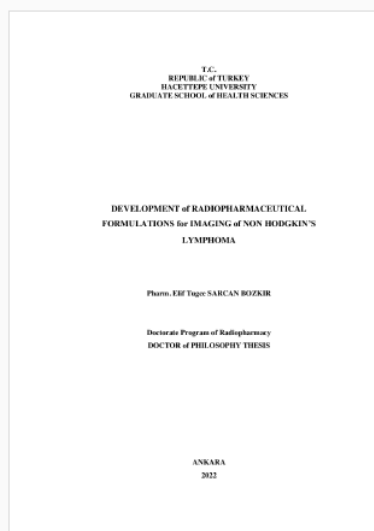


Digital Receipt

This receipt acknowledges that Turnitin received your paper. Below you will find the receipt information regarding your submission.

The first page of your submissions is displayed below.

Submission author: Elif Tugce Sarcen Bozkir
Assignment title: Development of Radiopharmaceutical Formulations for Imag...
Submission title: Development of Radiopharmaceutical Formulations for Imag...
File name: tez.docx
File size: 27.37M
Page count: 88
Word count: 18,055
Character count: 101,150
Submission date: 30-Sep-2022 01:40PM (UTC+0300)
Submission ID: 1912891085



9. CURRICULUM VITAE

PERSONAL INFORMATION

Name/Surname: Elif Tuğçe SARCAN BOZKIR